# Compensation Failure as the Mechanism of Psychosis in 22q11.2 Deletion Syndrome: A Falsifiable Model

Tyler M. Moore

Department of Psychiatry, Perelman School of Medicine, University of Pennsylvania; Lifespan Brain Institute, Penn Medicine and Children's Hospital of Philadelphia

Manuscript · November 2026 tymoore@pennmedicine.upenn.edu ORCID 0000-0002-1384-0151

DOI 10.5281/zenodo.24150977

Recommended citation: Moore, T. M. (2026). *Compensation failure as the mechanism of psychosis in 22q11.2 deletion syndrome: A falsifiable model*. Manuscript retrieved from https://mooremetrics.com/22q. https://doi.org/10.5281/zenodo.24150977

## Abstract

The 22q11.2 deletion raises psychosis risk roughly twentyfold, yet most carriers never become psychotic. That gap, rather than the deletion's biology, is what a theory of this syndrome has to explain, and most of the cellular literature cannot address it: it compares carriers who have schizophrenia with healthy controls, so what it identifies belongs to the combined deletion-and-illness group and cannot be assigned to the deletion alone. This article proposes that the deleted genes with demonstrated neural phenotypes are dosage-limiting for rates, gains and throughputs rather than for structures, so that hemizygosity narrows the range over which a controlled variable can be corrected. The predicted phenotype is bidirectional instability of set points, which is what is observed: connectivity is in surplus before puberty and in deficit after it in deletion mice and in carriers; synaptic transcripts rise while presynaptic proteins fall; neurons are more excitable while their evoked calcium transients are smaller. The model holds that every carrier compensates, and states itself in six separately defined quantities, each with a proposed measurement or proxy: demand, intrinsic capacity, effort, effective capacity, output and reserve. Its predictions can therefore differ in sign between quantities and cannot be averaged into one. Psychosis is placed where the rising demand of adolescent remodeling crosses a falling capacity, with the timing set by regulatory trajectories. The sharpest consequence inverts the usual case-control logic: on compensatory effort the protected carrier should be abnormal beyond controls rather than normal, and the one cellular study to have measured compensatory-effort variables in carriers with and without schizophrenia reports that ordering. Because the state is an imbalance rather than accumulated damage, positive symptoms should remit while negative symptoms and functional impairment persist, and they do. Dopamine is placed as a downstream compensator with a perceptual cost rather than a final common pathway. Four prespecified programs state what would falsify the model, with evidence for, evidence against, and inconclusive outcomes defined in advance.

*Keywords:* 22q11.2 deletion syndrome, psychosis, incomplete penetrance, compensation, developmental dysconnectivity, falsifiability

# Contents


| | |
|---|---|
| 1 | The Central Claim |
| 2 | Which Evidence Can Answer the Question |
| 3 | The Deleted Genes Are Regulators |
| 4 | The Signature Is Bidirectional Instability, Not Uniform Deficit |
| 5 | The Regulated Variable and Its Circuit Expression |
| 6 | Timing: A Crossing, Not a Gate |
| 7 | Symptom Dynamics: The State Is Reversible, and Its Components Dissociate |
| 8 | Dopamine as a Compensator with a Cost |
| 9 | Barrier and Immune Load |
| 10 | The Reciprocal Duplication as a Dose Test |
| 11 | Falsification: Four Decisive Programs |
| 12 | Scope |
| 13 | Synthesis |
| | Transparency and openness |
| | References |


# Supplemental Material


| | |
|---|---|
| S1 | How Evidence Was Selected and Weighted, and the Full Evidence Matrix |
| S2 | The Deleted Genes, Gene by Gene |
| S3 | The Bidirectionality Catalogue and the Circuit-Level Expression |
| S4 | What the Modifier Literature Says About the Character of the Modifiers |
| S5 | The Barrier and Immune Limb |
| S6 | Scope and the Extension to Idiopathic Psychosis |
| S7 | Design Specifications for the Four Falsification Programs |
| | Supplementary Figure |
| | Supplementary References |

# 1 The Central Claim

## 1.1 The question the syndrome can answer

The 22q11.2 deletion is the most informative natural experiment in psychiatric genetics, and the field has largely used it to answer a different question from the one it is best placed to answer. Carriers of the recurrent hemizygous deletion face a risk of psychotic illness some twentyfold above the population rate (Khan et al., 2020; McDonald-McGinn et al., 2015; Murphy et al., 1999). The 3-Mb form, in roughly 85 to 90% of cases, removes one copy of some 46 protein-coding genes; the nested 1.5-Mb form, in most of the remainder, removes about 28 to 30. About a quarter of carriers develop a schizophrenia-spectrum disorder by young adulthood (Gur et al., 2023), and 41% of those older than 25 in the International Brain and Behavior Consortium sample met criteria for a psychotic disorder (Schneider et al., 2014). The lesion is known in advance; the outcome is not. The scientific value of the syndrome lies in that discrepancy: it converts an intractable question about why some people develop psychosis into a tractable question about why some carriers of a specified lesion do.

Most of the cellular and molecular literature cannot answer that question, because of how its comparisons are built. Patient-derived neurons, organoids, fibroblasts and barrier models are overwhelmingly drawn from carriers who have schizophrenia and compared with cells from people who have neither the deletion nor the illness (Crockett et al., 2021; Li et al., 2019; Rao et al., 2025). A difference in that contrast is attributable to the deletion, to the illness, to medication, or to their combination, and the design cannot apportion it. Such studies identify abnormalities of the combined deletion-and-illness group; what distinguishes the carrier who becomes psychotic from the one who does not, they cannot establish. This article proposes a model built from the penetrance question outward, and states what would refute it.

## 1.2 The claim, and the quantities it is stated in

**The central claim is that the 22q11.2 deletion does not install a psychosis-producing lesion; it narrows the dynamic range of the regulatory systems that hold cortical circuits at their set points, and psychosis occurs in the minority of carriers in whom the rising demand of adolescent remodeling crosses a falling compensatory capacity.** The deleted genes that carry demonstrated neural phenotypes are dosage-limiting for a rate, a gain or a throughput rather than for the existence of a structure (Section 3). That is a claim about which of a gene's functions the second copy is required for, not a taxonomy sorting genes into regulators and effectors. The model's hypothesis, tested as such in Section 11 rather than entailed by reduced dosage, is that losing one copy narrows the range over which deviations can be corrected, so the phenotype is an instability of set points rather than a deficit of fixed size: bidirectional, sign-changing across development, and revealed under load.

A model of reserve is unfalsifiable unless its terms are distinct and separately predicted. The model is therefore stated in six quantities, and Table 1 fixes for each what it is, how it would be measured, and what it is predicted to do in every group. *Demand*, D, is the rate at which a

circuit requires its regulated variable, synaptic maintenance as specified in Section 5, to be supplied. *Intrinsic capacity*, $C_0$, is the maximal rate at which that process can run from gene dosage alone; it is identified from effective capacity with effort held at control level rather than measured directly, and it is the quantity predicted to vary monotonically with copy number. *Compensatory effort*, E, is the regulatory response recruited to close the gap. *Effective capacity*, C, is intrinsic capacity raised by effort with diminishing returns, which is the ceiling the model is named for. *Output*, O, is the maintained function, and *reserve*, R = C − D, is the margin by which it is maintained. Figure 1A plots that margin directly for the three groups, so that the model's threshold is the zero line and the transition into psychosis is predicted where a trajectory crosses it.

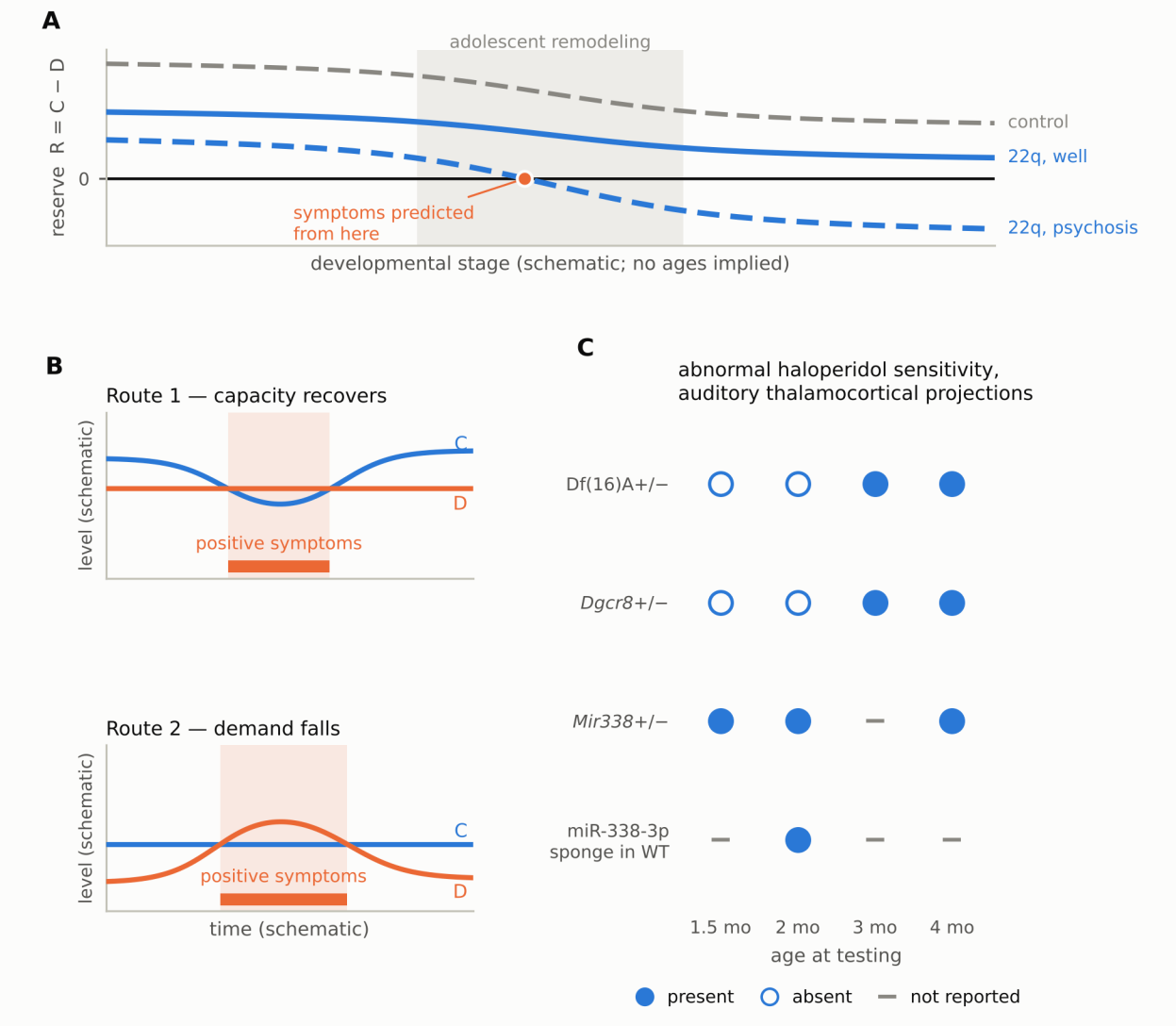



**Figure 1. The model as a reserve that narrows, the two routes to remission it permits, and an experiment that moved the age dependence of a circuit phenotype. (A)** Reserve, R = C − D, plotted directly, so that the model's threshold is the zero line. Developmental stages are illustrative and no ages are implied. A control (gray) retains a large margin. A carrier who remains well (blue, solid) runs on a margin that narrows but stays positive. A carrier who develops psychosis (blue, dashed) differs in starting capacity and rate of decline, and symptoms are predicted from the point at which reserve turns negative. Where capacity sits relative to controls is a separate question, set

out in Table 1 and tested in Study 1. **(B)** The two routes to remission, shown separately because the model permits both and they are empirically distinguishable. Positive symptoms are present only while reserve is negative. In Route 1, capacity recovers against flat demand. In Route 2 capacity stays flat throughout and demand does the work in both directions: it rises through remodeling until it crosses capacity, which is what produces the episode, and falls back below it as remodeling completes, which ends it (Section 11.3). **(C)** Abnormal haloperidol sensitivity of auditory thalamocortical projections at each age reported by Chun et al. (2017): present (filled), absent (open), or not reported (dash). In Df(16)A+/− and *Dgcr8*+/− mice it is absent at 1.5 and 2 months and present at 3 and 4 months, tracking the age-dependent decline of miR-338-3p; in *Mir338*+/− heterozygotes it is present at 1.5, 2 and 4 months; and a miR-338-3p sponge confers it on wild-type (WT) projections at 2 months. Manipulating one regulator therefore changes the age dependence of the phenotype it controls. Demand and capacity were not measured in these experiments, and no claim about this model's crossing follows directly from them.

**Demand is not constant across genotypes, and the model's arithmetic requires that it is not.** With equal demand, a carrier whose effective capacity exceeded a control's would have the *larger* reserve, which is the reverse of what this model asserts. The model predicts instead that **demand is higher in deletion carriers**. This is an assumption the article declares rather than a result it inherits, and it carries the rest of the structure. Demand has two components, measured in different places. *Per-cell maintenance demand*, the rate at which a neuron must supply its own synapses, is visible in a dish, and *CLDN5* hemizygosity adds to it by admitting a peripheral immune load that varies between carriers (Section 9). *Developmental remodeling load*, the synaptic architecture a circuit must eliminate and stabilize through adolescence, is not: a reprogrammed neuron is developmentally immature and has no surplus of synapses awaiting elimination, so no respirometry measurement on such a cell can speak to it. Its ground is that carriers arrive at puberty with more to remodel (Section 4), and its test must run in a system that has synapses to lose.

That converts an arithmetic problem into a quantitative commitment. For the carrier who passes through the risk window without psychosis, the model requires

$$\mathbf{D(well) - D(control) > C(well) - C(control) > 0,}$$

so that reserve is smaller than a control's *even though capacity is higher*. This is the model's sharpest arithmetic claim and the place a disconfirming result would strike first: a carrier group with raised capacity and no demand excess has the larger margin, and the clinical premise fails outright. It is also the claim this article is least able to support from existing work, which is why Study 1 measures demand as a named primary endpoint rather than assuming it.

The assays named in Table 1 are proxies for these quantities, not the quantities themselves: basal respiration indexes realized consumption rather than required demand, and uncoupler-elicited maximal respiration is not maximal physiological output under load. What would make them interpretable, and what follows for the model's threshold, is set out in Supplementary Section S7.2.

**What is entailed, and what is not.** Preserved output with lowered intrinsic capacity does not by itself require compensation: a carrier with an intrinsic capacity of 70 facing a demand of 50 meets it unassisted and has only a smaller unused margin. The entailment holds only where demand exceeds unassisted capacity, which is what the demand prediction above asserts. The

model therefore stakes two claims in order, the first carrying the second: **demand for the regulated process exceeds unassisted capacity in carriers, and effort is therefore recruited.** Neither follows from reduced dosage, and Study 1 tests them as separate contrasts. A third and stronger claim is that effort carries effective capacity above the *control* range, motivated by biology rather than arithmetic: controls recruit the biogenesis controllers minimally at rest, so a carrier running them chronically above control level should exceed that unrecruited baseline from a lower starting dosage, as a trained muscle exceeds an untrained one. Section 11.1 tests the three separately, so that losing the third costs the model its sharpest prediction without taking the architecture with it.

**Table 1** *The six quantities, how each would be measured, and the predicted position of each group relative to controls.*

| Quantity | How it would be measured | Control | 22q, well | 22q, psychosis | Duplication |
|---|---|---|---|---|---|
| **D, demand** | Maintenance component: basal respiration under controlled workload. Remodeling component: synaptic density before elimination, in organoids or mouse cortex | reference | above | above | at or below |
| **$C_0$, intrinsic capacity** | Not measured directly; identified from C with E at control | reference | below | below | above |
| **E, effort** | Resting PGC-1α (primary); PGC-1β, PPARα, PRKN | low | **highest** | raised without a matching rise in C | lowest |
| **C, effective capacity** | Maximal respiration after challenge (primary); accuracy of homeostatic restoration | reference | above controls (strong form); above the psychosis group (core form) | below | above, with E at or below control |
| **O, bioenergetic output** | ATP content; complex I activity | reference | at control | below | at control |
| **O, presynaptic output** | SV2A, NRXN1 protein, absolute and conditional on transcript | reference | absolute at control; transcript-adjusted below | both below | at or above control |
| **O, circuit output** | Long-range synchrony under load | reference | at or near control | below | at control |
| **R, reserve** | Spare respiratory capacity (maximal − basal), as an ordinal proxy only | large | smaller | smallest | large |

"22q, well" denotes a currently unaffected carrier with no lifetime psychotic disorder and no threshold psychosis-spectrum symptoms on a structured diagnostic interview, assessed at age 30 or older; "22q, psychosis" denotes a carrier with a schizophrenia-spectrum diagnosis at assessment, which in every existing cellular study is a cross-sectional classification rather than an observed transition. Age distributions are matched across groups and modeled (Supplementary Section S7.2); the age-30 floor selects the unaffected group and does not define the comparison. *Protected carrier* is used below as a label for the first group under this model's reading of it, not as a demonstrated property of a clinically selected sample. Challenge-evoked measures are primary wherever the biology permits. Three reading notes. The six quantities occupy eight rows because output is split into its bioenergetic, presynaptic and circuit forms. Spare respiratory capacity indexes reserve ordinally and nothing more: a negative value in a dish is not a validated psychosis threshold, and the sign of R in the model is not read off it (Supplementary Section S7.2). And the row entries are predicted positions, not measured ones, except where Section 2 marks them as reported.

### 1.3 Six propositions

**Proposition 1. The deleted genes with neural phenotypes are dosage-sensitive regulators.** They set rates, gains and throughputs rather than specifying a circuit, a receptor or a neuronal identity (Fernandez et al., 2019; Paterlini et al., 2005; Stark et al., 2008; Xu et al., 2013).

**Proposition 2. Regulator hemizygosity produces bidirectional set-point instability rather than uniform deficit**, with overshoot and undershoot coexisting, sign reversing across development, divergence growing under load, and transcript corresponding poorly with protein (Alvino et al., 2025; Khan et al., 2020; Nehme et al., 2022; Sun et al., 2020).

**Proposition 3. The regulated variable is synaptic maintenance in late-maturing association and hippocampal circuits, with presynaptic supply as the hypothesized bottleneck, and its circuit-level expression is dysconnection** (Fernandez et al., 2019; Nehme et al., 2022; Sigurdsson et al., 2010).

**Proposition 4. Compensation is active, costly and measurable, and strongest in carriers who do not become psychotic**, with mitochondrial biogenesis regulators above both controls and carriers with schizophrenia in induced neurons from carriers who remained well, and ATP content and complex I activity preserved (Li et al., 2021). The proposition commits in order to three things: that demand exceeds unassisted capacity, so that effort is required; that effort exceeds control level in carriers who remain well; and that it carries effective capacity above control level. The ordering is the prediction's signature, but no observational contrast can show that the response was *recruited*, since those were iPSC-derived neurons and reprogramming erases acquired state. The proposition therefore stands on Study 1's perturbation arm rather than on the three-group contrast (Section 11.1).

**Proposition 5. Psychosis occurs where rising demand crosses falling capacity, and the position of the crossing is set by the trajectories of regulatory variables rather than by a developmental program** (Alvino et al., 2025; Castellani et al., 2025; Chun et al., 2017; Gur et al., 2023; Vorstman et al., 2015).

**Proposition 6. Dopaminergic elevation is downstream of regulator loss, forms part of the compensatory response, and carries a perceptual cost; it is not a final common pathway.** Thalamic *Drd2* rises because an age-declining microRNA that represses it is depleted (Chun et al., 2014, 2017); striatal synthesis capacity varies inversely with copy number and tracks subclinical positive symptoms, while in antipsychotic-naive carriers it accompanies more control-like connectivity (Mancini et al., 2026; Rogdaki et al., 2023). These are distinct measures, linked by hypothesis rather than by equation.

Two of these claims are indispensable, in the sense that the model should be abandoned rather than repaired if either fails: the inversion on effort, from Proposition 4, and decline of capacity within persons before symptoms emerge, implicit in Proposition 5. If compensation indices prove to be stable traits that do not move within people, the model collapses into static liability accumulation with new vocabulary. Two further claims are separable and weaker: that the

decline is *consumption* rather than age, and that capacity recovers at remission, which the equation does not require (Sections 7 and 11.3). Section 11.5 sorts every claim into indispensable, distinctive and accessory.

**Table 2** *Crosswalk from propositions to falsification programs*

| Proposition | Distinguishing commitment | Decisive program(s) |
|---|---|---|
| **1. Regulators, not effectors** | Deleted genes set rates and gains; the phenotype is a narrowed correction range | Studies 1 and 2 (capacity under challenge; dose-response across the reciprocal CNV) |
| **2. Bidirectional instability** | Overshoot and undershoot coexist and reverse sign across development; transcript–protein discordance is expected | Study 1 (signed, prespecified directions per axis) |
| **3. Synaptic maintenance as the regulated variable, dysconnection as its expression** | Convergence is on synaptic supply, not on a single metabolite or a regional volume | Studies 1 and 4 (presynaptic protein conditional on transcript; benefit mediated by the supply variable) |
| **4. Compensation is active and strongest in the protected** | Non-monotonic three-group ordering with protected carriers beyond controls on effort and capacity | Study 1 (primary), Study 2 (dose extension) |
| **5. Crossing of rising demand and falling capacity** | Capacity is consumed before onset and recovered on remission; the crossing can be moved experimentally | Studies 3 and 4 |
| **6. Dopamine as compensator with a cost** | Dopaminergic elevation is downstream of regulator depletion; its coupling to network configuration is positive before onset and inverts across transition | Studies 2 and 3 |

# 2 Which Evidence Can Answer the Question

## 2.1 Four questions the literature runs together

Work on this syndrome routinely runs together four questions whose answers need not coincide: what the deletion causes (carriers versus noncarriers); what is associated with psychosis among carriers; what prospectively precedes psychosis; and what causally mediates it. A phenotype can answer the first while contributing nothing to the others. The calcium phenotype in 22q11.2 cortical neurons is robust, is phenocopied by *DGCR8* loss, is rescued by its restoration, and does not differ between donors with and without psychosis (Khan et al., 2020); it answers question one and not question two. The reverse error is subtler: a phenotype present in all carriers but *differing in magnitude or inducibility* between converters and non-converters answers question two, but only if the design includes both carrier groups. That design is rare, which is why this model weights a few studies heavily and many lightly.

## 2.2 Four tiers of causal evidence

Claims that mechanism A contributes to psychosis are graded at four tiers: presence; temporal precedence within persons; mediation or intervention; and necessity. The tiers are defined in Supplementary Section S1 and applied in Table 3, with the full matrix as Supplementary Table S1. Two conventions do real work. Tier 1 evidence from a carriers-versus-controls design is

recorded for the combined deletion-and-illness group rather than for penetrance, and carried in its own column. And tiers are reported separately for human and model-system evidence, because an intervention in a deletion mouse reaches Tier 3 for a conserved component mechanism and not for the human sequence: the Df(16)A, LgDel and Df(h22q11) lines are bred to fixed backgrounds and do not model clinical penetrance (Hiroi et al., 2012).

**Table 3** *Principal claims, the strongest human evidence for each, and whether that evidence compared carriers by psychosis status*

| Claim | Strongest human evidence (tier) | Within-carrier comparison? | Principal limitation |
|---|---|---|---|
| **1. Deleted genes act as dosage-sensitive regulators (Prop. 1)** | Locus-wide transcript reduction with non-proportional effects; 89% of differentially expressed genes lie outside the deletion (Nehme et al., 2022); miR-185 falls further than hemizygosity predicts (Khan et al., 2020; Xu et al., 2013) (Tier 1) | No | Regulator classification is interpretive, not a quantified enrichment; some deleted genes (*TBX1*) are patterning genes |
| **2. Phenotypes are bidirectional and reverse sign across development (Prop. 2)** | Thicker cortex with reduced surface area (Sun et al., 2020); synaptic transcripts up with presynaptic proteins down (Nehme et al., 2022); hyperconnectivity before puberty, hypoconnectivity after it (Alvino et al., 2025) (Tier 1) | No | Also compatible with many unrelated effects; human connectivity data are cross-sectional with puberty inferred from age |
| **3. Convergence on synaptic maintenance, expressed as dysconnection (Prop. 3)** | Reduced SV2A and NRXN1 protein against broadly upregulated synaptic transcripts in carrier neurons (Nehme et al., 2022); in idiopathic schizophrenia, synaptic density at 72% and terminal mitochondrial density at 64% of control (Roberts et al., 2015) (Tier 1) | No | Discovery proteomics in two carrier and two control donors; presynaptic specificity is a hypothesis, not a measurement |
| **4. Compensation is active and strongest in protected carriers (Prop. 4)** | Carriers without schizophrenia show PGC-1α, PGC-1β and PPARα above controls and above carriers with schizophrenia, and PRKN selectively elevated relative to carriers with schizophrenia; ATP and complex I reduced only in carriers with schizophrenia (Li et al., 2021) (Tier 1, design-appropriate) | **Yes** | iPSC-derived neurons, so an elevation is a constitutive difference and not a demonstrated recruitment (Section 1.3); no PRKN-versus-control statistic is reported; four lines per carrier group and six controls; mtDNA copy number exceeded carriers with schizophrenia but not controls; the peripheral replication had no control group and its groups differed in age at collection (26 vs 34 years, P = .02); nonpsychotic donors aged 22–26 remained in the risk window |
| **5. Rising demand crosses falling capacity (Prop. 5)** | Verbal IQ decline precedes psychosis (Vorstman et al., 2015); working-memory decline drives clinical change (Gur et al., 2023); accelerated thinning accompanies psychotic symptoms (Bagautdinova et al., 2021) (Tier 2 relative to onset) | Partly | Cognitive decline may be an early expression of illness; no human study has measured a compensation variable longitudinally |
| **6. Dopamine as a downstream compensator with a cost (Prop. 6)** | Synthesis capacity falls linearly with copy number ($B = -1.2 \times 10^{-3}$ min$^{-1}$ per copy, $p < 0.001$), with deletion carriers above controls ($d = 1.44$) and above duplication carriers ($d = 2.00$) (Rogdaki et al., 2023); higher synthesis capacity accompanies control-like connectivity (Mancini et al., 2026) (Tier 1) | Partly | Cross-sectional, 18–21 carriers, overlapping datasets; the duplication-versus-control contrast did not survive correction, so the three-way ordering is not established; compensatory direction is inferred from a correlation |

| Claim | Strongest human evidence (tier) | Within-carrier comparison? | Principal limitation |
|---|---|---|---|
| **7. The state is reversible rather than cumulative (Props. 4, 5)** | Positive psychosis-spectrum symptoms remitted in 16 of 41 symptomatic carriers over 2.8 years; negative symptoms and functional impairment persisted after remission (Tang et al., 2017) (Tier 1–2) | **Yes** | Subthreshold symptoms, not psychotic disorder; the impairment factor was higher at baseline in the emergent group (P = 0.03) but did not predict emergence in regression (P = 0.82); 41 symptomatic participants, so rate comparisons are imprecise, and the comparison cohort was followed for a shorter period (Section 7) |
| **8. Barrier and immune load contributes to penetrance** | Within carriers, IL-6 and IL-6/IL-10 (Mekori-Domachevsky et al., 2017), IL-8 (O'Hora et al., 2024) and Th17 percentage (Vergaelen et al., 2018) higher with psychosis or psychosis-risk symptoms (Tier 1) | **Yes** | Three small studies, each with a different marker; carrier-versus-control cytokine elevations did not replicate across them; the human cellular barrier work used cells of non-endothelial lineage (Lu et al., 2021); a claudin-5 variant association in a small carrier cohort (Greene et al., 2018) did not replicate in 490 (Guo et al., 2020) |
| **9. Modifiers act on regulatory and synaptic systems the deletion constrains** | Polygenic score predicts diagnosis and verbal IQ decline (Davies et al., 2020); rare duplications overlapping nervous-system genes, connected to deletion-region genes, enriched with schizophrenia (Bassett et al., 2017); genic tandem repeat expansions enriched, acting through splicing and methylation (Cheng et al., 2026); 110 modifier genes with rare coding variants acting in both directions (Lin et al., 2023) (Tier 1, strong) | **Yes** | Each class explains a minority of variance; network connectivity is a bioinformatic association; no study relates modifier burden to a measured compensation variable |

Three features of Table 3 govern the rest of the article. The within-carrier column is negative for most of the cellular and imaging literature and positive for most of the genetic and peripheral literature, so the biology studied most intensively is the biology least able to speak to penetrance. Of the two cellular studies that compared carriers by psychosis status, the one measuring a regulated output found no difference (Khan et al., 2020) and the one measuring compensatory machinery found the non-monotonic ordering the model predicts (Li et al., 2021). And the strongest model-system evidence has reached the necessity tier for a component mechanism (Chun et al., 2017).

### 2.3 Rival architectures

A model earns its structure only if some observation would favor it over rivals built from the same findings. Table 4 specifies five and gives what each predicts: H1, the account of Section 1.2; H2, static liability accumulation, with no distinct compensatory process, so biomarkers are monotonic across the three groups, stable within persons, and the same at rest and under challenge; H3, fixed vulnerability with stochastic trigger; H4, parallel subgroup routes through distinct primary lesions; and H5, developmental vulnerability with changing load. Figure 2 sets the H1 and H2 orderings side by side, quantity by quantity, and marks where data exist: the two coincide on presynaptic output, which is why no panel can stand for the set. H5 is the strongest comparator, and the only one worth the article's attention: it allows demand to rise and fall, modifiers to push risk in either direction and symptom components to run on

different timescales, and so reproduces most of the observations this model was built from. What it does not contain is an active compensatory process that is recruited, costly and capable of being suppressed.

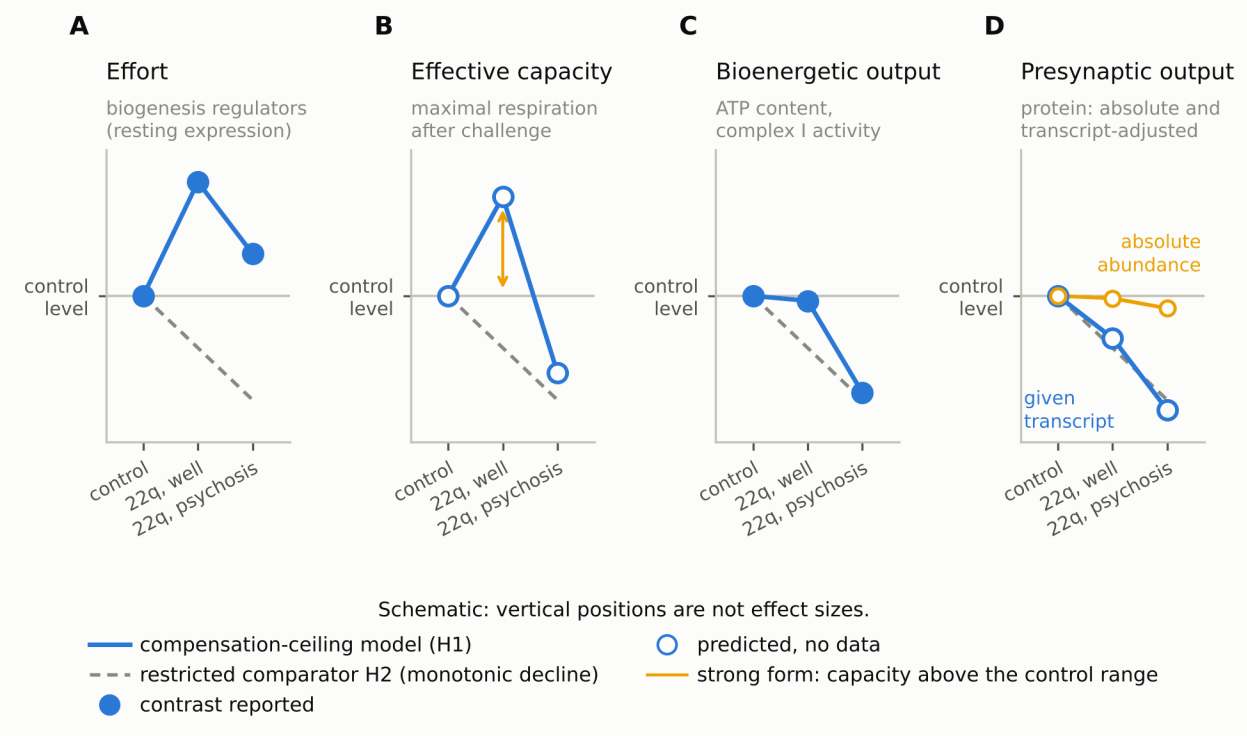



**Figure 2. Three-group orderings predicted by the compensation-ceiling model and by the restricted monotonic comparator, separated by quantity.** Vertical positions show predicted direction and shape, not effect sizes. H1 (blue) is the compensation-ceiling model. The dashed gray line is H2 *as specified in Table 4*, meaning monotonic decline in every quantity, and not a generic liability-threshold prediction; other threshold models make other orderings. Each quantity is a separate endpoint and they are never averaged into a composite (Section 11). "22q, psychosis" denotes carriers with a schizophrenia-spectrum diagnosis at assessment; in every existing cellular study this is a cross-sectional classification, not an observed transition. **(A)** Effort. Filled markers denote contrasts reported by Li et al. (2021) in induced neurons: PGC-1α, PGC-1β and PPARα higher in carriers without schizophrenia than in both other groups, and PRKN higher than in the psychosis group, with no PRKN-versus-control statistic reported. Mitochondrial DNA copy number exceeded the psychosis group but not controls and is not plotted. The psychosis group is drawn above the control line rather than on it, because Table 1 predicts effort raised in every carrier without a matching rise in capacity; the source is self-contradicting on the carrier-versus-control comparison, its Results text reporting the controllers unchanged between carrier groups and the legend to its own Figure 3 reporting them elevated in both carrier groups relative to controls. **(B)** Effective capacity. The core form requires only that carriers who remain well exceed the psychosis group; the strong form adds the overshoot above controls, marked by the amber arrow. No three-group capacity data exist. **(C)** Bioenergetic output, with the reported contrasts filled: ATP content and complex I activity reduced in the psychosis group and not different from controls in carriers who remain well. A nonsignificant difference is not equivalence, and this group's placement at control level is the model's prediction, not a demonstrated equality. **(D)** Presynaptic output under two distinct estimands. *Absolute* protein abundance (amber) is predicted to be roughly preserved; protein abundance *conditional on transcript* (blue), estimated by donor-level regression, is predicted to fall. The two are not alternatives and can hold together, since elevated transcript with preserved protein is exactly what a reduced transcript-adjusted estimand describes. On the conditional estimand both models predict monotonic decline, so this panel does not discriminate between them on its own; it is shown because its predicted direction is *opposite* to that of effort in panel A, which is why the two can never enter a common composite.

**Table 4** *Observations that discriminate the compensation-ceiling model from four specified rivals.*

| Observation | H1 predicts | H2 predicts | H3 predicts | H4 predicts | H5 predicts |
|---|---|---|---|---|---|
| **Three-group ordering on effort and challenge-evoked capacity** | Non-monotonic: protected carriers exceed controls; the psychosis group resembles or falls below them | Monotonic: controls, protected carriers, psychosis group | No carrier-group difference at rest | Varies by subgroup | Non-monotonic is possible; no recruited process |
| **Resting versus challenge-evoked measurement** | Separation larger under challenge | Similar under both, scaled by burden | Minimal in either | Varies by subgroup | Larger under challenge, from fixed capacity limits |
| **Within-person trajectory of compensation indices across transitions** | Decline before emergence, preceding cognitive change; at remission the balance returns by recovering capacity or falling demand, identifiably | Stable traits; baseline predicts outcome without within-person change | Stable; change follows the trigger | No common trajectory | Decline before emergence; no effort term |
| **Relation of genetic modifiers to the deletion** | Act on the systems the deletion constrains; predict trajectory, not only endpoint | Modifiers add independently; endpoint prediction suffices | Index exposure risk | Partition by subgroup | Act on the same systems; signed effects allowed |
| **Duplication carriers on capacity measures** | Exceed controls, with effort at or below control | At or near controls; protection is reduced liability | At controls | Varies | Exceed controls on capacity |
| **Dopamine–connectivity coupling across transition** | Positive before onset, flattening or inverting across it | No specific prediction | No specific prediction | One subgroup only | No specific prediction |
| **Durability of an intervention after it stops** | Set by whether dosing fell inside the regulator's window; endpoint-specific within an animal; sign set by the pretreatment deviation | Set by the size of the effect on liability while it is applied, with no window and no sign reversal | Irrelevant without trigger removal | One subgroup only | Set by the developmental window |
| **Suppressing the compensatory response in protected-carrier cells** | Degrades output under load, more than in controls | No distinct response to suppress | No effect | Confined to one subgroup | No effect beyond the dosage deficit |
| **Symptom dynamics** | Positive symptoms track the fast balance; negative symptoms and function track the slow architecture and persist | Positive and negative symptoms remit together as liability falls | Follows trigger removal | Differs by subgroup | Fast and slow components, as in H1 |

The rivals are restricted forms, stated in Section 2.3, not general statements of the traditions they come from; H5 is the closest comparator and matches H1 everywhere except on the recruited, costly, suppressible compensatory process itself.

H1 is itself a threshold model, and what distinguishes it from H2 is what lies on either side of the threshold: in H1 the liability is a within-person state composed of two separately measurable and manipulable terms, one of them an active process that overshoots. Over-readings of that difference are disclaimed in Supplementary Section S6. What survives is narrow and is the whole of what Table 4 claims: of the five forms, only H1 predicts an *actively*

*recruited, costly, suppressible* compensatory process strongest in carriers who remain well. H5 differs from H1 there and nowhere else, which is why Study 1's perturbation arm, and not any observational contrast, is what separates them.

## 3 The Deleted Genes Are Regulators

The organizing observation behind Proposition 1 is that the interval's neural relevance lies in genes that set the rate, gain or throughput of a process rather than in genes that specify a structure. This is a claim about the genes with demonstrated neural phenotypes, not a quantified enrichment across all 46, and *TBX1*, a patterning gene, does not fit it. Figure 3 maps the mechanism that this section and those following populate, marking each link as a definition, as a reported association, or as a hypothesis that Section 11 tests. The gene-by-gene case is in Supplementary Section S2; two genes carry the argument here.

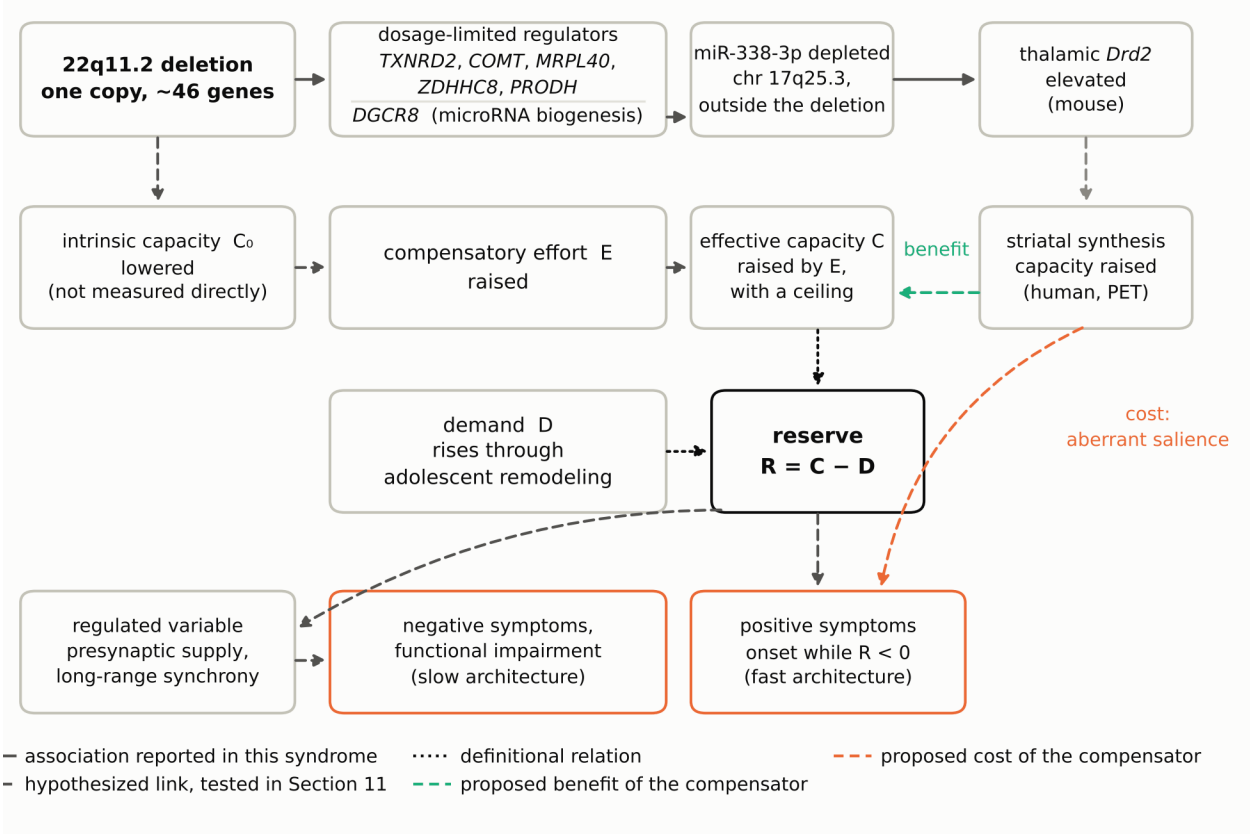



**Figure 3. The mechanism, with definitions, reported associations and hypothesized causal links distinguished.** Solid arrows mark associations reported in this syndrome at Tier 1 or above; dashed arrows mark hypothesized links that the programs of Section 11 test; dotted lines mark the definitional relation R = C − D, which is arithmetic rather than a hypothesis awaiting evidence. Two distinctions in the dopaminergic branch are deliberate. First, species and level of measurement: elevated thalamic *Drd2* is a mouse transcript finding and elevated striatal synthesis capacity is a human positron emission tomography finding, so the link between them is dashed rather than drawn as a chain, and each box names its species. Second, the two consequences are separate: elevated synthesis capacity is proposed to contribute to effective capacity by stabilizing network states, and independently to produce aberrant salience, which grades severity *within* the positive-symptom state rather than driving the transition into it. The transition is governed by the sign of reserve. These are tested separately in Study 3. miR-338-3p is not a deleted gene: human *MIR338* lies on chromosome 17q25.3 and is depleted because *DGCR8*, which

is deleted, is required for microRNA biogenesis; the arrow is routed from *DGCR8* accordingly. Intrinsic capacity is not measured directly, so the links into and out of it are dashed. Assays for each quantity are given in Table 1.

*TXNRD2* encodes the rate-limiting enzyme for clearance of mitochondrial hydrogen peroxide. Of six 22q11 mitochondrial genes screened by knockdown in wild-type cortical neurons, only *Txnrd2* depletion reproduced the LgDel reduction in axon and dendrite growth, its re-expression restored growth and returned reactive oxygen species to wild-type levels, and the deficit was confined to layer 2/3 projection neurons, whose long-range association projections impose the highest bioenergetic demand (Fernandez et al., 2019). That is a dosage-limited regulator whose consequences surface where demand is greatest. *COMT* makes the compensation point directly: in *Prodh*-deficient mice frontal *Comt* is upregulated at message and protein from the third postnatal week, chronic NMDA-receptor blockade in wild-type mice phenocopies the regional pattern, identifying the upregulation as a response to altered transmission, and COMT inhibition unmasks deficits in the mutants only (Paterlini et al., 2005). One deleted gene is the compensator for another.

## 4 The Signature Is Bidirectional Instability, Not Uniform Deficit

If the deletion removed one copy of a set of effectors, the expected phenotype would be partial deficits of roughly proportional size pointing in the same direction. That is not what is observed.

The clearest demonstration is longitudinal in mice and cross-sectional in carriers. LgDel mice scanned before and after puberty showed widely *increased* global functional connectivity as juveniles and *decreased* hippocampal connectivity as adults, in the same animals; in 139 carriers and 117 controls aged 6 to 30, prepubertal children showed foci of global hyperconnectivity while postpubertal carriers showed hippocampal and temporal hypoconnectivity (Alvino et al., 2025; Figure 4A, 4B). The anatomy behaves the same way: prefrontal spine density increased in juvenile mice and at wild-type level in adults, hippocampal density increased in juveniles and *reduced* in adults. The deletion does not produce too little connectivity. It produces the wrong amount, and which direction is wrong depends on when you look. The juvenile surplus is also what the demand term draws on, since a circuit arriving at puberty with more synapses has more to eliminate (Section 1.2).

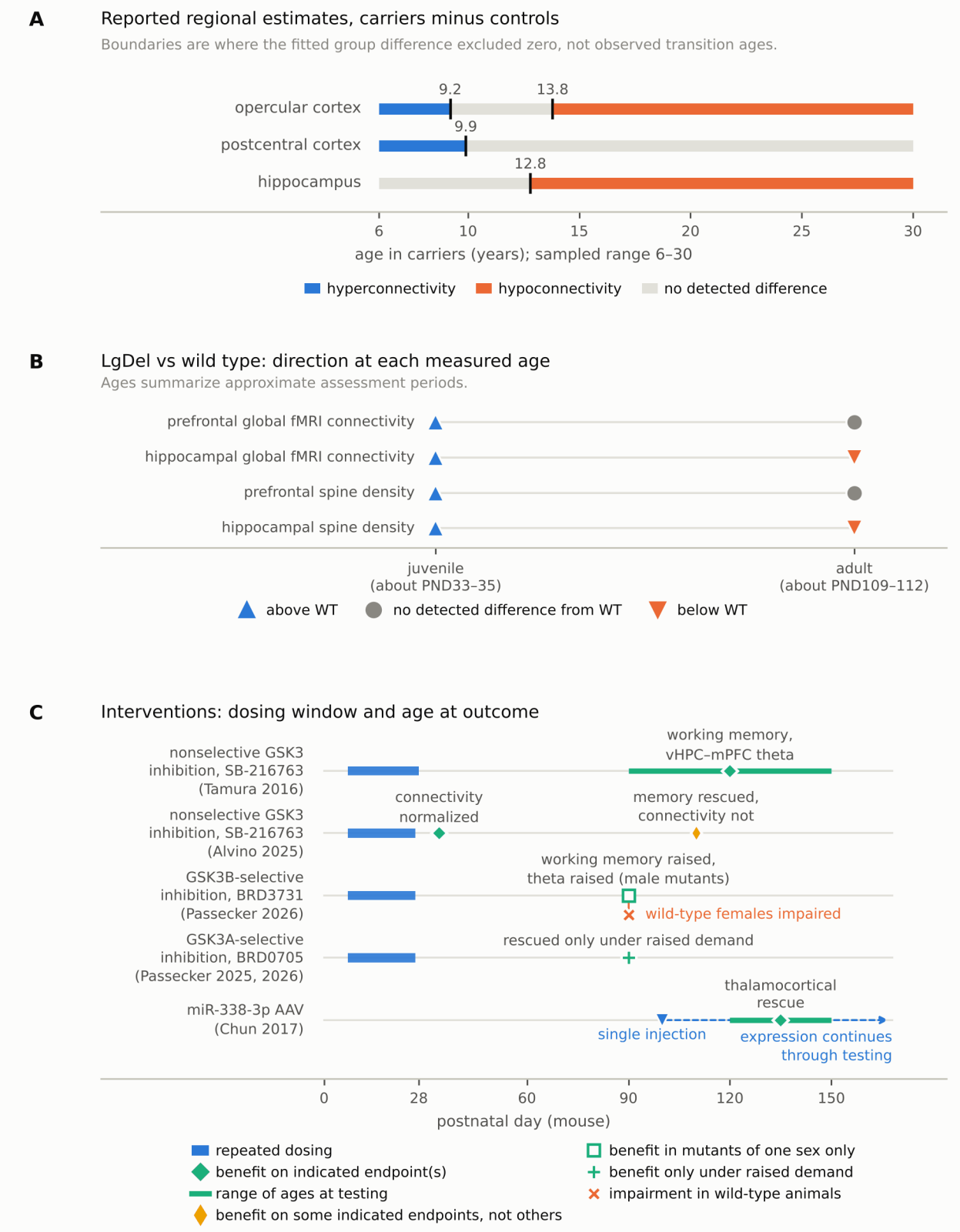



**Figure 4. The developmental reversal in each species, and what the intervention literature establishes. (A)** Carriers, cross-sectional, in 139 carriers and 117 controls aged 6 to 30 (Alvino et al., 2025). Regional estimates are shown as reported rather than combined into a

single fitted trajectory, which would imply a common crossing the data do not locate. The boundaries are 9.2 and 9.9 years for hyperconnectivity in opercular and postcentral cortex and 12.8 and 13.8 years for hypoconnectivity in hippocampus and opercular cortex, and they are the ages at which the confidence interval for the fitted group difference excluded zero rather than observed biological transition times. Gray marks ages at which no group difference was detected, which is not the same as an established absence of one. Pubertal status was inferred from an age cutoff, not measured. **(B)** LgDel mice. Direction of each endpoint relative to wild type (WT) at the two assessment periods, shown qualitatively because spine density and global functional magnetic resonance imaging connectivity carry different units. Gray denotes no detected difference from WT; equivalence was not tested. Ages summarize approximate assessment periods. Connectivity was measured longitudinally in the same animals, spine density in separate juvenile and adult animals. A pooled mean of a measure that changes sign depends on the age composition of the sample, which is why the model requires age-stratified analysis. **(C)** Interventions, on a postnatal-day (PND) axis. Nonselective GSK3 inhibition with SB-216763 from PND7 to PND28 restored working memory and ventral hippocampal (vHPC) to medial prefrontal (mPFC) theta synchrony, tested between three and five months (Tamura et al., 2016); the same compound on a near-identical schedule to PND27 rescued adult temporal-order memory at about PND110 while adult hippocampal hypoconnectivity was not rescued and the juvenile normalization of connectivity did not persist (Alvino et al., 2025); the GSK3B-selective inhibitor BRD3731, ten injections from PND7 to PND27, improved working memory and *raised* vHPC–mPFC theta coherence in adult male mutants, raised rather than restored because coherence was not significantly reduced in mutants of either sex at baseline, while the same compound impaired wild-type females, a deviation in sign that Study 4 is designed to resolve and for which no wild-type male comparison is reported (Passecker et al., 2026); and the GSK3A-selective BRD0705 on that schedule was null at baseline but rescued adult spatial working memory when the task was run under raised working-memory demand (Passecker et al., 2025, 2026), which is load dependence of the kind Proposition 2 predicts. Adeno-associated virus (AAV) miR-338-3p replenishment in the medial geniculate is a single injection whose expression continues through testing at four to five months, which is not comparable to a course of dosing that ends (Chun et al., 2017). Benefit outlasting *dosing* is therefore established; benefit outlasting verified *disengagement* of the proximal target has not been tested in any of them, and that is the gap Study 4 closes.

Eight further findings fit the same shape and are catalogued in Supplementary Section S3, among them increased hippocampal long-term potentiation (LTP) (Earls et al., 2012), overgrowing thalamocortical axons (Shin et al., 2024), thicker cortex with substantially reduced surface area (Sun et al., 2020), and neurons that fire spontaneously about four times as often while showing *smaller* evoked calcium transients (Khan et al., 2020). The deletion's effect is better described as loss of set-point control than as loss of function.

Transcript–protein discordance is expected under Proposition 4, where transcriptional upregulation is the compensatory response and its failure to normalize protein stoichiometry is compensation falling short at the step the deletion constrains. That reading is not the only one available, and the alternative comes from the same paper: Nehme et al. (2022) propose that reduced *TBX1* de-represses the activity-dependent transcription factor MEF2C, with JUN/FOS motifs most enriched among the upregulated genes, which would make the transcript elevation part of a developmental cascade and so part of the lesion rather than a response to it. That is a serious rival to the *compensatory* reading, and the two separate on prediction: a compensatory elevation should be larger in carriers who remain well and should worsen function when suppressed, whereas a MEF2C-driven elevation should track the deletion rather than psychosis status. Association with a favorable clinical status cannot distinguish beneficial compensation from differences in maturation, transcription, translation or degradation correlated with that status. Only perturbation can, which is why Study 1 carries a perturbation arm.

Two consequences follow. Signed averages across measures that move in opposite directions, and age-pooled contrasts on measures that reverse sign, both cancel, so the model requires signed, age-resolved, prespecified hypotheses for each quantity (Section 11). And

bidirectionality alone is compatible with a 46-gene deletion simply producing many unrelated effects; what distinguishes Proposition 2 is that divergence should grow *under load*, which makes challenge-evoked measurement the discriminating design.

## 5 The Regulated Variable and Its Circuit Expression

"Compensation" without a specified object is unfalsifiable. Proposition 3 names the object as synaptic maintenance in late-maturing association and hippocampal circuits, and makes a narrower bet about the bottleneck: presynaptic supply. The broad claim is what the evidence supports now; the narrow one is what Study 1 measures.

Five lines of evidence converge on synaptic maintenance, none presynaptic-specific on its own, and they are set out in Supplementary Section S3. Two carry the weight. Carrier neurons show broadly upregulated synaptic transcripts against reduced presynaptic protein, with 37 of the 182 downregulated SynGO-annotated synaptic proteins upregulated at the transcript level (Nehme et al., 2022). And *Txnrd2* dosage limits synaptic vesicle density and presynaptic specializations in the layer 2/3 neurons whose projections impose the highest demand (Fernandez et al., 2019), with *Mrpl40* hemizygosity disrupting presynaptic calcium handling under load (Devaraju et al., 2017). Adolescent remodeling is elimination and selective stabilization, and stabilization is the metabolically expensive half.

The circuit expression of a supply constraint is loss of the long-range coordination that depends on it. Hippocampal–prefrontal synchrony during working memory is drastically reduced in Df(16)A+/− mice, the line also designated Df(16)1/+ and called by the first name throughout this article, and coherence at the onset of training predicted how long acquisition took (Sigurdsson et al., 2010): a circuit measure that predicts the *rate at which an animal can learn* indexes capacity rather than damage. Naming the variable sets a boundary as well as a target. The model does not claim that bioenergetic failure is a universal bottleneck, or that metabolic demand explains regional vulnerability.

## 6 Timing: A Crossing, Not a Gate

Proposition 5 holds that psychosis is timed by the point at which rising demand crosses falling capacity, rather than by a developmental gate that opens at a fixed age. Four lines of evidence support reading the timing as a crossing.

First, the deletion's consequences are latent and then expressed within the same genotype without further genetic change. Hippocampal LTP in Df(16)A+/− mice is indistinguishable from wild-type at 8–10 weeks and markedly elevated at 16–20 weeks (Earls et al., 2012), and thalamocortical *Drd2* elevation with haloperidol sensitivity is present in Df(16)A+/− and *Dgcr8*+/− mice from three months and in neither at 1.5 or 2 months (Chun et al., 2017). What changes between those ages is the value of a regulatory variable in a maturing circuit, not the lesion. That the LTP result is an *overshoot* arriving after puberty, where the developmental claim of

Section 4 is surplus before puberty and deficit after it, is not a conflict: that claim is about long-range connectivity, while what is dated here is the age at which a controlled variable first leaves its set point. Which direction it leaves in is set by the limiting controller; that it leaves at all, within one genotype between two ages, is the timing fact.

Second, and most important, the timing can be moved. miR-338-3p is enriched in thalamus, represses *Drd2* through a conserved seed site, and declines with age; *Dgcr8* hemizygosity exaggerates that decline. If the age dependence of the circuit phenotype is produced by that trajectory, removing the regulator should remove the age dependence, and it does: *Mir338*+/− heterozygotes show the thalamocortical deficit, its haloperidol sensitivity and the prepulse inhibition abnormality at every age tested, and a miR-338-3p sponge confers haloperidol sensitivity on wild-type projections at 2 months (Chun et al., 2017; Figure 1C). Conversely, replenishment by adeno-associated virus (AAV) in the medial geniculate, given well after the phenotype has appeared, rescues it; of five depleted *Drd2*-targeting microRNAs, only miR-338-3p did. Two qualifications hold. Human *MIR338* lies on chromosome 17q25.3, outside the deleted interval, so it is a downstream regulator rather than a deleted gene. And the depletion is demonstrated in mouse models, not in human carriers, where the corresponding observation is in schizophrenia postmortem thalamus; that carriers show it is a prediction of this model rather than a fact. These experiments measured neither demand nor capacity. What they show is that a regulator's trajectory sets the clock.

Third, the adolescent inflection is selective: in LgDel/+ mice, social deficits, the failed adolescent increase in prelimbic thickness and microglial *C4* elevation all appear at adolescence, while sensorimotor gating deficits are present from postnatal day 19 (Castellani et al., 2025). Some consequences of the deletion are constitutive and some adolescence-dependent, and it is the latter that track the human risk period. Fourth, what changes in carriers before psychosis indexes the capacity to meet cognitive demand rather than structural loss: verbal IQ declines more steeply in those who go on to psychotic illness (Vorstman et al., 2015), polygenic burden predicts that decline (Davies et al., 2020), and youth with prominent psychosis-spectrum features declined specifically in working memory (Gur et al., 2023). Carriers with psychosis differ from carriers without in cortical thickness (Bagautdinova et al., 2021) but *not* in surface area (Sun et al., 2020), the measure that most strongly separates carriers from controls: the deletion sets surface area, and remodeling sets who converts.

## 7 Symptom Dynamics: The State Is Reversible, and Its Components Dissociate

If psychosis in this syndrome were accumulated damage, symptoms should be largely monotonic once established. They are not. Among 72 carriers with a longitudinal clinical classification, followed for a mean of 2.8 years, psychosis-spectrum symptoms were

consistently absent in 22, emergent in 9, remitted in 16 and persistent in 25 (Tang et al., 2017). Sixteen of 41 symptomatic carriers crossed back out of the symptomatic state within three years, which is the observation the model needs: a state that resolves is a balance, not a scar.

What that cohort cannot establish is an *asymmetry* between entry and exit, and this article does not claim one. The comparison group, non-deleted youth from the Philadelphia Neurodevelopmental Cohort, was followed for 2.0 years against the carriers' 2.8, and cumulative proportions over unequal windows are not comparable. Converted to annual hazards, emergence runs at 0.115 per year in carriers against 0.084, a ratio of 1.4 rather than the doubling the raw proportions suggest; remission runs at 0.162 against 0.286, a ratio of 0.57. A narrowed margin predicts that pattern once both of its terms are allowed to move, but so does an accumulating lesion, so the comparison does not discriminate and is not used to. With 41 symptomatic carriers the remission estimate is imprecise in any case. What the model requires from this cohort is that exit occurs at all, and it does.

The discriminating observation is the dissociation *within* the symptoms. Negative symptoms and functional impairment continued to mark carriers whose positive symptoms had remitted, and were higher at baseline in the group whose positive symptoms later emerged ($P = 0.03$), although that factor did not significantly predict emergence or persistence once entered in a regression ($P = 0.82$) (Tang et al., 2017). The persistence half is the load-bearing one, and it is unambiguous. Deriving it requires saying which quantity is fast and which is slow, because a single C cannot be both. Effort and the effective capacity it buys are fast and recoverable, being expression and activity levels in a regulatory system. Demand is slow and, through adolescence, monotonic. Slow and only partly reversible is the architecture of the regulated variable: synapses formed or lost, long-range synchrony, and the structural consequences of having run with negative reserve. Positive symptoms track the sign of reserve, which is fast because one of its terms is; negative symptoms and functional impairment track the architecture, which is why restoring the balance returns the first and not the second. Of the rivals in Table 4, only H1 predicts that ordering rather than stipulating it.

The same accounting constrains what remission shows. Because $R = C - D$, the balance can be restored either by capacity recovering or by demand falling, and the model asserts that both routes exist rather than requiring the first. Figure 1B draws them separately, because they are empirically distinguishable. That is testable, and no rival makes the prediction: the routes should dominate at different ages. Remission late in the risk window should occur with demand falling and capacity flat; remission earlier, while demand is still rising, should require capacity to recover.

Three limits are developed in Supplementary Section S6: remission of subthreshold symptoms is not remission of a psychotic disorder; symptom remission does not show that structural abnormalities have resolved; and affective comorbidity moves with symptom course, so Study 3 measures affective state rather than assuming it away.

# 8 Dopamine as a Compensator with a Cost

Proposition 6 departs from the framing in which striatal hyperdopaminergia is the final common pathway for psychosis. Three lines of evidence support the departure, and they concern three different measures the model connects by hypothesis.

The mechanistic evidence places *thalamic receptor expression* downstream of regulator loss: thalamic *Drd2* elevation is attributable to *Dgcr8* hemizygosity, and its proximate cause is depletion of miR-338-3p, which is necessary and sufficient for the phenotype (Chun et al., 2014, 2017). The human imaging evidence establishes the dosage relationship: in 21 deletion carriers, 12 duplication carriers and 26 controls, all antipsychotic-naive, copy number had an inverse linear effect on whole-striatal $K_i^{cer}$ ($B = -1.2 \times 10^{-3}$ $min^{-1}$ per copy, $p < 0.001$), with deletion carriers exceeding controls by $d = 1.44$ (Rogdaki et al., 2023). Synthesis capacity was also associated with psychosis-risk symptom severity ($B = 730.5$, $SE = 310.2$, $p < 0.05$), estimated across the *combined* deletion and duplication sample with copy-number group in the model, so the symptom association is adjusted for copy number rather than demonstrated within deletion carriers alone.

The multimodal evidence concerns *network configuration* and resists the reading that hyperdopaminergia is simply pathogenic. Across antipsychotic-naive carriers and controls, with group in the model, higher striatal synthesis capacity was associated with functional connectivity profiles *more* like those of controls ($p = 0.011$), while connectivity showed no relationship with subclinical symptoms (Mancini et al., 2026). The within-carrier version of that association is weaker and sensitivity-dependent, and a profile more similar to controls is a resemblance rather than a demonstrated benefit. Taken together the three lines describe a variable raised by loss of a regulator, varying inversely with regulatory dosage, accompanying more normative network organization and accompanying more severe psychosis-risk symptoms. Under Proposition 6 that is what a compensator with a perceptual cost looks like: elevated presynaptic dopamine raises the gain with which salience is assigned, stabilizing network states under degraded input and raising the probability that neutral stimuli acquire significance.

The proposition therefore makes two claims, tested separately because neither implies the other. **The benefit claim:** raising synthesis capacity improves a circuit property the deletion degrades, measured against performance or stability rather than resemblance. **The cost claim:** the same elevation increases aberrant salience. Dopamine can do both at once across the whole observed range, so a positive dopamine–connectivity association does not show the cost is absent. The cost claim predicts specifically that the symptom association survives adjustment for connectivity; if positive symptoms track dopamine only through network disruption, the proposition loses half its content.

Placing dopamine beside the reserve equation forces a choice, because the two could otherwise generate symptoms independently. **Reserve governs the transition; dopaminergic state governs severity within a state.** Crossing into, and out of, the psychosis-spectrum state

requires a change in the sign of reserve. Dopaminergic gain modulates how intense symptoms are and how often subthreshold experiences occur within a state, and can move with no change in capacity or demand. This is what makes Study 3's falsifier coherent: a *transition* with no measurable movement in either term would refute the balance account, whereas fluctuation in severity without such movement would not. It is also a claim in its own right, and it fails if transitions track dopaminergic measures with reserve held constant.

A third and weaker prediction is retained as an additional test rather than a decisive one, and is set out in Supplementary Section S4: the sign of the dopamine–connectivity relationship should invert across transition, which no rival in Table 4 predicts but which medication, illness stage, sampling and range restriction can also produce.

## 9 Barrier and Immune Load

The model assigns the barrier and immune limb a specific and now load-bearing role: *CLDN5* hemizygosity destabilizes barrier tone, admitting a peripheral immune load that varies between carriers and adds to demand. It supplies the maintenance component of the demand excess (Section 1.2), and it is the component that varies *within* the carrier group, which makes it a candidate source of penetrance variation rather than a uniform deletion effect. The animal evidence is causal and places barrier tone upstream: neonatal intranasal oxytocin in LgDel/+ mice raised claudin-5, sealed the barrier, prevented microglial *C4* and *C1q* elevation and prevented the adolescent social deficit (Castellani et al., 2025). The human limb is weak on both sides, and Supplementary Section S5 sets out why. Because the demand prediction rests partly on this limb, Study 1 measures immune load alongside the bioenergetic endpoints.

## 10 The Reciprocal Duplication as a Dose Test

The locus supplies something almost no other psychiatric risk variant does: a reciprocal duplication with an opposite phenotype. In 21,138 schizophrenia cases and 25,867 controls, duplications occurred in 0.014% of cases and 0.085% of controls, odds ratio 0.17 (95% CI 0.05–0.56); the same duplication *raises* risk of intellectual disability, developmental delay and congenital malformation (OR 3.75, 2.29–6.15) and of autism spectrum disorder (OR 3.29, 1.63–6.61) (Rees et al., 2014; Supplementary Figure S1). That dissociation is the most constraining fact available to any theory of the locus: an account on which the deletion impairs brain development along a single dimension has to explain how adding a copy moves one outcome down while moving two others up. A developmental account accommodates it by positing distinct dosage-sensitive processes with opposite requirements, so what the dissociation refutes is not developmental accounts as a class but any version in which one quantity of developmental burden orders all three outcomes.

The compensation-ceiling model is constrained by it and accommodates it. Under Proposition 1, increased dosage of rate- and gain-setting genes raises intrinsic capacity, which is protective during the adolescent window when correction is rate-limiting and *harmful* during early construction, when developmental programs require accurately timed derepression rather than maximal throughput: excess microprocessor capacity silences targets that should be expressed. That is falsifiable in a specific way. It requires duplication carriers to exceed controls on *capacity with effort at or below control level*, which is the signature of raised intrinsic capacity rather than of recruited compensation, and not merely to sit opposite deletion carriers on a regulated output, which is all the existing dopamine data show (Rogdaki et al., 2023). Study 2 tests that stronger version and supplies the program's sharpest specificity comparison: a capacity measure relevant to psychosis protection should not track intellectual disability or autism severity in the same direction.

## 11 Falsification: Four Decisive Programs

A model that accommodates any observation explains nothing. The four programs below state what would refute this one, each as claim at risk, prediction, design and falsifying result.

*One rule for every contrast, and no composites.* Every primary contrast fixes a minimum meaningful effect, δ, and reports a 90% interval; the four outcomes it can return are defined in Supplementary Section S7.1, as is what counts as a carrier who remains well. Because the model predicts opposite directions for different quantities on different scales, a signed average cancels, so each quantity keeps its own endpoint and direction, and primary hypotheses are signed and challenge-evoked wherever the biology permits. Where the model predicts a *pattern*, global support requires every component contrast to meet its criterion, an intersection–union rule conservative in the direction of not claiming support. **Falsification is not the mirror image of that rule.** Failing to establish a conjunction is not evidence that any component is false. A component counts as evidence against only when its own upper bound lies below δ, and the model as a whole is refuted when at least one such bound lies below δ under *simultaneous* limits across the required contrasts. Simultaneity, rather than a majority vote, is what stops several components from manufacturing repeated chances to reject (Supplementary Section S7.3).

### 11.1 Study 1: The three-group compensation assay

**Claim at risk.** Compensatory effort is raised in carriers who remain well, it buys effective capacity, and the response is beneficial rather than merely correlated with being well (Proposition 4). The *core* form is the model's defining commitment; the *strong* form adds capacity above the control range and is tested separately.

**Prediction.** Four quantities, four endpoints, four directions, with one primary measure for each so that the decision rule applies to a named contrast rather than a family. *Demand*, maintenance component: basal respiration under controlled workload is **higher** in both

carrier groups than in controls. *Demand*, remodeling component: synaptic density before the elimination window is higher in carriers, measured where a surplus can exist, which means cortical organoids at a matched differentiation stage with mouse spine density as the cross-species anchor. A monolayer of reprogrammed neurons has no architecture to eliminate and cannot report this quantity whatever its respiration shows. Together these are the prediction the rest of the arithmetic depends on. *Effort*: resting PGC-1α is higher in carriers who remain well than in controls and than in carriers with psychosis, with PGC-1β, PPARα and PRKN secondary. *Capacity*: maximal respiration after substrate challenge is higher than in the psychosis group, and in the strong form higher than in controls. *Output*: presynaptic protein is at control level in absolute terms in carriers who remain well and below control conditional on transcript.

**Prediction, perturbation arm.** This arm, not the three-group contrast, is what Proposition 4 stands on. No observational contrast can show that a response is beneficial, since any variable correlated with clinical status produces one, and none can show it was *recruited*, since reprogramming erases acquired state and leaves a constitutive difference looking exactly like a spent one. The decisive test is perturbation inside protected-carrier cells: suppressing the controllers should degrade output under load, and more than in control cells; restoring them should recover it. The four controllers are fixed in advance as the definition of effort, so elevations elsewhere cannot be reclassified afterward as unsuccessful effort. The source demands that commitment: ERRα was elevated in both carrier groups relative to controls on the figure legend's reading and unchanged between carrier groups on the Results text's, and a definition fixed afterward could accommodate either (Li et al., 2021).

**Design.** Excitatory neurons, cortical organoids and a lineage-authenticated brain endothelial system from the three groups, at least two clones per donor, groups matched on age distribution. Derivation method is prespecified because it decides what the assay can see: directly converted neurons retain donor age-associated transcriptomic signatures that induced pluripotency erases (Mertens et al., 2015). The dosage and effort hypotheses are therefore tested in iPSC-derived neurons, the decline hypothesis in directly converted neurons from the same donors, and the remodeling component of demand in organoids. The primary intersection–union test runs in directly converted neurons, with the other systems as prespecified replications. Sample size is simulated for the named primary endpoints under stipulated planning effects, and reaches 93% at 40 donors per group for a planning effect of d = 0.8 (Supplementary Section S7.2 and S7.3). Fifty donors per group across three groups and two derivation routes is consortium-scale against the fourteen lines of the study it builds on, and is staged: 20 per group first, as a pilot estimating the variance components the full target depends on.

**Falsifying result.** Each contrast is judged by the rule above, so an interval spanning zero and δ leaves its claim undecided rather than refuted. The demand prediction fails if basal respiration in carriers is not above control level with an upper bound below δ, and its failure is the most consequential of all: without a demand excess, raised capacity gives carriers the *larger* margin

and the clinical premise of Section 1.2 collapses. The core form fails if the effort contrasts reach evidence against, not merely if they fail to reach support. The second half of Proposition 4 fails if effort is raised while capacity does not exceed the psychosis group; the strong form fails if capacity does not exceed controls while both carrier-group contrasts hold. Only the perturbation result separates this model from H5: if suppressing the controllers in protected-carrier cells does not degrade output under load more than in control cells, there is no recruited compensatory process to speak of.

### 11.2 Study 2: The reciprocal copy-number dose test

**Claim at risk.** Capacity is set by dosage, so the duplication raises it above the control range with no effort recruited, and the capacity that protects against schizophrenia is schizophrenia-specific (Propositions 1 and 6).

**Prediction and design.** On the Study 1 capacity endpoints, duplication carriers exceed controls *with effort at or below control level*. The joint position is the prediction, and it separates endowment from compensation: a well deletion carrier is also predicted above controls on capacity, but only with effort above them. Intrinsic capacity is the quantity predicted to be monotonic in copy number; effective capacity is not, because effort intervenes. The design is a three-arm comparison on the Study 1 endpoints, with autism and intellectual-disability phenotypes measured dimensionally (Supplementary Section S7.5): capacity should be associated with better psychosis outcomes and with equal or worse autism and intellectual-disability outcomes.

**Falsifying result.** The dosage–capacity link of Proposition 1 reaches evidence against if the duplication-versus-control capacity contrast has an upper bound below $\delta$; a contrast that merely fails to exclude zero leaves the link undecided. If duplication carriers exceed controls on capacity *and* on effort, they are compensating rather than endowed, and the quantity measured is not intrinsic capacity. The schizophrenia-specific reading fails if capacity is associated with lower adverse scores across psychosis, autism and intellectual disability alike, which would indicate a general developmental-burden measure.

### 11.3 Study 3: Is capacity consumed before emergence, and what restores the balance?

**Claim at risk.** Capacity declines within persons before symptoms emerge, and the decline is a cost of prior compensation rather than a property of age (Propositions 4 and 5). The first half, with Study 1, is the model's other indispensable claim. The second half is separable: a decline that precedes symptoms establishes temporal precedence but not consumption, since age-related change in regulatory expression, maturation or an illness process already under way would produce the same trajectory. The model therefore commits to something sharper, that *earlier effort predicts later capacity loss* once age and demand are in the model. If that fails, the word consumption is withdrawn while temporal precedence survives.

**Prediction.** (a) In carriers whose symptoms emerge, a validated compensation index declines within person beforehand, and before cognitive change. This is the indispensable one, and onset is where the model is properly exposed: stable capacity with rising demand would also produce a transition, so the model commits to capacity *falling* and not merely to the balance crossing. (b) Cumulative effort over the preceding interval predicts the magnitude of that loss, with age and demand in the model, which is the test that distinguishes consumption from age. (c) At remission the balance is restored by one of two identifiable routes, and which one is age-dependent: late in the window, developmental demand falls with capacity flat; earlier, either capacity recovers or an additional load falls (Section 9). (d) Whichever route operates, the *reserve* index recovers further than measures of the regulated variable. (e) The cognitive signature preceding emergence is disproportionately load-dependent.

**Design.** A multisite prospective cohort entered uniformly between ages 12 and 18 and followed to 25, with six-monthly symptom assessment, an annual biological battery and event-triggered sampling within eight weeks of any status change (Supplementary Section S7.7). The primary compensation index is peripheral bioenergetic capacity under challenge, with biogenesis transcripts as the effort term and basal consumption as the demand term, so that capacity and demand are measured separately rather than inferred from a single margin. It becomes primary only on meeting prespecified thresholds for reliability, for responsiveness to a challenge of known direction, and for correspondence between its change and change in a central measure.

**Falsifying result.** Compensation is a liability marker rather than a dynamic variable if carriers whose symptoms emerge show no within-person decline beforehand among those with adequately timed samples, and the indispensable dynamic claim then fails. It is a consequence rather than an antecedent if the index declines only after cognitive change or after onset. The consumption claim fails, while temporal precedence survives, if cumulative effort does not predict subsequent capacity loss with age and demand in the model. The balance account fails if a *transition* occurs with no measurable movement in either term. Fluctuation in severity without such movement does not count, since the model assigns severity to dopaminergic state (Section 8).

### 11.4 Study 4: What makes an intervention's benefit outlast it

**Claim at risk.** Durable benefit is produced by intervening inside the developmental window in which a regulator sets a circuit's trajectory, not by whether the target lies inside the deleted interval; durability is endpoint-specific within the same animal; and the *sign* of an intervention's effect is set by the direction in which the regulator deviates before treatment. The first two claims are shared with H5. Only the sign claim is distinctive, because only this model ties the direction of a treatment effect to a measurable pretreatment deviation, and it is the model's most consequential practical prediction.

**What the literature establishes.** Four studies gave a GSK3 inhibitor from postnatal day 7 and tested animals months later; Figure 4C places them on a common age axis and Supplementary Section S7.9 sets them out. Two nonselective courses produced benefit at three to five months and at about postnatal day 110 (Alvino et al., 2025; Tamura et al., 2016). The paralog-selective pair is more informative, because together they turn this model's own methodological prescription into a result. GSK3B-selective BRD3731 improved working memory in adult male mutants and *raised* ventral hippocampal (vHPC) to medial prefrontal (mPFC) theta coherence in them ($p = 0.048$), raised rather than restored, since coherence was not significantly reduced in mutants of either sex at baseline (Passecker et al., 2026). GSK3A-selective BRD0705 was null in that experiment — but the same group, in the same model and window, found it restored adult spatial working memory when the task was run under increased working-memory demand (Passecker et al., 2025). A compound that is null at baseline and effective under load is not a failed intervention; it is Proposition 2 arriving as pharmacology, and it is why every endpoint here is challenge-evoked wherever the biology permits. Durability is endpoint-specific within one experiment: in the animals whose adult memory was rescued, juvenile normalization of connectivity did not survive, adult hippocampal hypoconnectivity was unaffected, and sociability was not rescued at either age (Alvino et al., 2025).

**Mechanism of persistence.** The model owes one, because $R = C - D$ has no memory: if raising capacity is followed by the regulator returning toward its untreated state, nothing in the equation explains why benefit remains. The specified mechanism is developmental. Inside the window, the regulator sets the trajectory along which a circuit matures, and a circuit that has matured along a corrected trajectory is self-maintaining afterward; what persists is the structure, not the regulatory state that produced it.

Sex is where the sign claim meets its nearest existing test, and the fit has to be described exactly. BRD3731 improved working memory in male mutants, had no effect in female mutants, and *impaired* it in wild-type females, while *Gsk3b* expression was higher in male mutants than male wild types and lower in female mutants than female wild types (Passecker et al., 2026). The animals with reduced expression are therefore not the animals that were harmed. Read as a deviation rule rather than a level rule the pattern is informative: the inhibitor corrected an upward deviation and helped, and moved wild-type females away from their own set point and harmed them. But the comparison that would complete it, drug against vehicle in wild-type *males*, is not reported, nothing was tested within animals, and expression is not kinase activity, which was not measured (Supplementary Section S7.8).

**Prediction.** Four hypotheses, tested separately, with sex crossed throughout. (a) *Window*: benefit outlasting cessation follows dosing inside the window and not outside it, whatever the target. (b) *Endpoint specificity*: persistence differs across endpoints within the same animals, and is greater for endpoints still maturing during dosing. (c) *Sign*: the direction of effect is predicted by the pretreatment direction of the regulator's deviation, measured per animal. (d) *Mediation*: benefit is mediated by change in the regulated variable, with target class adding little once that change is in the model.

**Design.** A factorial experiment in LgDel/+ or Df(h22q11)/+ mice crossing target class with dosing window, the windows being pre-adolescent, peri-adolescent at the inflection, and post-adolescent, with sex crossed and each arm titrated to a prespecified fractional restoration of its proximal variable. Endpoints are chosen in pairs whose maturation windows differ demonstrably, since uniform persistence across endpoints that mature together would say nothing about specificity. Cessation must be real and engagement measured at outcome: none of the four studies above assayed target engagement months after dosing. The sign arm carries a measurement problem the design must solve rather than assume away, since an animal cannot be sampled for a regional brain transcript and then followed (Supplementary Section S7.8).

**Falsifying result.** The window claim fails if persistence after verified disengagement tracks target identity rather than dosing window, and in particular if late restoration of a deleted regulator outlasts disengagement while early action on a node outside the interval does not. Endpoint specificity fails if persistence is uniform across endpoints within animals. The sign claim fails if pretreatment regulator direction does not predict the direction of response, which would leave Proposition 2 without treatment-relevant content. Mediation fails if an intervention restores its variable with verified engagement and leaves the phenotype unchanged.

### 11.5 What would falsify the model as a whole

**Two claims are indispensable.** The inversion, in its core form: on effort, carriers who pass through the risk window without psychosis lie above controls and above carriers with psychosis, and suppressing that response degrades function under load (Study 1). And consumption: capacity declines within persons before symptoms emerge (Study 3). If either produces evidence against under the decision rule, the model should be abandoned rather than repaired.

What replaces it should be stated with the same care as the model itself. Evidence against those two claims rejects the specified form of H1 and leaves the specified form of H2 standing; it does not establish H2 against every alternative, since a compensatory process on a variable this program did not measure would remain compatible. That is why the measured quantities are prespecified and named. The honest statement of a negative result is that the compensation architecture, as specified and measured here, is not what distinguishes carriers who become psychotic.

**Four claims are distinctive**, and their failure leaves an ordered developmental account standing while collapsing this model into a neighbor: the strong form of the inversion (Study 1); the window and sign claims about intervention durability (Study 4); the dose extension (Study 2); and the biological counterpart of the symptom dissociation (Study 3), whose clinical form already has support (Tang et al., 2017).

**Three claims are accessory:** which quantity dominates; the interchangeability of two regulator-restoring routes; and the identity of the executor of synaptic elimination. The barrier and immune limb is not among them, and nor is it indispensable. It supplies the maintenance component of the demand excess (Section 1.2), so its failure costs the model one of two independent grounds for that excess and leaves the remodeling component standing; it is load-bearing for a claim that does not rest on it alone.

**What would not count.** Six results that would not count against the model are listed in Supplementary Section S7.10, among them any null on resting measures without challenge-evoked ones, any null pooled across puberty on a measure known to reverse sign, and an upper bound below δ reported as evidence that compensation does not exist when what it rejects is an effect of at least δ.

## 12 Scope

Five boundaries govern what the model claims, and Supplementary Section S6 develops them. The syndrome licenses a claim about process, not sequence: the deletion engages the same biology as distributed schizophrenia liability (Cheng et al., 2026; Cleynen et al., 2021; Davies et al., 2020; Lin et al., 2023; Nehme et al., 2022), which does not make the two routes to illness the same. The compensation signature is measurable outside the deletion (Das et al., 2022), but as a two-group finding rather than a replication of the three-group inversion. The model specifies one component of synaptic accounts of idiopathic schizophrenia (Howes & Onwordi, 2023; Moore, 2026). The programs test transitions in psychosis-spectrum status, not whether the state entered is specifically schizophrenia (Schneider et al., 2014). And a cellular model of a consumed state is constrained by its derivation.

## 13 Synthesis

The 22q11.2 deletion removes one copy of a set of genes that, where their neural phenotypes are known, are dosage-limiting for a rate, a gain or a throughput. The model holds that losing one copy narrows the range over which a controlled variable can be corrected; that the resulting instability of set points is what the syndrome shows, most clearly in a connectivity phenotype in surplus before puberty and in deficit after it in both species; that every carrier compensates, in six distinct and separately predicted quantities; and that psychosis occurs where the demand of adolescent remodeling crosses a capacity falling because the regulators the deletion constrains decline with age. The clock is a regulatory variable, not a program. The state is a balance, not a scar.

Separating the quantities is what makes the model refutable, and also what shows where it is most exposed. That a carrier who maintains output from lowered dosage is expending effort follows from the structure. That the effort carries capacity above the *control* range does not; it is a further bet, and the program that tests it is built so that losing the bet costs the model its

sharpest claim without taking the architecture down. Capacity declining before onset is indispensable, because a compensation index that never moves within a person is a liability marker with a new name.

The model's first demonstration is twenty years old and two genes wide: frontal *Comt* upregulated as a homeostatic response to *Prodh* loss, with carriers hemizygous for both, so that the locus impairs synaptic function and the compensatory response to it together (Paterlini et al., 2005). The most recent is narrower still and points the same way. A GSK3B-selective inhibitor given from postnatal day 7 to 27 improves working memory and raises prefrontal–hippocampal synchrony in adult male deletion mice, does nothing in female mutants and impairs wild-type females, in a line where *Gsk3b* expression deviates from wild type in opposite directions by sex; its GSK3A-selective counterpart is null at baseline and effective under increased load (Passecker et al., 2025, 2026). A regulator deviating in opposite directions, an intervention that helps where it opposes a deviation and harms where it creates one, and a benefit visible only when the circuit is pushed: three of this model's commitments arriving as pharmacology, though not yet as a test of them, since no animal's own pretreatment level predicted its own response. What it implies is a treatment principle rather than a treatment — measure the direction of the deviation before pushing on it, and measure the effect under load.

The value of this syndrome has never been that it is a window onto mechanism; there is no shortage of mechanism. Its value is that it holds the lesion fixed and lets the outcome vary, which makes the question of why outcome varies answerable, and answerable means refutable.

## Transparency and Openness

*Generative artificial intelligence.* The author used Claude Opus 4.8, Claude Fable 5.1, GPT-5.5 Pro Extended, and Grok 4.3 to prepare and revise drafts and for proofreading. The author reviewed and edited all content and takes full responsibility for it. No AI tool was used to generate or analyze empirical data for this theoretical article.

*Data and materials.* This article reports no new empirical data. Every quantitative value cited is taken from the published source indicated, and the simulation inputs and outputs for the cohort projections in Supplementary Section S7.7 are stated there in full so that they can be reproduced.

*Declaration of competing interest.* The author declares no competing interests.

*Funding.* This work received no specific grant from any funding agency.

## References

Alvino, F. G., Gini, S., Minetti, A., Pagani, M., Sastre-Yagüe, D., Barsotti, N., De Guzman, E., Schleifer, C., Stuefer, A., Kushan, L., Montani, C., Galbusera, A., Papaleo, F., Kates, W. R., Murphy, D., Lombardo, M. V., Pasqualetti, M., Bearden, C. E., & Gozzi, A. (2025). Synaptic-dependent developmental dysconnectivity in 22q11.2 deletion syndrome. *Science Advances, 11*(11), eadq2807. https://doi.org/10.1126/sciadv.adq2807

Bagautdinova, J., Zöller, D., Schaer, M., Padula, M. C., Mancini, V., Schneider, M., & Eliez, S. (2021). Altered cortical thickness development in 22q11.2 deletion syndrome and association with psychotic symptoms. *Molecular Psychiatry, 26*(12), 7671–7678. https://doi.org/10.1038/s41380-021-01209-8

Bassett, A. S., Lowther, C., Merico, D., Costain, G., Chow, E. W. C., van Amelsvoort, T., McDonald-McGinn, D., Gur, R. E., Swillen, A., Van den Bree, M., Murphy, K., Gothelf, D., Bearden, C. E., Eliez, S., Kates, W., Philip, N., Sashi, V., Campbell, L., Vorstman, J., … Marshall, C. R., & International 22q11.2DS Brain and Behavior Consortium. (2017). Rare genome-wide copy number variation and expression of schizophrenia in 22q11.2 deletion syndrome. *American Journal of Psychiatry, 174*(11), 1054–1063. https://doi.org/10.1176/appi.ajp.2017.16121417

Castellani, G., Ciampoli, M., Benedetti, A., Ferretti, V., Trigilio, G., Barcik, W., Busnelli, M., Contarini, G., Paolini, C., Devroye, C., Rodriguez Aburto, M., Cucinelli, A., Antonelli, F., Maltese, F., Braccia, C., Pacinelli, G., Managò, F., Rodríguez-Gimeno, A., Mazzarella, M. A., … Papaleo, F. (2025). Oxytocin seals the blood–brain barrier, improving 22q11.2 deletion syndrome trajectories. *Brain, 148*(9), 3184–3198. https://doi.org/10.1093/brain/awaf112

Cheng, M., Yin, Y., Engchuan, W., Heung, T., International 22q11.2 Brain Behavior Consortium, Morrow, B. E., Bassett, A. S., & Yuen, R. K. C. (2026). Genome-wide tandem repeat expansions modify schizophrenia risk in the presence of a 22q11.2 deletion. *Molecular Psychiatry, 31*, 4934–4946. https://doi.org/10.1038/s41380-026-03574-8

Chun, S., Du, F., Westmoreland, J. J., Han, S. B., Wang, Y.-D., Eddins, D., Bayazitov, I. T., Devaraju, P., Yu, J., Mellado Lagarde, M. M., Anderson, K., & Zakharenko, S. S. (2017). Thalamic miR-338-3p mediates auditory thalamocortical disruption and its late onset in models of 22q11.2 microdeletion. *Nature Medicine, 23*(1), 39–48. https://doi.org/10.1038/nm.4240

Chun, S., Westmoreland, J. J., Bayazitov, I. T., Eddins, D., Pani, A. K., Smeyne, R. J., Yu, J., Blundon, J. A., & Zakharenko, S. S. (2014). Specific disruption of thalamic inputs to the auditory cortex in schizophrenia models. *Science, 344*(6188), 1178–1182. https://doi.org/10.1126/science.1253895

Cleynen, I., Engchuan, W., Hestand, M. S., Heung, T., Holleman, A. M., Johnston, H. R., Monfeuga, T., McDonald-McGinn, D. M., Gur, R. E., Morrow, B. E., Swillen, A., Vorstman, J. A. S., Bearden, C. E., Chow, E. W. C., van den Bree, M., Emanuel, B. S., Vermeesch, J. R., Warren, S. T., Owen, M. J., … Bassett, A. S. (2021). Genetic contributors to risk of schizophrenia in the presence of a 22q11.2 deletion. *Molecular Psychiatry, 26*(8), 4496–4510. https://doi.org/10.1038/s41380-020-0654-3

Crockett, A. M., Ryan, S. K., Hernandez Vásquez, A., Canning, C., Kanyuch, N., Kebir, H., Ceja, G., Gesualdi, J., Zackai, E., McDonald-McGinn, D., Viaene, A., Kapoor, R., Benallegue, N., Gur, R., Anderson, S. A., & Alvarez, J. I. (2021). Disruption of the blood–brain barrier in 22q11.2 deletion syndrome. *Brain, 144*(5), 1351–1360. https://doi.org/10.1093/brain/awab055

Das, S. C., Hjelm, B. E., Rollins, B. L., Sequeira, A., Morgan, L., Omidsalar, A. A., Schatzberg, A. F., Barchas, J. D., Lee, F. S., Myers, R. M., Watson, S. J., Akil, H., Bunney, W. E., & Vawter, M. P. (2022). Mitochondria DNA copy number, mitochondria DNA total somatic deletions, Complex I activity, synapse number, and synaptic mitochondria number are altered in schizophrenia and bipolar disorder. *Translational Psychiatry, 12*(1), 353. https://doi.org/10.1038/s41398-022-02127-1

Davies, R. W., Fiksinski, A. M., Breetvelt, E. J., Williams, N. M., Hooper, S. R., Monfeuga, T., Bassett, A. S., Owen, M. J., Gur, R. E., Morrow, B. E., McDonald-McGinn, D. M., Swillen, A., Chow, E. W. C., van den Bree, M., Emanuel, B. S., Vermeesch, J. R., van Amelsvoort, T., Arango, C., Armando, M., … Vorstman, J. A. S. (2020). Using common genetic variation to examine phenotypic expression and risk prediction in 22q11.2 deletion syndrome. *Nature Medicine, 26*(12), 1912–1918. https://doi.org/10.1038/s41591-020-1103-1

Devaraju, P., Yu, J., Eddins, D., Mellado-Lagarde, M. M., Earls, L. R., Westmoreland, J. J., Quarato, G., Green, D. R., & Zakharenko, S. S. (2017). Haploinsufficiency of the 22q11.2 microdeletion gene *Mrpl40* disrupts short-term synaptic plasticity and working memory through dysregulation of mitochondrial calcium. *Molecular Psychiatry, 22*(9), 1313–1326. https://doi.org/10.1038/mp.2016.75

Earls, L. R., Fricke, R. G., Yu, J., Berry, R. B., Baldwin, L. T., & Zakharenko, S. S. (2012). Age-dependent microRNA control of synaptic plasticity in 22q11 deletion syndrome and schizophrenia. *The Journal of Neuroscience, 32*(41), 14132–14144. https://doi.org/10.1523/JNEUROSCI.1312-12.2012

Fernandez, A., Meechan, D. W., Karpinski, B. A., Paronett, E. M., Bryan, C. A., Rutz, H. L., Radin, E. A., Lubin, N., Bonner, E. R., Popratiloff, A., Rothblat, L. A., Maynard, T. M., & LaMantia, A.-S. (2019). Mitochondrial dysfunction leads to cortical under-connectivity and cognitive impairment. *Neuron, 102*(6), 1127–1142. https://doi.org/10.1016/j.neuron.2019.04.013

Greene, C., Kealy, J., Humphries, M. M., Gong, Y., Hou, J., Hudson, N., Cassidy, L. M., Martiniano, R., Shashi, V., Hooper, S. R., Grant, G. A., Kenna, P. F., Norris, K., Callaghan, C. K., Islam, M. N., O'Mara, S. M., Najda, Z., Campbell, S. G., Pachter, J. S., … Campbell, M. (2018). Dose-dependent expression of claudin-5 is a modifying factor in schizophrenia. *Molecular Psychiatry, 23*(11), 2156–2166. https://doi.org/10.1038/mp.2017.156

Guo, Y., Singh, L. N., Zhu, Y., Gur, R. E., Resnick, A., Anderson, S. A., & Alvarez, J. I. (2020). Association of a functional Claudin-5 variant with schizophrenia in female patients with the 22q11.2 deletion syndrome. *Schizophrenia Research, 215*, 451–452. https://doi.org/10.1016/j.schres.2019.09.014

Gur, R. E., McDonald-McGinn, D. M., Moore, T. M., Gallagher, R. S., McClellan, E., White, L., Ruparel, K., Hillman, N., Crowley, T. B., McGinn, D. E., Zackai, E., Emanuel, B. S., Calkins, M. E., Roalf, D. R., & Gur, R. C. (2023). Psychosis spectrum features, neurocognition and functioning in a longitudinal study of youth with 22q11.2 deletion syndrome. *Psychological Medicine, 53*(14), 6763–6772. https://doi.org/10.1017/S0033291723000259

Hiroi, N., Hiramoto, T., Harper, K. M., Suzuki, G., & Boku, S. (2012). Mouse models of 22q11.2-associated autism spectrum disorder. *Autism Open Access, S1*, 001. https://doi.org/10.4172/2165-7890.S1-001

Howes, O. D., & Onwordi, E. C. (2023). The synaptic hypothesis of schizophrenia version III: A master mechanism. *Molecular Psychiatry, 28*(5), 1843–1856. https://doi.org/10.1038/s41380-023-02043-w

Khan, T. A., Revah, O., Gordon, A., Yoon, S.-J., Krawisz, A. K., Goold, C., Sun, Y., Kim, C. H., Tian, Y., Li, M.-Y., Schaepe, J. M., Ikeda, K., Amin, N. D., Sakai, N., Yazawa, M., Kushan, L., Nishino, S., Porteus, M. H., Rapoport, J. L., … Pașca, S. P. (2020). Neuronal defects in a human cellular model of 22q11.2 deletion syndrome. *Nature Medicine, 26*(12), 1888–1898. https://doi.org/10.1038/s41591-020-1043-9

Li, J., Ryan, S. K., Deboer, E., Cook, K., Fitzgerald, S., Lachman, H. M., Wallace, D. C., Goldberg, E. M., & Anderson, S. A. (2019). Mitochondrial deficits in human iPSC-derived neurons from patients with 22q11.2 deletion syndrome and schizophrenia. *Translational Psychiatry, 9*(1), 302. https://doi.org/10.1038/s41398-019-0643-y

Li, J., Tran, O. T., Crowley, T. B., Moore, T. M., Zackai, E. H., Emanuel, B. S., McDonald-McGinn, D. M., Gur, R. E., Wallace, D. C., & Anderson, S. A. (2021). Association of mitochondrial biogenesis with variable penetrance of schizophrenia. *JAMA Psychiatry, 78*(8), 911–921. https://doi.org/10.1001/jamapsychiatry.2021.0762

Lin, J.-R., Zhao, Y., Jabalameli, M. R., Nguyen, N., Mitra, J., International 22q11.2DS Brain and Behavior Consortium, Swillen, A., Vorstman, J. A. S., Chow, E. W. C., van den Bree, M., Emanuel, B. S., Vermeesch, J. R., Owen, M. J., Williams, N. M., Bassett, A. S., McDonald-McGinn, D. M., Gur, R. E., Bearden, C. E., Morrow, B. E., & Zhang, Z. D. (2023). Rare coding variants as risk modifiers of the 22q11.2 deletion implicate postnatal cortical development in syndromic schizophrenia. *Molecular Psychiatry, 28*(5), 2071–2080. https://doi.org/10.1038/s41380-023-02009-y

Lu, T. M., Houghton, S., Magdeldin, T., Barcia Durán, J. G., Minotti, A. P., Snead, A., Sproul, A., Nguyen, D.-H. T., Xiang, J., Fine, H. A., Rosenwaks, Z., Studer, L., Rafii, S., Agalliu, D., Redmond, D., & Lis, R. (2021). Pluripotent stem cell-derived epithelium misidentified as brain microvascular endothelium requires ETS factors to acquire vascular fate. *Proceedings of the National Academy of Sciences, 118*(8), e2016950118. https://doi.org/10.1073/pnas.2016950118

Mancini, V., Rogdaki, M., Jauhar, S., Moretto, M., Veronese, M., Turkheimer, F., Howes, O. D., & McCutcheon, R. A. (2026). Striatal dopaminergic function and cortical functional connectivity in 22q11.2 deletion syndrome: An integrative multimodal 18F-DOPA PET and magnetic resonance imaging study. *Molecular Psychiatry*. Advance online publication. https://doi.org/10.1038/s41380-026-03839-2

McDonald-McGinn, D. M., Sullivan, K. E., Marino, B., Philip, N., Swillen, A., Vorstman, J. A. S., Zackai, E. H., Emanuel, B. S., Vermeesch, J. R., Morrow, B. E., Scambler, P. J., & Bassett, A. S. (2015). 22q11.2 deletion syndrome. *Nature Reviews Disease Primers, 1*, 15071. https://doi.org/10.1038/nrdp.2015.71

Mekori-Domachevsky, E., Taler, M., Shoenfeld, Y., Gurevich, M., Sonis, P., Weisman, O., Weizman, A., & Gothelf, D. (2017). Elevated proinflammatory markers in 22q11.2 deletion syndrome are associated with psychosis and cognitive deficits. *Journal of Clinical Psychiatry, 78*(9), e1219–e1225. https://doi.org/10.4088/JCP.16m11207

Mertens, J., Paquola, A. C. M., Ku, M., Hatch, E., Böhnke, L., Ladjevardi, S., McGrath, S., Campbell, B., Lee, H., Herdy, J. R., Gonçalves, J. T., Toda, T., Kim, Y., Winkler, J., Yao, J., Hetzer, M. W., & Gage, F. H. (2015). Directly reprogrammed human neurons retain aging-associated transcriptomic signatures and reveal age-related nucleocytoplasmic defects. *Cell Stem Cell, 17*(6), 705–718. https://doi.org/10.1016/j.stem.2015.09.001

Moore, T. M. (2026). *Schizophrenia as ordered synaptic fragility* [Manuscript under review].

Murphy, K. C., Jones, L. A., & Owen, M. J. (1999). High rates of schizophrenia in adults with velo-cardio-facial syndrome. *Archives of General Psychiatry, 56*(10), 940–945. https://doi.org/10.1001/archpsyc.56.10.940

Nehme, R., Pietiläinen, O., Artomov, M., Tegtmeyer, M., Valakh, V., Lehtonen, L., Bell, C., Singh, T., Trehan, A., Sherwood, J., Manning, D., Peirent, E., Malik, R., Guss, E. J., Hawes, D., Beccard, A., Bara, A. M., Hazelbaker, D. Z., Zuccaro, E., … Eggan, K. (2022). The 22q11.2 region regulates presynaptic gene-products linked to schizophrenia. *Nature Communications, 13*(1), 3690. https://doi.org/10.1038/s41467-022-31436-8

O'Hora, K. P., Amir, C. M., Chiem, E., Schleifer, C. H., Grigoryan, V., Kushan-Wells, L., Chiang, J. J., Cole, S., Irwin, M. R., & Bearden, C. E. (2024). Differential inflammatory profiles in carriers of reciprocal 22q11.2 copy number variants. *Psychoneuroendocrinology, 169*, 107135. https://doi.org/10.1016/j.psyneuen.2024.107135

Passecker, J., Aloimonos, C. M., Dagunts, A., Wagner, F. F., Kupferschmidt, D. A., Gogos, J., & Gordon, J. A. (2025). Developmental selective GSK3α inhibition rescues working memory deficits in a mouse model of schizophrenia predisposition. *Complex Psychiatry, 11*(1), 131–141. https://doi.org/10.1159/000547800

Passecker, J., Chang, C.-Y., Dagunts, A., Aloimonos, C. M., Leitner, L., Petryk, A., Wagner, F. F., Myroshnychenko, M. V., Kupferschmidt, D. A., Gogos, J. A., & Gordon, J. A. (2026). Divergent transcriptomic pathways underlie sex-biased cognitive rescue by developmental GSK3B inhibition in a mouse model of 22q11.2 deletion syndrome. *Translational Psychiatry, 16*(1), 415. https://doi.org/10.1038/s41398-026-04108-0

Paterlini, M., Zakharenko, S. S., Lai, W.-S., Qin, J., Zhang, H., Mukai, J., Westphal, K. G. C., Olivier, B., Sulzer, D., Pavlidis, P., Siegelbaum, S. A., Karayiorgou, M., & Gogos, J. A. (2005). Transcriptional and behavioral interaction between 22q11.2 orthologs modulates schizophrenia-related phenotypes in mice. *Nature Neuroscience, 8*(11), 1586–1594. https://doi.org/10.1038/nn1562

Rao, S. B., Sun, Z., Brundu, F., Chen, Y., Sun, Y., Zhu, H., Shprintsen, R. J., Tomer, R., Rabadan, R., Leong, K. W., Markx, S., Kushner, S. A., Xu, B., & Gogos, J. A. (2025). Aberrant pace of cortical neuron development in brain organoids from patients with 22q11.2 deletion syndrome-associated schizophrenia. *Nature Communications, 16*(1), 6986. https://doi.org/10.1038/s41467-025-62187-x

Rees, E., Kirov, G., Sanders, A., Walters, J. T. R., Chambert, K. D., Shi, J., Szatkiewicz, J., O'Dushlaine, C., Richards, A. L., Green, E. K., Jones, I., Davies, G., Legge, S. E., Moran, J. L., Pato, C., Pato, M., Genovese, G., Levinson, D., Duan, J., … Owen, M. J. (2014). Evidence that duplications of 22q11.2 protect against schizophrenia. *Molecular Psychiatry, 19*(1), 37–40. https://doi.org/10.1038/mp.2013.156

Roberts, R. C., Barksdale, K. A., Roche, J. K., & Lahti, A. C. (2015). Decreased synaptic and mitochondrial density in the postmortem anterior cingulate cortex in schizophrenia. *Schizophrenia Research, 168*(1–2), 543–553. https://doi.org/10.1016/j.schres.2015.07.016

Rogdaki, M., Devroye, C., Ciampoli, M., Veronese, M., Ashok, A. H., McCutcheon, R. A., Jauhar, S., Bonoldi, I., Gudbrandsen, M., Daly, E., van Amelsvoort, T., Van Den Bree, M., Owen, M. J., Turkheimer, F., Papaleo, F., & Howes, O. D. (2023). Striatal dopaminergic alterations in individuals with copy number variants at the 22q11.2 genetic locus and their implications for psychosis risk: A [18F]-DOPA PET study. *Molecular Psychiatry, 28*(5), 1995–2006. https://doi.org/10.1038/s41380-021-01108-y

Schneider, M., Debbané, M., Bassett, A. S., Chow, E. W. C., Fung, W. L. A., van den Bree, M., Owen, M., Murphy, K. C., Niarchou, M., Kates, W. R., Antshel, K. M., Fremont, W., McDonald-McGinn, D. M., Gur, R. E., Zackai, E. H., Vorstman, J., Duijff, S. N., Klaassen, P. W. J., Swillen, A., … International Consortium on Brain and Behavior in 22q11.2 Deletion Syndrome. (2014). Psychiatric disorders from childhood to adulthood in 22q11.2 deletion syndrome: Results from the International Consortium on Brain and Behavior in 22q11.2 Deletion Syndrome. *American Journal of Psychiatry, 171*(6), 627–639. https://doi.org/10.1176/appi.ajp.2013.13070864

Shin, D., Kim, C. N., Ross, J., Hennick, K. M., Wu, S.-R., Paranjape, N., Leonard, R., Wang, J. C., Keefe, M. G., Pavlovic, B. J., Donohue, K. C., Moreau, C., Wigdor, E. M., Larson, H. H., Allen, D. E., Cadwell, C. R., Bhaduri, A., Popova, G., Bearden, C. E., … Nowakowski, T. J. (2024). Thalamocortical organoids enable in vitro modeling of 22q11.2 microdeletion associated with neuropsychiatric disorders. *Cell Stem Cell, 31*(3), 421–432. https://doi.org/10.1016/j.stem.2024.01.010

Sigurdsson, T., Stark, K. L., Karayiorgou, M., Gogos, J. A., & Gordon, J. A. (2010). Impaired hippocampal–prefrontal synchrony in a genetic mouse model of schizophrenia. *Nature, 464*(7289), 763–767. https://doi.org/10.1038/nature08855

Stark, K. L., Xu, B., Bagchi, A., Lai, W.-S., Liu, H., Hsu, R., Wan, X., Pavlidis, P., Mills, A. A., Karayiorgou, M., & Gogos, J. A. (2008). Altered brain microRNA biogenesis contributes to phenotypic deficits in a 22q11-deletion mouse model. *Nature Genetics, 40*(6), 751–760. https://doi.org/10.1038/ng.138

Sun, D., Ching, C. R. K., Lin, A., Forsyth, J. K., Kushan, L., Vajdi, A., Jalbrzikowski, M., Hansen, L., Villalon-Reina, J. E., Qu, X., Jonas, R. K., van Amelsvoort, T., Bakker, G., Kates, W. R., Antshel, K. M., Fremont, W., Campbell, L. E., McCabe, K. L., Daly, E., … Bearden, C. E. (2020). Large-scale mapping of cortical alterations in 22q11.2 deletion syndrome: Convergence with idiopathic psychosis and effects of deletion size. *Molecular Psychiatry, 25*(8), 1822–1834. https://doi.org/10.1038/s41380-018-0078-5

Tamura, M., Mukai, J., Gordon, J. A., & Gogos, J. A. (2016). Developmental inhibition of Gsk3 rescues behavioral and neurophysiological deficits in a mouse model of schizophrenia predisposition. *Neuron, 89*(5), 1100–1109. https://doi.org/10.1016/j.neuron.2016.01.025

Tang, S. X., Moore, T. M., Calkins, M. E., Yi, J. J., McDonald-McGinn, D. M., Zackai, E. H., Emanuel, B. S., Gur, R. C., & Gur, R. E. (2017). Emergent, remitted and persistent psychosis-spectrum symptoms in 22q11.2 deletion syndrome. *Translational Psychiatry, 7*(7), e1180. https://doi.org/10.1038/tp.2017.157

Vergaelen, E., Schiweck, C., Van Steeland, K., Counotte, J., Veling, W., Swillen, A., Drexhage, H., & Claes, S. (2018). A pilot study on immuno-psychiatry in 22q11.2 deletion syndrome: A role for Th17 cells in psychosis? *Brain, Behavior, and Immunity, 70*, 88–95. https://doi.org/10.1016/j.bbi.2018.03.022

Vorstman, J. A. S., Breetvelt, E. J., Duijff, S. N., Eliez, S., Schneider, M., Jalbrzikowski, M., Armando, M., Vicari, S., Shashi, V., Hooper, S. R., Chow, E. W. C., Fung, W. L. A., Butcher, N. J., Young, D. A., McDonald-McGinn, D. M., Vogels, A., van Amelsvoort, T., Gothelf, D., Weinberger, R., … International Consortium on Brain and Behavior in 22q11.2 Deletion Syndrome. (2015). Cognitive decline preceding the onset of psychosis in patients with 22q11.2 deletion syndrome. *JAMA Psychiatry, 72*(4), 377–385. https://doi.org/10.1001/jamapsychiatry.2014.2671

Xu, B., Hsu, P.-K., Stark, K. L., Karayiorgou, M., & Gogos, J. A. (2013). Derepression of a neuronal inhibitor due to miRNA dysregulation in a schizophrenia-related microdeletion. *Cell, 152*(1–2), 262–275. https://doi.org/10.1016/j.cell.2012.11.052

# Supplemental Material

## Compensation Failure as the Mechanism of Psychosis in 22q11.2 Deletion Syndrome: A Falsifiable Model

Section numbers in the form S*n* are in this supplemental material; section numbers without the S, Tables 1–4 and Figures 1–4 are in the main text. Works cited here are listed in the Supplementary References at the end.


| | |
|---|---|
| S1 | How Evidence Was Selected and Weighted, and the Full Evidence Matrix |
| S2 | The Deleted Genes, Gene by Gene |
| S3 | The Bidirectionality Catalogue and the Circuit-Level Expression |
| S4 | What the Modifier Literature Says About the Character of the Modifiers |
| S5 | The Barrier and Immune Limb |
| S6 | Scope and the Extension to Idiopathic Psychosis |
| S7 | Design Specifications for the Four Falsification Programs |
| | Supplementary Figure |
| | Supplementary References |

# S1 How Evidence Was Selected and Weighted, and the Full Evidence Matrix

## S1.1 Selection and weighting

This is a theory-building narrative synthesis rather than a systematic review. Sources were chosen to represent foundational formulations, methodologically decisive studies, causal or interventional evidence, major replications, and findings that threaten the model. Human evidence outranks model-system evidence for claims about the human sequence; within human evidence, intervention outranks within-person longitudinal measurement, which outranks cross-sectional comparison in living carriers, which outranks postmortem tissue; within model systems, controlled intervention outranks observation. Within a design, larger, preregistered and replicated studies outrank smaller discovery samples.

One additional criterion, specific to this syndrome, is applied throughout and recorded explicitly in Table S1: whether the design compared carriers by psychosis status. A study comparing carriers with schizophrenia to healthy controls is marked as uninformative for penetrance regardless of its quality, because no analysis of such data can separate the deletion from the illness or from its treatment. Such a study is not thereby irrelevant: a phenotype present in every carrier may be the necessary background on which the penetrance variable acts. The filter distinguishes mechanisms of background vulnerability from mechanisms of variation in outcome, and the model is a model of the latter.

Negative and discordant findings were sought for every load-bearing link. Four are treated as serious rather than incidental: the absence of a psychosis-status difference in the calcium phenotype (Khan et al., 2020); the absence of a functional-connectivity relationship with subclinical symptoms in carriers, in a study that found a robust connectivity–dopamine relationship in the same participants (Mancini et al., 2026); the finding that cortical surface area, the measure most strongly separating carriers from controls, does not separate carriers with psychosis from those without (Sun et al., 2020); and the failure of developmental GSK3 inhibition to prevent adult hippocampal hypoconnectivity despite normalizing the juvenile phenotype it was given to correct (Alvino et al., 2025).

Two arrived with the immune literature. Carrier-versus-control elevations of IL-6, CRP and TNFα reported in one sample (Mekori-Domachevsky et al., 2017) were absent in a study with a larger total sample but slightly fewer deletion carriers: 166 participants of whom 45 carried the deletion, against 79 of whom 49 did (O'Hora et al., 2024). And a claudin-5 variant associated with schizophrenia in a small carrier cohort (Greene et al., 2018) was not associated among 490 (Guo et al., 2020).

A third cuts directly against a row of Table 1. The same study found IL-8 elevated specifically in *duplication* carriers relative to controls (O'Hora et al., 2024), while this model treats immune load as a demand term and predicts duplication demand at or below control level. Two things are worth separating before the finding is counted either way. Peripheral cytokine

concentration is not load delivered to the brain, and the quantity in the model is the latter; duplication carriers have an additional copy of *CLDN5*, so on this model's own logic their barrier should be *tighter* than a control's, and an elevated peripheral signal need not cross it. That is a reconciliation and not a result, and it converts the discordance into a measurement: the prediction is that peripheral and central immune load dissociate by copy number, with barrier permeability measured alongside the cytokines rather than inferred from them. If duplication carriers show elevated central load, the demand row for that group is wrong.

A fourth is a discordance between two papers from one group, and resolving it supplies a finding the model had not claimed. A GSK3α-selective inhibitor had no significant behavioral effect in one experiment (Passecker et al., 2026) and restored adult spatial working memory in the same model on the same schedule in another, where the task was run under increased working-memory demand (Passecker et al., 2025). Read together, the compound is null at baseline and effective under load, which is the signature Proposition 2 predicts and the reason challenge-evoked measures are primary throughout Section 11.

### S1.2 Four tiers of causal evidence

Claims that mechanism A contributes to psychosis in this syndrome are graded at four tiers. Tier 1, presence: A is abnormal in carriers, or in carriers with psychosis. Tier 2, temporal precedence: within persons, change in A precedes the outcome. Tier 3, mediation or intervention: manipulating A changes the outcome, or the effect runs demonstrably through A under the assumptions mediation requires. Tier 4, necessity: removing A abolishes the outcome. Explaining more of the outcome than a rival does is comparative explanatory importance rather than necessity, and is recorded at Tier 3, not here.

Three rules keep the grading honest. Tier 1 evidence from a carriers-versus-controls design is recorded as Tier 1 for the deletion, not for penetrance, and the distinction is carried in a separate column rather than blurred into a strength rating. Precedence relative to clinical onset is recorded separately from precedence between biological nodes. And the measured outcome is recorded with the tier: rescue of a downstream synaptic phenotype by restoring a microRNA is Tier 3 evidence about that phenotype and not about progenitor developmental tempo, and causal evidence for a circuit phenotype in a mouse is not evidence of necessity for human psychosis.

Tiers are reported separately for human evidence and for model systems. An intervention in a deletion mouse or a patient-derived culture reaches Tier 3 for a conserved component mechanism, not for the human sequence and not for penetrance. The Df(16)A, LgDel and Df(h22q11) lines are bred to fixed backgrounds; a restricted background does not guarantee complete phenotypic penetrance within strain, but these lines do not model human clinical penetrance, and they are strong tools for Propositions 1, 2, 3, 5 and 6 and nearly silent on Proposition 4 except where background is deliberately varied, which is a model of modifier effects rather than of compensation (Hiroi et al., 2012).

**Table S1** *Evidence matrix for the principal claims, graded by the highest tier reached, with explicit recording of whether the cited design compared carriers by psychosis status*

| Claim | Human evidence: highest tier (strength) | Model-system evidence: highest tier (strength) | Within-carrier | Principal contradictory or null findings |
|---|---|---|---|---|
| **1. Deleted genes act as dosage-sensitive regulators of tempo, throughput, redox tone and trafficking (Prop. 1)** | Tier 1, strong: locus-wide transcript reduction with non-proportional effects; 89% of differentially expressed genes lie outside the deletion (Nehme et al., 2022); miR-185 falls further than hemizygosity predicts (Khan et al., 2020; Xu et al., 2013) | Tier 3, strong: *Dgcr8* hemizygosity accounts for the locus-level miRNA biogenesis defect (Stark et al., 2008); single-gene manipulation reproduces and reverses locus-level phenotypes (*Dgcr8*, *Mirta22*, *Mir338*, *Mrpl40*, *Txnrd2*) (Chun et al., 2017; Earls et al., 2012; Fernandez et al., 2019; Li et al., 2019; Xu et al., 2013); *Comt* upregulation compensates for *Prodh* loss and COMT inhibition unmasks deficits (Paterlini et al., 2005) | No | Deletion-versus-control designs. Regulator classification is interpretive and not a quantified enrichment; categories overlap, since enzymes and transporters both implement functions and set their rates; *TBX1* and other patterning genes do not fit |
| **2. Phenotypes are bidirectional and reverse sign across development (Prop. 2)** | Tier 1, moderate: thicker cortex with reduced surface area (Sun et al., 2020); upregulated synaptic transcripts with reduced presynaptic proteins (Nehme et al., 2022); global fMRI hyperconnectivity before puberty giving way to hippocampal and temporal hypoconnectivity after it, cross-sectionally with puberty inferred from age (Alvino et al., 2025) | Tier 1–3, strong: longitudinal hyper- to hypoconnectivity reconfiguration in the same LgDel mice; prefrontal spine density in surplus as juveniles and at wild-type level as adults, hippocampal density in surplus as juveniles and in deficit as adults, in separate animals (Alvino et al., 2025); increased hippocampal LTP (Earls et al., 2012); thalamocortical axon overgrowth (Shin et al., 2024); greater spontaneous firing with smaller evoked calcium transients (Khan et al., 2020) | No | Bidirectionality is also compatible with heterogeneous independent effects rather than a common loss of set-point control; opposite-direction abnormalities across outcomes do not by themselves demonstrate set-point instability |
| **3. Convergence on synaptic maintenance, with presynaptic supply as the hypothesized bottleneck, expressed as dysconnection (Prop. 3)** | Tier 1, moderate: reduced SV2A, SYT11 and NRXN1 protein against broadly upregulated synaptic transcripts, with 37 of the 182 downregulated synaptic proteins carrying SynGO annotations, about one fifth, upregulated at the transcript level (Nehme et al., 2022); in idiopathic schizophrenia, anterior cingulate synaptic density at 72% and terminal mitochondrial density at 64% of controls (Roberts et al., 2015), and reduced PSD95-defined synapse number with reduced mitochondria–synapse colocalization in women (Das et al., 2022) | Tier 3, strong: mitochondrial transporter interactome required for synapse function and behavior (Gokhale et al., 2019); *Mirta22* reduction reverses dendritic and spine alterations in vivo (Xu et al., 2013); *Txnrd2* dosage limits layer 2/3 axon and dendrite growth, synaptic vesicle density and presynaptic specializations, rescued by re-expression and by N-acetylcysteine (Fernandez et al., 2019); fMRI dysconnectivity covaries with spine density and both respond to the same manipulation (Alvino et al., 2025); hippocampal–prefrontal synchrony reduced and predictive of learning rate (Sigurdsson et al., 2010) | No | Discovery proteomics used two carrier and two control donors; dendritic spines are postsynaptic, static protein abundance does not measure turnover, and PSD95–TOM40 colocalization is not a presynaptic measure, so presynaptic specificity remains a hypothesis; postmortem synaptic data are from idiopathic schizophrenia; the complex I reduction in Das et al. (2022) was attributable to medication |

| Claim | Human evidence: highest tier (strength) | Model-system evidence: highest tier (strength) | Within-carrier | Principal contradictory or null findings |
|---|---|---|---|---|
| **4. Compensation is active and strongest in protected carriers (Prop. 4)** | Tier 1, moderate but design-appropriate: in induced neurons, carriers without schizophrenia show PGC-1α, PGC-1β and PPARα above both controls and carriers with schizophrenia and PRKN selectively elevated; mtDNA copy number above carriers with schizophrenia but not above controls; ATP and complex I activity reduced in carriers with schizophrenia relative to carriers without, with carriers without not different from controls (Li et al., 2021). In lymphoblastoid lines from a separate two-group sample, carriers without schizophrenia exceeded carriers with on mitochondrially encoded transcripts and complex I and IV activity | Tier 3 for the components: a miR-181a/b antagomir and bezafibrate each raised ATP and complex I activity in neurons from carriers with schizophrenia (Li et al., 2021) | **Yes** | Six control and four lines per carrier group; cross-sectional; the peripheral sample had no control group, so the inversion was not retested peripherally; some nonpsychotic donors aged 22–26 remained within the risk window; in blood, a co-expression module containing aerobic-respiration and protein-folding genes was *higher* in carriers with psychosis (Jalbrzikowski et al., 2015), which the model reads as effort without matching capacity and which is why the two are measured separately. Das et al. (2022) is a two-group design compatible with mitochondrial adaptation, not a replication of the three-group ordering |
| **5. Crossing of rising demand and falling capacity (Prop. 5)** | Tier 2 relative to onset, moderate: verbal IQ decline precedes psychosis (Vorstman et al., 2015); executive and specifically working-memory decline distinguishes carriers with emerging psychosis features and drives clinical change (Gur et al., 2023); accelerated cortical thinning accompanies psychotic symptoms (Bagautdinova et al., 2021); the hyper-to-hypoconnectivity transition is dated to puberty cross-sectionally (Alvino et al., 2025) | Tier 3–4, strong: the LTP phenotype is absent at 8–10 weeks and present at 16–20 weeks and is rescued by restoring miR-25 and miR-185 (Earls et al., 2012); thalamic *Drd2* rises and antipsychotic sensitivity appears from 3 months in Df(16)A+/− and *Dgcr8*+/− mice, and *Mir338*+/− mice show the phenotype at 1.5, 2 and 4 months (Chun et al., 2017); adolescence is the inflection for social behavior, prefrontal thickness, microglial activation and myeloid infiltration in LgDel/+ (Castellani et al., 2025) | Partly | Gur et al. and Vorstman et al. compare carriers by outcome. Cognitive decline could be an early expression of the illness rather than an antecedent; no human study has measured a compensation variable longitudinally; the claim that demand rises while capacity falls is a model prediction, not an established joint trajectory |

| Claim | Human evidence: highest tier (strength) | Model-system evidence: highest tier (strength) | Within-carrier | Principal contradictory or null findings |
|---|---|---|---|---|
| **6. Dopamine as a downstream compensator with a cost (Prop. 6)** | Tier 1, moderate: striatal synthesis capacity falls linearly with copy number ($B = -1.2 \times 10^{-3}$ $min^{-1}$ per copy, $p < 0.001$), with deletion carriers above controls ($d = 1.44$) and above duplication carriers ($d = 2.00$), while the duplication-versus-control contrast did not survive correction (Rogdaki et al., 2023); higher synthesis capacity associated with more control-like connectivity, estimated across the combined deletion and duplication sample with copy-number group in the model (Mancini et al., 2026); synthesis capacity associated with psychosis-risk symptom severity in that same combined sample (Rogdaki et al., 2023); thalamic miR-338-3p reduced in schizophrenia postmortem (Chun et al., 2017) | Tier 3–4, strong: *Dgcr8* hemizygosity elevates thalamic *Drd2* and confers antipsychotic sensitivity on thalamocortical projections (Chun et al., 2014); miR-338-3p depletion is necessary and sufficient, and its replenishment in mature mice rescues the phenotype under continued expression (Chun et al., 2017) | Partly | Thalamic receptor expression, striatal synthesis capacity, network configuration and positive symptoms are different constructs linked here by hypothesis; both imaging studies are cross-sectional and small (18–21 carriers) from overlapping datasets; connectivity was unrelated to symptoms (Mancini et al., 2026); the compensatory interpretation is an inference, not a demonstrated direction |
| **7. The state is reversible rather than cumulative (Props. 4 and 5)** | Tier 1–2, moderate: over 2.8 years, positive psychosis-spectrum symptoms remitted in 16 of 41 symptomatic carriers and emerged in 9 of 31 asymptomatic ones; negative symptoms and functional impairment persisted after positive symptoms remitted, and were higher at baseline in the emergent group ($P = 0.03$) though not predictive in regression ($P = 0.82$) (Tang et al., 2017) | Tier 3, strong: replenishing miR-338-3p in mature mice rescues an already-established thalamocortical deficit (Chun et al., 2017); nonselective GSK3 inhibition normalizes juvenile connectivity and spine surplus transiently (Alvino et al., 2025) | **Yes** | 75 participants aged 8–35 enrolled, of whom 72 received a longitudinal clinical classification; remission of subthreshold symptoms is not remission of a psychotic disorder, five participants developed threshold psychosis, and symptom remission does not establish the absence of persisting pathology; the comparison cohort was followed for 2.0 years against these carriers' 2.8, so cumulative proportions are not comparable across them and the entry-versus-exit asymmetry claimed in earlier accounts of this cohort does not survive conversion to annual hazards (Section 7) |
| **8. Barrier compromise contributes to the immune limb** | Tier 1, weak: reduced transendothelial resistance and elevated ICAM-1 in patient-derived barrier models; reduced claudin-5 in postmortem tissue (Crockett et al., 2021); claudin-5 variant rs10314 reduces expression and was weakly associated with schizophrenia in a small carrier cohort (Greene et al., 2018) | Tier 3, moderate: neonatal intranasal oxytocin raises claudin-5, seals the barrier, reduces myeloid infiltration, improves the constitutive gating deficit and prevents the adolescent social deficit in LgDel/+ (Castellani et al., 2025); inducible claudin-5 suppression produces barrier disruption, behavioral phenotypes and seizures, and antipsychotics raise claudin-5 dose-dependently (Greene et al., 2018) | Partly | Patient lines were all from carriers with schizophrenia; the induced barrier cells lack vascular lineage identity (Lu et al., 2021); the rs10314 association was not replicated in 490 carriers (overall $P = 0.27$; female subgroup $P = 0.053$) (Guo et al., 2020) |

| Claim | Human evidence: highest tier (strength) | Model-system evidence: highest tier (strength) | Within-carrier | Principal contradictory or null findings |
|---|---|---|---|---|
| **9. Immune skew contributes to penetrance** | Tier 1, weak to moderate, three small within-carrier studies with different markers: IL-6 and IL-6/IL-10 higher in 13 carriers with psychosis than 36 without (Mekori-Domachevsky et al., 2017); IL-8 higher in carriers with psychosis-risk symptoms than without, robust to antipsychotic adjustment (O'Hora et al., 2024); Th17 percentage higher in carriers with psychotic symptoms (Vergaelen et al., 2018); a blood co-expression module with immune and respiratory genes higher with psychosis (Jalbrzikowski et al., 2015) | Tier 3, moderate: regulatory T-cell reduction and microglial *C4* and *C1q* elevation in adolescent LgDel/+, both preventable by neonatal oxytocin (Castellani et al., 2025) | **Yes** | Carrier-versus-control elevations of IL-6, CRP and TNFα in one sample were absent in another, which found only IL-8 elevated and only in duplication carriers (O'Hora et al., 2024); 12 of 13 psychotic carriers in the IL-6 study were on antipsychotics; depleting microglia or regulatory T cells did not abolish the oxytocin benefit, placing both downstream of barrier tone |
| **10. Modifiers act on regulatory and synaptic systems and interact with the deletion (Section S4)** | Tier 1, strong: schizophrenia polygenic score higher in carriers with schizophrenia and predictive of verbal IQ decline (Cleynen et al., 2021; Davies et al., 2020); rare duplications overlapping nervous-system genes enriched in carriers with schizophrenia and showing network connectivity with deletion-region genes (Bassett et al., 2017); rare genic tandem repeat expansions enriched at an effect comparable to polygenic score, concentrated in intronic and splice-adjacent regions (Cheng et al., 2026) | Tier 3, moderate: strain background determines expression of social phenotypes (Hiroi et al., 2012) | **Yes** | Each class explains a minority of variance; the network-connectivity result is a bioinformatic association, not a demonstrated interaction; gene interaction does not by itself imply statistical nonadditivity on a liability scale; no study has tested whether modifier burden predicts a measured compensation variable |
| **11. Developmental tempo is slowed at the progenitor stage** | Tier 1, moderate: G1 accumulation and S-phase depletion, reduced CTIP2+ neuron yield, 15 of 19 differentially expressed miRNAs downregulated including *hsa-mir-185* (Rao et al., 2025) | Tier 1, moderate: *Dgcr8* hemizygosity reproduces the locus-level miRNA biogenesis defect (Stark et al., 2008). Rescue of downstream synaptic phenotypes by restoring microRNAs (Chun et al., 2017; Earls et al., 2012) is Tier 3 evidence about those phenotypes, not about progenitor tempo | No | Patient lines were selected for schizophrenia with no carrier-without-schizophrenia group; cannot distinguish a deletion effect from a schizophrenia effect, as the authors note |

Tiers: 1 = presence; 2 = temporal precedence within persons; 3 = mediation, intervention or greater explanatory importance than a rival; 4 = necessity, meaning that removing the mechanism abolishes the outcome. Strength ratings summarize replication and sample size within the tier reached.

## S2 The Deleted Genes, Gene by Gene

The organizing observation behind Proposition 1 is that the 22q11.2 interval is unusually poor in genes that specify a neural structure and unusually rich in genes that set the rate, gain or throughput of a process (Karayiorgou & Gogos, 2004; Kolar et al., 2023). This is a claim about

the genes with demonstrated neural phenotypes rather than a quantified enrichment across all 46, and *TBX1*, with its patterning role in pharyngeal and cardiac development, does not fit it. The categories also overlap, since enzymes, transporters, ribosomal proteins and junctional proteins both implement functions and set their rates; the claim is about where the weight of the interval's neural relevance lies, and the inference drawn from it, a narrowed correction range, is a hypothesis tested in the main text rather than an entailment.

*DGCR8* encodes the RNA-binding component of the microprocessor complex and is therefore a regulator of the rate at which primary microRNAs are converted to precursors. Its hemizygosity does not remove a neural function; it broadly and partially reduces the fidelity of post-transcriptional timing across hundreds of targets. In the Df(16)A+/− mouse, the locus-level alteration in brain microRNA biogenesis was traced to *Dgcr8* hemizygosity specifically, and *Dgcr8*+/− animals reproduced the relevant neuronal and behavioral deficits (Stark et al., 2008). The consequences observed are consistently those of mistimed rather than absent processes: in patient-derived organoids, progenitors accumulate in G1 and are depleted from S phase, terminal neuronal yield falls to roughly half, and the dominant cellular signature is a slowing of developmental tempo rather than a failure of fate specification, with 15 of 19 differentially expressed microRNAs reduced, including *hsa-mir-185* from within the interval (Rao et al., 2025).

*MIR185* illustrates the regulatory logic more sharply still. Its reduction in deletion models is substantially greater than hemizygosity alone would produce, which already indicates that the locus is embedded in feedback rather than acting as a simple dosage element (Xu et al., 2013). Its principal downstream consequence is sustained derepression of *Mirta22*, a Golgi-localized inhibitor of dendritic and spine development with a prenatal expression bias. Reducing *Mirta22* reverses the dendritic and spine alterations of Df(16)A+/− mice both in vitro and in vivo (Xu et al., 2013). The lesion is a failure to release a developmental brake on schedule, and restoring the schedule restores the structure.

A second microRNA makes the same point with the clearest causal evidence in the syndrome. miR-338-3p is enriched in thalamus in both mice and humans, represses *Drd2* through a conserved seed site, and declines with age; *Dgcr8* hemizygosity exaggerates that decline, so that thalamic *Drd2* rises and auditory thalamocortical transmission is disrupted in older but not younger deletion mice (Chun et al., 2014, 2017). The regulator is not required to build the circuit. It is required to hold a receptor at its set point, and the circuit fails when it can no longer do so.

*MRPL40* encodes a mitochondrial ribosomal protein and so regulates the translational throughput of the thirteen mitochondrial-genome-encoded subunits of the respiratory chain. The specificity of its consequence is diagnostic: in patient-derived neurons, complex I and complex IV activities fall while complexes II, III and V are spared, and the pattern follows the number of mitochondrially encoded subunits each complex contains: seven and three for complexes I and IV, versus zero, one and two for II, III and V (Li et al., 2019). Introducing a

heterozygous loss-of-function mutation into a single *MRPL40* allele in a control line reproduced this pattern together with an approximately 30% ATP reduction. In mouse models, *Mrpl40* hemizygosity produces abnormally elevated calcium transients in presynaptic cytosol and mitochondrial matrix during high-frequency stimulation, with mitochondrial permeability transition pore-dependent calcium extrusion as the proximal mechanism (Devaraju et al., 2017).

The subunit-count pattern does not survive unchanged into the later three-group study from the same laboratory, and the discrepancy is instructive rather than fatal. There, complex V was reduced in the psychosis group (P = .02) while complex IV was not significantly reduced (P = .15) (Li et al., 2021), close to the inverse of the Li et al. (2019) ordering. Three differences separate the studies: the comparison is carrier-with-psychosis against carrier-without rather than carrier against control, the later samples are lymphoblastoid rather than neuronal, and the two therefore ask different questions. The subunit-count argument is about what *hemizygosity* does to the chain and is tested against controls; the three-group contrast is about what distinguishes carriers who become ill, and under this model that difference is a demand-and-effort difference rather than a second dosage effect. The two patterns are only in conflict if one assumes the within-carrier difference must be the deletion's dosage signature repeated, which is precisely what the model denies. This is a direct prediction: in the design of Section 11.1, the subunit-count ordering should appear in the carrier-versus-control contrast, and should *not* reproduce in the psychosis-versus-well contrast, which should instead track effort. If the subunit-count ordering also separates the two carrier groups, the dosage reading of complex-specific loss is wrong.

*SLC25A1*, which lies within the deleted interval at 22q11.21, encodes the mitochondrial citrate transporter and sits with *SLC25A4* at 4q35.1 as the two principal nodes of a mitochondrial transporter interactome. Both proteins are reduced by at least half in fibroblasts from deletion carriers relative to unaffected family members, and the two transporters regulate one another's abundance: loss of either raises the other in single-gene models, with *SLC25A4* loss raising *SLC25A1* some 3.6-fold (Gokhale et al., 2019). A system in which two transporters buffer each other's levels is a regulated system, and partial loss of both simultaneously removes exactly the buffering that would otherwise absorb the perturbation. In *Drosophila*, haploinsufficiency of the orthologues altered synapse morphology, neurotransmission and sleep, which places the interactome's output at the synapse rather than at bulk cellular energetics.

*TXNRD2* encodes thioredoxin reductase 2, the rate-limiting enzyme for clearance of hydrogen peroxide in the mitochondrial matrix. In LgDel mice, layer 2/3 projection neurons, but not layer 5/6 neurons, show reduced long-distance cortico-cortical connectivity, shorter and less branched dendrites, swollen mitochondria with disordered cristae, and dilated presynaptic terminals with few vesicles. Among six 22q11 mitochondrial genes screened by shRNA in wild-type layer 2/3 neurons (*Mrpl40*, *Txnrd2*, *Slc25a1*, *Prodh*, *Tango2*, *Zdhhc8*), only *Txnrd2* depletion reproduced the growth deficit, raising mitochondrial and cytosolic reactive oxygen species by

about a quarter; *Txnrd2* re-expression in LgDel neurons restored growth and returned reactive oxygen species to wild-type levels; heterozygous *Txnrd2* deletion in single layer 2/3 neurons in vivo reduced apical dendrite length by 21% and branching by up to half; and N-acetylcysteine from birth restored dendritic growth, mitochondrial morphology, synapse frequency and reversal learning in young adult LgDel mice (Fernandez et al., 2019). The laminar selectivity is itself informative: the neurons affected are those whose long-range projections impose the highest bioenergetic demand, which is where a dosage-limited regulator of redox tone should fail first.

*ZDHHC8* encodes a Golgi palmitoyltransferase and therefore regulates the membrane targeting of a large set of synaptic substrates rather than performing a synaptic function directly. *RANBP1* regulates RAN-GTPase-dependent nucleocytoplasmic transport. *CLDN5*, expressed in brain endothelium at far higher levels than other claudins, sets tight-junction tone rather than constituting the barrier alone, and its expression is dosage-sensitive in a way that matters: inducible suppression in mice produces localized barrier disruption, deficits in learning and memory, anxiety-like behavior and sensorimotor gating, and seizures with death after three to four weeks, while antipsychotic drugs dose-dependently increase claudin-5 expression in vitro and in vivo (Greene et al., 2018). *PRODH* regulates the flux of proline through the mitochondrial matrix, and its haploinsufficiency raises plasma proline roughly twofold, producing cytosolic concentrations at which proline competitively inhibits glutamate decarboxylase and selectively impairs sustained high-frequency GABAergic transmission (Crabtree et al., 2016; Jacquet et al., 2002; Liu et al., 2002). *COMT* regulates the clearance rate of synaptic catecholamines.

*COMT* and *PRODH* together supply the oldest demonstration of the model's logic. In homozygous *Prodh*-knockdown mice on a 129/SvEv background, hippocampal CA3–CA1 transmission is enhanced through increased glutamate release probability, with reduced paired-pulse facilitation and a decreased dynamic range of presynaptic plasticity; the animals show deficits in associative learning and potentiated locomotor responses to amphetamine, while working memory is spared, which the authors read as "the emergence of cortical compensations." Transcriptional profiling of frontal cortex implicated three processes, namely translational initiation, mitochondrial function and presynaptic neurotransmitter release, and the top upregulated gene in the third was *Comt*, elevated by about 25% at the message and reproducibly at the protein level, selectively in frontal cortex and not striatum, from the third postnatal week, together with reduced DRD1 and DARPP-32 and elevated calcineurin. Chronic MK801 treatment of wild-type mice phenocopied the frontal-selective *Comt* elevation, identifying it as a homeostatic response to altered transmission. The COMT inhibitor tolcapone, which had no effect in wild-type animals, potentiated the amphetamine response, increased working memory errors, and reduced prepulse inhibition in the mutants (Paterlini et al., 2005). The authors' conclusion is the compensation model at the level of two genes: because carriers are deficient for both, they are "perhaps unable to compensate efficiently,

through COMT, for the cortical dopaminergic hyperactivity induced by PRODH deficiency," and the locus contributes to illness "by impairing both synaptic function and the development of compensatory response."

# S3 The Bidirectionality Catalogue and the Circuit-Level Expression

## S3.1 Findings that fit the bidirectional signature

Long-term potentiation at CA3–CA1 synapses is *increased*, not decreased, in deletion models, through presynaptic SERCA2 overexpression that enhances endoplasmic reticulum calcium loading and neurotransmitter release; the increase is recapitulated by *Dgcr8* hemizygosity alone and is reversed by restoring miR-25 and miR-185 to presynaptic neurons (Earls et al., 2012). Thalamocortical axons *overgrow* rather than undergrow, through elevated *FOXP2* and depletion of the repulsive guidance receptor *ROBO2*, with striatal PKCδ-positive axon density increased in Df(h22q11)/+ mice and axonal outgrowth increased in patient-derived thalamic organoids (Shin et al., 2024). Cortex in carriers is overall *thicker* than in controls, with left and right effect sizes of 0.61 and 0.65, while cortical surface area is substantially *reduced*, at −1.01 and −1.02 (Sun et al., 2020). Neurons from carriers are approximately four times more likely to fire spontaneously and have a more depolarized resting membrane potential, yet show *smaller* depolarization-induced calcium transients, because the depolarized resting potential inactivates voltage-gated calcium channels (Khan et al., 2020). Transcripts of synaptic genes are broadly *upregulated* in mature patient-derived neurons, with 193 of 2,173 upregulated transcripts carrying synaptic annotations and strongest enrichment for the synaptic vesicle cycle, while presynaptic proteins including SV2A, SYT11 and NRXN1 are *reduced* at the protein level in discovery proteomics on two carrier and two control donors, with 37 of the 182 downregulated SynGO-annotated synaptic proteins, about one fifth, upregulated at the transcript level (Nehme et al., 2022). The schizophrenia heritability enrichment in these neurons is carried disproportionately by the *upregulated* genes, at 1.31-fold enrichment with Bonferroni-adjusted $p = 0.001$ against 1.20-fold for all differentially expressed genes, and the same analysis found rare loss-of-function burden from SCHEMA enriched in the upregulated set at $p = 5.08 \times 10^{-6}$ and a MAGMA competitive enrichment at $p = 7.93 \times 10^{-8}$. Enrichment of liability among upregulated transcripts is consistent with the compensatory reading of those transcripts; it does not by itself show that they are beneficial.

The longitudinal mouse and cross-sectional human connectivity findings are described in the main text (Section 4). Two features of the design should be kept in view. In the mouse, fMRI was longitudinal in the same animals (PND35 ± 2 and PND111 ± 7) while spine density was measured in separate juvenile and adult animals, so the claim that the same animals passed through a spine surplus to a deficit is not what was measured; the claim that the same animals passed from hyper- to hypoconnectivity is. In the human cohort (139 carriers, 117 controls), the analysis was cross-sectional with pubertal status inferred from an 11-year age cutoff, and

the age anchors (hyperconnectivity to 9.2 and 9.9 years, hypoconnectivity from 12.8 years in hippocampus and 13.8 years in opercular cortex) come from a nonlinear model fitted across individuals, not from followed individuals (Alvino et al., 2025).

### S3.2 The circuit-level expression

A synaptic supply constraint has to show itself at the level of circuits if it is to explain a psychiatric phenotype, and in this syndrome it does, in four measurements that are usually discussed separately.

The first is long-range synchrony. In Df(16)A+/− mice performing a working memory task, synchronization between hippocampus and prefrontal cortex was drastically reduced, measured both as phase-locking of prefrontal units to hippocampal theta and as coherence of local field potentials; the mice were impaired at acquiring the task, and the magnitude of hippocampal–prefrontal coherence at the onset of training predicted how long acquisition took (Sigurdsson et al., 2010). A circuit measure that predicts the rate at which an animal can learn is a measure of functional capacity rather than of damage, which is the quantity the model requires and the kind of measure it needs more of.

The second is the pubertal reconfiguration. The hippocampal localization of the adult phenotype is consistent across modalities. Deletion carriers show elevated hippocampal Glx and reduced hippocampal GABA+ relative to controls, with large effects, and hippocampal Glx is higher in carriers with psychotic symptoms than in those without (Mancini et al., 2023). Within carriers, higher hippocampal Glx was associated with greater hippocampal volume loss measured across a mean interval of roughly three years ($\beta = -0.39$), although the spectroscopy was acquired at one time point only, so the direction of that relationship is not established.

The third is the thalamocortical projection to auditory cortex, which is disrupted specifically in deletion models through elevated thalamic *Drd2*, and which acquires an abnormal sensitivity to antipsychotics as a result (Chun et al., 2014). The circuit is of obvious interest given that auditory hallucinations are the symptom antipsychotics most reliably relieve, and the mechanism is a regulator failure: the elevation of *Drd2* follows depletion of the microRNA that represses it (Chun et al., 2017).

The fourth comes from a different model line and a different question. In LgDel mice, long-distance cortico-cortical connectivity from medial frontal association cortex is reduced and short-distance connectivity increased, selectively from layer 2/3 projection neurons, through a *Txnrd2*-dependent redox mechanism; the deficit, its cellular correlates, and the associated reversal-learning impairment are all restored by antioxidant treatment (Fernandez et al., 2019). What unifies the four is a single functional description: each is a system whose performance depends on precise, sustained, high-frequency coordination of distant populations, and each degrades in a way that tracks the state of synaptic supply rather than the loss of a structure.

## S4 What the Modifier Literature Says About the Character of the Modifiers

Because the genetic modifier studies are the part of this literature that reliably uses a penetrance design, what they report deserves separate treatment. Three findings bear on the model, and none of them is simply that modifiers exist.

First, modifiers predict trajectory and not only endpoint. In 962 carriers, schizophrenia polygenic score was associated not only with schizophrenia-spectrum diagnosis but with decline in verbal IQ, and nominally with subthreshold psychosis; comparing tail deciles, 33% of carriers in the highest polygenic decile had schizophrenia against 9% in the lowest (Davies et al., 2020). A liability-threshold account expects modifiers to shift the probability of crossing a threshold. That they also predict the rate at which a capacity-sensitive measure deteriorates is what a model of consumed reserve expects, although it does not by itself exclude an account in which the same variants independently accelerate cognitive decline and raise liability.

Second, modifiers act in both directions, and through coding as well as regulatory routes. The directional point first. Among 456 European-ancestry carriers from the International Brain and Behavior Consortium, 223 with schizophrenia and 233 without, an integrated gene-network and mouse-phenotype method identified 110 candidate modifier genes in which rare nonsynonymous variants explained about 4.6% of variance in schizophrenia status (99% CI 3.7–5.6%, adjusted $P = 9.4 \times 10^{-4}$), of which about 4.0% was independent of common polygenic risk; combining the two explained about 8.9%. Of those genes, 54 carried higher weighted burden in cases and 56 in unaffected carriers, so variants in this set can raise or lower risk (Lin et al., 2023). A model in which liability accumulates predicts modifiers that add; a model of set-point instability predicts modifiers that push in both directions, and that is what is observed. Synonymous variants contributed nothing, which is the specificity check.

Modifiers act through coding and regulatory routes together rather than through either alone. The same study found enrichment among loss-of-function-intolerant ($P = 9.4 \times 10^{-6}$) and missense-constrained genes ($P = 3.2 \times 10^{-5}$), which is a coding signal, *and* associations with rare and low-frequency noncoding variants in neuronal transcription-factor binding sites ($P = 1.9 \times 10^{-4}$) and brain enhancers ($P = 4.7 \times 10^{-4}$) of the same genes. Nothing in the model requires the two routes to be alternatives. What the regulatory evidence adds is a second, independent class: rare genic tandem repeat expansions were enriched in carriers with schizophrenia relative to carriers without, with odds ratios of 1.75 and 2.14 in trio and singleton cohorts and a contribution to liability comparable to that of polygenic score; the expansions were concentrated in intronic and splice-adjacent regions, with evidence that they act by altering methylation and splicing, and the genes affected were differentially expressed in prefrontal excitatory and inhibitory neurons and included synaptic organizers such as *DLGAP2* (Cheng et al., 2026). Rare intergenic expansions showed no enrichment.

Third, modifiers engage the same systems and the same developmental window as the deletion rather than an independent one. The modifier genes above were enriched for synaptic genes ($P = 8.3 \times 10^{-9}$) and developmental-disorder genes ($P = 9.7 \times 10^{-4}$), and were coexpressed with 22q11.2 deletion-region genes, *SLC25A1*, *COMT* and *PI4KA* among them, in cortical modules spanning late infancy to young adulthood, which is the window in which this model locates the crossing (Lin et al., 2023). Among 329 carriers compared by psychosis status with the nonpsychotic group restricted to age 25 or older, rare duplications overlapping genes in a mouse abnormal-nervous-system set were enriched in the schizophrenia group and survived stepwise model selection; a connectivity analysis using 22q11.2 deletion-region genes as bait found that this gene set was significantly more connected to deletion-region genes than expected (Bassett et al., 2017). This is a bioinformatic association rather than a demonstrated biological interaction, gene interaction does not automatically imply statistical nonadditivity on a liability scale, and the result should not be over-read. But it is the observation a compensation model predicts: the modifiers that matter are those that further narrow a range the deletion has already narrowed, rather than any additional liability drawn from anywhere in the genome. A purely additive account is compatible with this pattern too, so the observation is consistent with the model rather than decisive for it; what would discriminate is a modifier that narrows the same range showing a larger effect than a modifier of equal main effect that does not, which no study has tested.

Taken together, the modifier literature supplies something the cellular literature has not: penetrance-relevant evidence, at scale, that what varies between carriers who do and do not develop psychosis is regulatory and synaptic, affects trajectory, and overlaps the deletion's own network. None of this establishes that compensation is the mediating variable. It does establish that the modifiers behave as the model requires, and it motivates the direct test in Study 1, whose secondary analysis asks whether modifier burden predicts measured compensatory capacity within carriers.

## S5 The Barrier and Immune Limb

The immune and barrier evidence in this syndrome is mechanistically attractive and, in its human cellular form, considerably weaker than it is usually presented. Setting out why is necessary, because the model assigns this limb a real but subordinate role, and because the reasoning illustrates the penetrance filter of Section S1.

*CLDN5* lies within the deleted interval and encodes the tight-junction protein expressed at far higher levels than other claudins in brain endothelium. Patient-derived barrier models from carriers show reduced transendothelial electrical resistance, disorganized claudin-5 without a change in its message or total protein, elevated ICAM-1, increased monocyte transmigration, and reduced thrombomodulin in transmigrated cells; Df(h22q11)/+ mice show increased perivascular extravasation of IgG and fibrinogen in prefrontal cortex and elevated perivascular astrocytic GFAP and IL-6; and postmortem 22q11.2 tissue shows reduced claudin-5 (Crockett et

al., 2021). Claudin-5 dosage is consequential in its own right: targeted AAV-mediated suppression in mouse brain produces localized barrier disruption and behavioral change, an inducible knockdown produces impairments in learning and memory, anxiety-like behavior and sensorimotor gating followed by seizures and death after three to four weeks, antipsychotic medications dose-dependently increase claudin-5 expression in vitro and in vivo, and claudin-5 expression is discontinuous in postmortem schizophrenia cortex (Greene et al., 2018).

Two problems limit what the human cellular component establishes. The first is the design: all five patient lines in the barrier study came from carriers with schizophrenia, compared with five healthy controls, and the postmortem donors' psychosis status was undefined. The authors state the limitation themselves and call for studies including carriers without schizophrenia. The barrier finding is therefore evidence about the deletion, not about penetrance. The second is cellular identity. The induced barrier model used in this and much related work derives from protocols whose products have been shown, by transcriptomic meta-analysis validated against physiological assays, to lack vascular lineage gene expression and to express neuroectodermal epithelial programs; they acquire endothelial identity only when endothelial ETS transcription factors are overexpressed (Lu et al., 2021). Measures of barrier tightness in such cells cannot be interpreted straightforwardly as measures of brain endothelial function. This does not refute the barrier hypothesis; the mouse and postmortem findings are unaffected. It does mean the human cellular limb should be re-established in an authenticated endothelial system before it is treated as established, and Study 1 specifies that requirement.

The within-carrier genetics of the barrier are, at present, null. The rs10314 variant in the claudin-5 3′ untranslated region reduces protein expression from the allele carrying it by roughly 75% in vitro. A deletion carrier already expresses from one allele, so a carrier with the variant on the remaining copy is predicted to express about a quarter of what that single allele would otherwise produce, which is about an eighth of the diploid level. The fraction matters because the model's claim concerns absolute barrier tone, not relative loss. The variant was present in 9 of 15 carriers with schizophrenia and 8 of 44 without (P = 0.039) (Greene et al., 2018). In 490 carriers from the International Brain and Behavior Consortium genotyped by whole-genome sequencing, the variant was carried by 14.7% of 252 with schizophrenia and 11.3% of 238 without (P = 0.27), with no association in males (P = 0.80) and a marginal signal in females (18.3% versus 10.1%, P = 0.053) (Guo et al., 2020). A sample more than eight times larger did not reproduce the association, and the female subgroup result is a hypothesis for a further sample, not a finding.

The animal evidence is stronger and, unusually for this literature, includes a causal dissection. In LgDel/+ mice, neonatal intranasal oxytocin given from postnatal days 1 to 7 raised claudin-5 and claudin-1, reduced barrier permeability to cadaverine, reduced myeloid cell infiltration into parenchyma, restored splenic regulatory T cells, prevented the pro-inflammatory activation of prefrontal microglia including the elevation of *C4*, improved the sensorimotor gating deficit, which in this line is present at every age from postnatal day 19, in both

adolescence and adulthood, and prevented the adolescent emergence of the social deficit (Castellani et al., 2025). Depleting microglia with a CSF1R inhibitor during the treatment window, or blocking regulatory T-cell function with a p300 inhibitor, did not abolish the benefit, while the barrier effects persisted. Within this model, barrier tone is upstream and the immune changes are consequences.

The human within-carrier immune evidence comes from three small studies that agree in design and disagree in marker. Among 49 carriers (13 with a psychotic disorder, 36 without) and 30 controls, carriers had higher CRP, IL-6, TNFα and IL-10 than controls, and carriers with psychosis had higher IL-6 and a higher IL-6/IL-10 ratio than carriers without and than controls, with IL-6 correlating with the severity of cognitive deficit; 12 of the 13 psychotic carriers were taking antipsychotics (Mekori-Domachevsky et al., 2017). Among 45 deletion carriers, 29 duplication carriers and 92 controls, with age, sex and body mass index modeled and false-discovery-rate correction applied, the only group difference was elevated IL-8 in duplication carriers relative to controls; within deletion carriers, those with psychosis-risk symptoms on structured interview had higher IL-8 than those without and than controls, and inclusion of antipsychotic use as a covariate did not change the result (O'Hora et al., 2024). Among 34 adults with the deletion and 34 matched controls, Th1, Th17 and memory T-helper percentages were elevated in carriers, and within carriers Th17 percentage was higher in those with psychotic symptoms and related to positive symptom severity (Vergaelen et al., 2018). In peripheral blood transcriptome from 46 carriers, 141 probes were differentially expressed between the 6 with a psychotic disorder and the 40 without, with over-representation of mitochondrial organization and transport, and a co-expression module of 237 probes, 75% brain-expressed and enriched for protein folding, acetyl-CoA metabolism and aerobic respiration, was predominantly upregulated in carriers with psychosis and correlated with positive symptom severity ($r = 0.54$), unrelated to antipsychotic use and overlapping with modules previously associated with idiopathic schizophrenia; immune-response enrichment in that module did not survive correction (Jalbrzikowski et al., 2015). The within-carrier signal is therefore replicated in kind, across four studies with four different markers, all in the direction of greater inflammatory or metabolic activation with psychosis, and not in marker, and the carrier-versus-control cytokine elevations have not replicated across studies.

The model's position is correspondingly bounded. Barrier tone is one of the regulated variables whose set point the deletion destabilizes, through *CLDN5* hemizygosity, and its destabilization admits peripheral immune influence that constitutes an additional, variable load on the system. It is a load term, not the mechanism of conversion. The elevation of microglial *C4* in adolescent deletion mice is noted as a possible link between this limb and synaptic elimination, given the established relationship between complement component 4 and synaptic pruning in schizophrenia risk (Sekar et al., 2016), but that link is a plausible conjunction of two literatures rather than a demonstrated pathway in this syndrome, and the model does not depend on it.

## S6 Scope and the Extension to Idiopathic Psychosis

Five boundaries on the model's scope are stated explicitly, because the temptation to extend an account of a rare, high-penetrance variant to common illness is strong and usually premature.

The first concerns what the syndrome licenses. The 22q11.2 deletion concentrates into one lesion a set of regulatory perturbations that, in idiopathic schizophrenia, are distributed across hundreds of common variants of small effect and a smaller number of rare variants of larger effect. The genomic signals do overlap: genes dysregulated in deletion-carrier neurons are enriched for common schizophrenia heritability and for rare loss-of-function burden from exome sequencing, and the enrichment is concentrated in the upregulated set (Nehme et al., 2022). The modifier literature supplies a second kind of overlap, and a more direct one: the additional genetic variants that distinguish carriers who develop schizophrenia from those who do not are, so far as has been tested, the same variants that contribute to schizophrenia risk in the general population (Cheng et al., 2026; Cleynen et al., 2021; Davies et al., 2020). That supports the claim that the deletion engages the same biological processes as distributed liability. It does not establish that the two produce illness by the same sequence, and the model does not claim that it does.

The second concerns whether the compensation signature is specific to this syndrome. In postmortem dorsolateral prefrontal cortex from people with schizophrenia and bipolar disorder, mitochondrial DNA copy number was elevated while complex I activity and PSD95-defined synapse number were reduced, with primary visual cortex and nucleus accumbens largely spared (Das et al., 2022). Machinery up, output down, in association cortex: that is a pattern compatible with mitochondrial adaptation, and it shows that the quantities the model names are measurable in human association cortex outside the deletion. It is not a replication of the three-group inversion, because the study compared patients with controls and had no protected group, and its complex I reduction was attributable to medication exposure. What it establishes is that the extension is testable rather than rhetorical.

The third concerns the relationship to synaptic accounts of idiopathic schizophrenia. This model is a specification of one component of such accounts rather than a competitor to them. Synaptic theories hold that distributed liability biases synaptic construction, that adolescent remodeling exposes the resulting fragility, and that dysconnection of association circuits is the proximate substrate of the failures of inference and self-monitoring that give psychosis its content (Howes & Onwordi, 2023; Moore, 2026). What the present model adds, and what the 22q11.2 syndrome is uniquely positioned to supply, is an account of the moderator: why, given the same construction bias, some systems survive remodeling and others do not. The answer proposed, that compensatory capacity is a measurable, exhaustible, recoverable, dosage-sensitive quantity and that the protected individual is distinguished by active overcompensation rather than by absence of deficit, is a claim about reserve that has been

difficult to operationalize in idiopathic samples precisely because the upstream lesion there is unknown and heterogeneous. In this syndrome it is known. That is the methodological argument for doing the work here.

The fourth concerns outcome definition. The programs test transitions in psychosis-spectrum status among deletion carriers. They do not test whether the state entered is specifically schizophrenia, and they do not test whether the same account applies to the intellectual disability, autism, anxiety and mood phenotypes that are more common in this population than psychosis is (Schneider et al., 2014). The duplication's dissociated risk profile makes the independence of these outcomes a substantive issue: whatever capacity protects against psychosis apparently does not protect against intellectual disability or autism, and a complete account of the locus will need to explain all of these outcomes.

A fifth boundary is methodological and applies to the whole field. Several of the most-cited findings in this literature rest on designs that cannot address the question they are used to answer, several on cellular systems whose identity has since been questioned, and several more on cross-sectional comparisons of a measure now known to reverse sign across puberty. Building penetrance claims on carriers-versus-controls comparisons, barrier claims on cells of uncertain lineage, and developmental claims on age-pooled samples has produced a confident narrative with a thin foundation. The remedy is not more mechanisms. It is three-group designs, challenge-evoked measurement, authenticated cellular systems, age-stratified analysis, and longitudinal sampling through the risk window, which is what Section 11 of the main text specifies.

### S6.1 The form of the comparison, and the over-readings it rules out

One point of form is conceded at the outset. H1 is itself a threshold model: psychosis occurs when D − C exceeds zero. What distinguishes it from H2 is what lies on either side of the threshold: in H1 the liability is a within-person state composed of two separately measurable and manipulable terms, one of which is an active process that overshoots; in H2 it is a fixed sum with no such process. Every discriminating observation in Table 4 follows from that difference. Liability models that add a compensatory process to H2 converge on H1 and are tested by the same observations, and the claim that "no rival predicts" a result is made throughout against these five specified forms, not against every model that could be written.

That restriction has to be honored in both directions, and five over-readings are disclaimed because the main argument depends on not committing them.

First, statistical additivity does not require biological pathways to operate independently, so demonstrating pathway interaction does not by itself defeat H2.

Second, additivity does not require every coefficient to be positive, so modifiers that lower risk are fully compatible with it.

Third, a fixed reduction in maximum capacity can produce disproportionate impairment under high load without any compensatory overshoot, so load-dependence alone does not establish active compensation.

Fourth, persistent structural abnormality is compatible with fluctuating symptoms, so the symptom dynamics of Section 7 do not by themselves establish that the underlying state is a balance rather than a lesion.

Fifth, an age-dependent regulatory trajectory is one way to implement a developmental program rather than an alternative to one, and dopamine being downstream of regulator loss, or beneficial before illness, does not exclude its acting as a convergent mediator of positive symptoms at onset.

What survives these concessions is narrow, and is the whole of what Table 4 claims: among the five specified forms, only H1 predicts an *actively recruited, costly, suppressible* compensatory process that is strongest in carriers who remain well. H5 matches H1 on timing, on signed modifiers and on symptom timescales, and differs from it only there, which is why Study 1's perturbation arm, and not any observational contrast, is what separates them.

## S7 Design Specifications for the Four Falsification Programs

The four programs in Section 11 of the main text are stated there as claim at risk, prediction, design, falsifying result and current state. This section carries the specifications a reader would need in order to run them.

### S7.1 The decision rule, stated in full

For every primary contrast the preregistration fixes a minimum meaningful effect δ and reports a 90% confidence interval. Four outcomes are defined, and each label is restricted to what the interval supports.

*Evidence against the stipulated magnitude*: the upper bound lies below δ. What this rejects is an effect as large as δ, which is what the model's claims are about; it does not establish that the quantity is unchanged, and it must not be reported as showing that compensation does not exist.

*A positive effect compatible with the stipulated magnitude*: the lower bound lies above zero and the upper bound is not below δ. With δ = 0.4, an interval of [0.05, 0.45] falls here. It establishes a positive effect and leaves δ compatible with the data; it does not establish an effect of at least δ, and must not be reported as though it did.

*Evidence for an effect at least as large as δ*: the lower bound exceeds δ. This is the only outcome that licenses the stronger statement, and the power calculations below show it is out of reach at feasible samples unless the true effect is well above δ.

*Inconclusive*: anything else. An interval of −0.2 to +0.9 against δ = 0.4 includes both zero and a meaningful effect and decides nothing; it is reported as inconclusive and the study is treated as underpowered for that contrast.

Two definitions are fixed here because every program uses them. A **carrier who remains well** is a currently unaffected adult aged at least 30 at sampling, assessed with a structured diagnostic interview and free both of psychotic disorder and of threshold psychosis-spectrum symptoms; the age floor matters because the risk period extends into the twenties, so the 22-to-26-year-old donors in existing cellular work were still inside it (Li et al., 2021; Schneider et al., 2014) and a protected classification based on them is provisional. And every primary hypothesis is **signed** in the direction Table 1 gives and specified **challenge-evoked** wherever the biology permits, because the model's claims are about what a system can be made to do under load rather than about resting levels. This intersection–union rule replaces both the composite rule and any majority-of-axes rule; where a pattern is predicted, support requires every component, while refutation requires at least one component's upper bound below δ under simultaneous limits across the required contrasts.

Composite endpoints are not used. The model predicts opposite directions for different quantities, so a signed average cancels and a sign-reversed average would reward the largest protein deficit; and the quantities carry different units, so no common scale exists without a measurement model. Where the model predicts a pattern across quantities, the primary analysis is an intersection–union test in which every required contrast must meet its criterion. This replaces both the composite rule and any majority-of-axes rule.

### S7.2 Study 1: cellular systems, derivation method and lineage authentication

Derivation method is prespecified rather than left to convenience, because it determines which of the model's claims a cellular assay can address. Induced pluripotency resets age-associated signatures, so iPSC-derived neurons from a 35-year-old carrier who remained well assay what that donor's genome specifies, not what their biology has been through. Direct conversion of fibroblasts to induced neurons bypasses the pluripotent state and retains more of the donor's acquired signature. The two hypotheses are therefore assigned to the two systems: the dosage hypothesis, that intrinsic capacity is set by copy number, is tested in iPSC-derived neurons, where erasure of acquired state is an advantage; the consumption hypothesis, that capacity is spent during the risk period, is tested in directly converted neurons from the same donors, where it is not. Donor age at or above 30 in the unaffected carrier group improves clinical classification and does nothing by itself to guarantee that derived cells retain the residue of having passed through the risk period; the derivation choice is what addresses that, and it is a limitation of the consumption arm rather than a solved problem. Where the two systems disagree, the disagreement is reported as a finding about derivation rather than resolved in favor of either.

The endothelial arm requires a methodological correction before it can contribute. Cells are generated either by transcription-factor-directed specification with verified vascular lineage identity or by an alternative protocol, and lineage authentication against primary brain endothelium is a prespecified gate that must be passed before barrier endpoints are analyzed, because the widely used induced protocol yields cells of neuroectodermal epithelial rather than endothelial identity (Lu et al., 2021).

Three assay definitions are fixed in advance, because each has been conflated with a different quantity in this literature. Respirometry reports basal, maximal and spare respiration as three numbers: maximal respiration is the capacity measure, basal respiration is the demand proxy, and spare respiratory capacity, their difference, is the reserve. Reporting the margin alone would allow a fall in demand to be read as a rise in capacity, which is the distinction the model exists to preserve. Adenosine triphosphate is measured as content, which is what the luminescent assay reports and what Li et al. (2021) measured; production flux is a different quantity and is not claimed from it. Presynaptic protein abundance is an abundance measure and not a measure of turnover or maintenance rate, and the endpoint is protein conditional on transcript in a donor-level regression rather than a ratio of ratios.

**Each of those three is a proxy, and none of them is the quantity itself.** Basal oxygen consumption indexes *realized* consumption rather than required demand, since a cell that cannot meet its requirements does not thereby report the size of the shortfall, and it includes proton leak, which is not work done on the regulated variable. Maximal respiration is elicited by chemical uncoupling and is therefore an upper bound on electron transport rather than maximal physiological ATP production under load. Spare respiratory capacity inherits the error in both. Three consequences follow for what the cellular program can claim. A negative spare capacity in a dish is not a validated psychosis threshold, and nothing in this design makes it one. Respiration and the accuracy of firing-rate restoration cannot enter the same subtraction unless a demand term is defined on each scale, which is why the two are reported separately and never combined. And making the margin interpretable as a threshold would require three things this literature does not yet have: a controlled workload rather than a resting measurement, a physiological output measured on the same cells, and a demonstrated correspondence between the assay margin and the clinical construct. Until those exist, the respirometry endpoints test the model's *orderings*, which is what Study 1 is powered for, and not its threshold.

### S7.3 Study 1: primary analysis, minimum meaningful effect and sample size

The primary analysis is an intersection–union test over three prespecified contrasts, each with its own direction and each evaluated under the rule of Section S7.1: effort higher in carriers who remain well than in controls; effort higher in carriers who remain well than in carriers with psychosis; and effective capacity higher in carriers who remain well than in carriers with psychosis. All three run in directly converted neurons, the preparation assigned in Section S7.2 to consumption and to maintenance demand, so that the primary result is a statement about

per-cell energetic load in cells that retain donor age. The iPSC-derived and organoid arms are prespecified replications of the same three contrasts, and the organoid arm alone carries the remodeling-demand endpoint, which a monolayer cannot express. Agreement across preparations strengthens the result; disagreement is reported as such and does not substitute for the primary test. The pattern counts as supported only if all three criteria are met, and failure of any one is evidence against the pattern. The strong form adds a fourth contrast, effective capacity above controls, and is evaluated separately so that its failure does not propagate to the core. Donor, clone within donor, and differentiation batch are random effects. The minimum meaningful effect is fixed in advance at a standardized difference of 0.4, roughly half the effect reported by Li et al. (2021), so that a substantially attenuated true effect still counts.

Falsification is not the mirror image of this rule, and the preregistration separates them. An intersection–union test is conservative for *support*: every contrast must pass, and the global type I error is controlled at the level of each. It is not conservative for *rejection*. If the model were declared falsified whenever any one of three contrasts had an upper bound below δ, three chances to reject would be taken at the nominal level of one, and the probability of a false global rejection would exceed it. Global rejection is therefore governed by its own prespecified rule: simultaneous 90% bounds across the three contrasts, with the model counted as falsified only when at least one bound lies below δ under those simultaneous limits, or, equivalently, a calibrated joint criterion whose false-rejection rate under the model is fixed in advance by the same simulation that fixes the sample size. A single contrast whose interval contains both zero and δ is inconclusive for that contrast and contributes to neither decision.

Where the model predicts that the psychosis group sits near control level, that is assessed against a prespecified equivalence bound and reported as equivalence or as indeterminate. A nonsignificant difference is never reported as evidence of equality.

Sample size is computed for this rule rather than for a conventional two-sided test of a single axis, by simulation. Twenty thousand datasets were generated per condition with two correlated endpoints per donor ($r = 0.3$), equal group sizes, and each contrast required to have a 90% interval excluding zero. If the true standardized effects are as large as those reported by Li et al. (2021), around $d = 0.8$, the conjunction is satisfied in 57% of simulated studies at 20 donors per group, 93% at 40 and 97% at 50. At $d = 0.6$ the same rule reaches 78% at 50 per group, 86% at 60 and 95% at 80. At $d = 0.4$, which is δ itself, it reaches 43% at 60 per group, 72% at 100 and 82% at 120. The cost of the conjunction is substantial and is the price of testing a pattern rather than a single contrast: at $d = 0.4$ and 60 donors per group, the average single contrast has about 70% power while the conjunction has 43%.

The stricter tier is harder still. Requiring the lower bound to exceed δ on all three contrasts is attained in 82% of simulated studies only at 120 donors per group with $d = 0.8$, in 17% at 120 per group with $d = 0.6$, and essentially never when the true effect equals δ. The proposed expectation is therefore the compatible-positive tier, which would be stated in the

preregistration in advance so that the weaker label is not presented afterward as the stronger one. The proposed target is 50 donors per group with an interim assessment of the variance components; a 20-per-group stage is a pilot that estimates those components and is not the test. Clones improve reliability and partition variance but are not independent donors and do not substitute for them.

### S7.4 Study 1: secondary analyses relating modifier burden to compensatory capacity

Donor-level schizophrenia polygenic score, rare copy-number burden, and rare genic tandem repeat burden are related to the compensation vector within the carrier groups. The model predicts that each modifier class is negatively associated with measured capacity, which is what it means to claim that modifiers act by narrowing an already-narrowed range rather than by adding independent liability (Bassett et al., 2017; Cheng et al., 2026; Davies et al., 2020). A null here would not falsify Proposition 4, but it would sever the model's link to the one body of penetrance-relevant human genetic evidence that exists, and Section S4 would have to be withdrawn.

### S7.5 Study 2: covariate handling and specificity comparisons

Intelligence quotient is treated as a covariate with a prespecified estimand, not as a matching variable and not as an automatic adjustment. Reduced IQ is an intrinsic feature of the deletion and matching on it misrepresents the phenotype (Mancini et al., 2026); the duplication's association with intellectual disability creates the same problem in the opposite direction; and adjusting for a variable that lies on the causal path from dosage to capacity would remove part of the effect under study. The primary estimand is therefore the total effect of copy number on capacity without IQ adjustment. IQ-adjusted estimates are reported as a sensitivity analysis and are described as *IQ-adjusted associations*. Calling such a coefficient a direct effect unmediated by general cognitive ability would require a causal model with assumptions this design does not supply, and that description is not used.

Autism and intellectual disability phenotypes are measured dimensionally in all three groups. They are *specificity comparisons*, not negative controls: the genetic exposure affects them, so they fail the defining condition of a negative control. Two inferences are licensed and a third is not. If a capacity measure tracks intellectual disability and autism severity in the same direction in which it tracks protection from psychosis, it indexes general neurodevelopmental burden and the model's explanation of the dissociated risk profile fails. If it tracks protection from psychosis and not the other two, the schizophrenia-relevant interpretation survives this test. But a capacity measure associated with better outcomes across several domains does not refute the model on its own, because the duplication may raise autism and intellectual-disability risk through a route the model locates elsewhere, in the timing requirements of early construction rather than in correction capacity (Section 10 of the main text).

### S7.6 Study 3: assessment schedule, proxy validation and estimands

Clinical assessment is six-monthly, with structured psychosis-spectrum interview and affective measures at every wave, and biological sampling is annual with an additional event-triggered collection within eight weeks of any change in symptom status.

The sampling scheme bounds what can be concluded, and the bound is stated rather than left implicit. A sample collected after a transition cannot reconstruct a decline over the preceding months, and treatment begun at transition may itself alter the post-transition measure. Event-triggered sampling therefore detects that a change has occurred; it does not recover the biology that preceded it. Three consequences are fixed in the preregistration. The temporal prediction is evaluated only in participants with a biological sample within a prespecified interval before the event. Onset is treated as interval-censored between assessment waves rather than dated to a visit. And participants without an adequately timed pre-event sample are counted as uninformative for the temporal test, not as instances of "no preceding decline"; reporting them as the latter would convert a sampling limitation into evidence.

The peripheral compensation index must clear a two-layer validation before it is used as primary, because a marker can correlate with central biology between people while failing to track central change within a person, and it is within-person change that this study is about. The first layer is cross-sectional correspondence: against induced-neuron measures of effort and capacity from the same donors in a subset, and against a central measure in the scanned subsample. The second layer is longitudinal, and it is the one that licenses the inference: prespecified thresholds for test–retest reliability over an interval matched to the sampling schedule, for responsiveness to a challenge of known direction, and for correspondence of *change* in the peripheral index with change in the central or induced-neuron measure. Until the second layer is met, a peripheral null is uninterpretable with respect to the central mechanism and is reported as such rather than as evidence against the model. The requirement is sharpened by the one blood transcriptome study to date having found respiratory and protein-folding transcripts elevated in carriers *with* psychosis (Jalbrzikowski et al., 2015), which under the model's definitions is effort rather than capacity, so the index must separate the two before either can be tracked.

Within-person estimands are fitted in models that separate stable between-person differences from within-person change, such as random-intercept cross-lagged or latent growth formulations, because conventional cross-lagged panel coefficients conflate the two (Hamaker et al., 2015). The primary within-person estimand is whether change in the compensation index predicts subsequent change in symptom severity after adjustment for age, sex, deletion extent, medication, cannabis exposure and baseline symptoms, with the reverse-ordered model fitted as the comparator. At remission, the two routes the model permits are distinguished by fitting change in capacity and change in the demand proxy as separate predictors, so that remission with capacity flat and demand falling is recorded as such rather than as a failure of the model. Affective state is modeled as a time-varying covariate because

dysphoric mood and anxiety predict both emergence and remission in this population (Tang et al., 2017). With two imaging occasions, the identifiable dopamine–connectivity estimand is the baseline-to-second-occasion change in coupling contrasted between those who transition and those who do not; pre-transition, transition and post-remission trajectories within one person are not identifiable with two scans and are not claimed. The benefit and cost claims of Proposition 6 are estimated separately, and the symptom association is additionally fitted with connectivity in the model, since a cost that disappears on adjustment for connectivity is not a separate consequence. Medication status, illness stage and range restriction are modeled explicitly, because each can produce a change in the sign of a coupling estimate without any change in the underlying mechanism. Measurement-specific least-significant-change thresholds are established from test–retest data so that apparent declines smaller than measurement error are not interpreted.

### S7.7 Study 3: expected transition counts

Sample size is governed by transition count rather than cohort size, and the relevant transitions run in both directions. Four event types are counted separately, because they have different base rates and different scopes of inference: emergence of subthreshold psychosis-spectrum symptoms; onset of threshold psychotic disorder; remission of positive symptoms; and recurrence within the same participant. The preregistration reports the simulated distribution of each separately and never a pooled figure.

The estimate below is reproducible from the assumptions in the table, which is its purpose; the figures are planning inputs, not findings.

| Input | Assumed value | Source or basis |
|---|---|---|
| **Cohort size at entry** | 400 carriers | Planning assumption, consortium-scale |
| **Entry age** | Uniform, 12 to 18 years | Design |
| **Follow-up** | To age 25; mean planned follow-up 10 years for uniform entry at 12 to 18 | Design |
| **Symptomatic at entry** | 57% | 41 of 72 clinically classified participants were remitting or persistent (Tang et al., 2017) |
| **Emergence, initially asymptomatic** | 29% per ~3 years | Tang et al. (2017) |
| **Remission, initially symptomatic** | 39% per ~3 years | Tang et al. (2017) |
| **Cumulative threshold disorder by young adulthood** | 25% | Gur et al. (2023); Schneider et al. (2014) |
| **Annual attrition** | 8% | Planning assumption |
| **Recurrence after remission** | Permitted; same hazard as first emergence | Planning assumption |

Under those inputs, and counting only transitions that occur while a participant is still enrolled, a cohort of 400 yields on the order of 85 first emergences of subthreshold symptoms, 210 remissions, 75 recurrences and 55 onsets of a threshold disorder, which is about 370 observed status transitions in all. Attrition is the dominant loss: at 8% per year, about 43% of the cohort remains after ten years, and roughly 175 participants complete follow-up to age 25.

The counts that matter are smaller again, and they are not interchangeable. The temporal falsifier requires a usable biological sample inside a prespecified interval before the event, which at 90% visit completion and 90% assay yield with annual sampling retains about four fifths: roughly 70 emergences, 170 remissions, 60 recurrences and 45 threshold onsets. The figure that bears on the indispensable claim of Section 11.5, that capacity declines within person *before* symptoms emerge, is the first of those, about 70, and not a pooled 290. A pooled count is dominated by remissions, which test a different prediction, and reporting it as though it powered the temporal falsifier would overstate that test fourfold. The preregistration reports the four distributions separately and never a pooled figure, and Study 3 is powered on the emergence count.

Two scope conditions follow and would be stated in the preregistration. A cohort powered on subthreshold emergence tests the model's claims about transitions in psychosis-spectrum status, and does not automatically test every claim that has been made about schizophrenia onset or about remission from established schizophrenia. And the temporal falsifier is restricted to participants with an adequately timed pre-event sample; onset timing is interval-censored between assessments, treatment initiation at transition is modeled as a potential influence on post-transition measures, and participants without such a sample are counted as uninformative for that test rather than as evidence of no preceding decline. Existing consortium infrastructure makes this feasible at a scale no single site could reach (Davies et al., 2020; Gur et al., 2023; Lin et al., 2023; Schneider et al., 2014).

### S7.8 Study 4: dosing windows, engagement and assessment schedule

Interventions are not sorted by whether their target lies inside the deleted interval, and the model makes no prediction that turns on that distinction. Three considerations rule it out. GSK3 is itself a regulatory node, so a target outside the interval is not thereby confined to correcting a level. Benefit outlasting cessation is already established for that target: the nonselective GSK3 inhibitor SB-216763, from P7 to P28, restored working memory and ventral hippocampal–prefrontal theta synchrony in Df(16)A+/− mice tested at three to five months (Tamura et al., 2016); the same compound on a near-identical schedule, to P27, rescued adult temporal-order memory in LgDel mice at about PND110 (Alvino et al., 2025); and the GSK3B-selective inhibitor BRD3731, ten injections from P7 to P27, improved working memory and *raised* vHPC–prefrontal theta coherence in adult male Df(16)A+/− mice, raised rather than restored, since coherence was not significantly reduced in mutants of either sex at baseline (Passecker et al., 2026). The GSK3A-selective BRD0705 was null in that experiment but restored adult spatial working memory in the same model and window when the task was run under

increased working-memory demand (Passecker et al., 2025), which is the load-dependence Proposition 2 predicts and the reason Study 4's endpoints are specified challenge-evoked. And durability is endpoint-specific within a single experiment rather than a property of an intervention class: in the same animals in which adult temporal-order memory was rescued, the juvenile normalization of functional connectivity did not persist, adult hippocampal hypoconnectivity was unaffected, and sociability deficits were not rescued at either age (Alvino et al., 2025).

The design therefore crosses *dosing window* with target class rather than varying target class alone. Three windows are used, namely pre-adolescent, peri-adolescent at the inflection, and post-adolescent after the phenotype has emerged, and sex is crossed throughout, because the existing data make it a factor and not a covariate: BRD3731 improved working memory in male mutants, did nothing in female mutants, and impaired it in wild-type females, with a sex-by-treatment interaction and no sex difference in brain drug concentration, in a line where *Gsk3b* expression runs above the wild-type level in males and below it in females at P7 and P28 (Passecker et al., 2026). Note that the harmed group is the wild-type females, not the group with reduced expression, so the result establishes sex-dependent treatment effects and opposite genotype-related expression differences by sex; it does not itself establish a within-animal rule relating pretreatment deviation to the direction of response, which is what the sign arm of this study tests.

Testing that sign prediction requires knowing each animal's pretreatment regulator level, and the proposed regulators are regional brain transcripts and microRNAs that are ordinarily obtained from tissue. Three routes are available, and the preregistration states which inference each arm supports. A validated live reporter of the regulator, or a nondestructive peripheral proxy with demonstrated correspondence to the regional measure, supports the within-animal prediction as stated. Sentinel littermates sampled at the time of dosing support only a group-level version, in which arms with larger mean deviations show larger mean benefit. Terminal sampling at outcome cannot support either, since the level measured then is post-treatment. Arms without a reporter or a validated proxy are analyzed and reported at the group level only.

Candidate interventions, classified by target for the factorial rather than for prediction: AAV replenishment of miR-338-3p (Chun et al., 2017) or of miR-25 and miR-185 (Earls et al., 2012); re-expression of *Txnrd2* (Fernandez et al., 2019); enhancement of mitochondrial biogenesis (Li et al., 2021); neonatal intranasal oxytocin, which raises claudin-5 (Castellani et al., 2025); nonselective and GSK3B-selective GSK3 inhibition (Alvino et al., 2025; Passecker et al., 2026; Tamura et al., 2016); N-acetylcysteine (Fernandez et al., 2019); and D2 antagonism (Chun et al., 2014; Khan et al., 2020). Each arm is titrated in pilot work to a prespecified fractional restoration of its proximal variable. Because equal fractional restoration of two different proximal variables does not imply equal functional potency, the interchangeability question is addressed only where dose–response curves on a common functional mediator can be estimated for both arms, and unequal benefit at equal fractional restoration is not by itself read as evidence for a privileged pathway.

Cessation must be demonstrable and engagement must be measured at outcome, which is the design problem the existing literature leaves open: none of the four GSK3 studies assayed target engagement months after dosing, so what they establish is benefit outlasting *dosing*, not benefit outlasting *disengagement*. For microRNA replenishment, the construct is placed under inducible control so that expression can be switched off at a defined time, or expression is reversed by antagomir delivery, and disengagement is verified by measuring the restored microRNA and its target after cessation. For drugs, washout is followed by verification that the proximal variable has returned toward its pretreatment value. Persistence is defined as benefit that survives verified disengagement.

The pretreatment level and direction of the targeted regulator are measured in every animal before dosing, so that the sign prediction can be tested directly rather than inferred from a group difference: the model predicts that animals whose regulator is deviated in the direction the intervention opposes will benefit, and that animals deviated the other way will be harmed by the same dose.

Outcomes are measured at three levels and at two times, immediately after treatment and after verified cessation: the targeted proximal variable; the synaptic supply variable of Proposition 3 and the circuit measures of Section 5; and the adolescence-dependent behavioral phenotypes, with the constitutive sensorimotor gating deficit measured as a specificity control, since the model predicts window effects only for the former. Persistence is analyzed per endpoint rather than per intervention, because the Alvino result shows the two can diverge within one animal.

### S7.9 Current state of the evidence for each program

**Study 1.** One study has measured compensatory machinery in a three-group design, in four lines per carrier group and six controls, finding the predicted ordering on the four regulators, with mtDNA copy number above the psychosis group but not above controls and output reduced only in the psychosis group (Li et al., 2021). No challenge-evoked measure, no presynaptic protein-to-transcript contrast, no perturbation arm and no barrier measure has been obtained in a three-group design.

**Study 2.** The protective effect and the dissociated risk profile are established (Rees et al., 2014). The inverse dose-response rests on one study of 21 deletion carriers, 12 duplication carriers and 26 controls (Rogdaki et al., 2023). No capacity or effort measure exists in duplication carriers.

**Study 3.** No study has measured any compensation variable longitudinally in this population. Symptom dynamics are established (Tang et al., 2017), cognitive decline before onset is established (Davies et al., 2020; Gur et al., 2023; Vorstman et al., 2015), the dopamine–connectivity coupling has been measured once, cross-sectionally (Mancini et al., 2026), and within-carrier peripheral signals exist but have not been related to capacity (Jalbrzikowski et al., 2015; Mekori-Domachevsky et al., 2017; O'Hora et al., 2024).

**Study 4.** Benefit outlasting dosing is established for developmental GSK3 inhibition on cognitive and prefrontal–hippocampal synchrony endpoints across four studies and two mouse lines (Alvino et al., 2025; Passecker et al., 2025, 2026; Tamura et al., 2016), and absent for resting connectivity and sociability in one of them. Benefit under raised demand from a compound null at baseline is established in one of them (Passecker et al., 2025). Late restoration of a depleted regulator rescues a mature circuit phenotype under continued expression (Chun et al., 2017), and *Txnrd2* re-expression and N-acetylcysteine each rescue the layer 2/3 phenotype under continuous conditions (Fernandez et al., 2019). No study has verified disengagement at outcome, crossed target class with dosing window, stratified on pretreatment regulator direction, or titrated two interventions to equal fractional restoration.

### S7.10 What would not count as evidence against the model

Six results are specified in advance as uninformative rather than disconfirming, so that the model cannot be credited with surviving tests it never faced and cannot be rejected on tests it never licensed.

A null on resting measures alone, where no challenge-evoked measure was obtained, because resting output in a compensating carrier is predicted to be normal — the model's content is in what a system can be made to do under load.

A null in a sample pooled across puberty on a measure known to reverse sign with age (Alvino et al., 2025), since a pooled mean of a quantity that changes sign depends on the age composition of the sample.

A deletion phenotype that fails to separate carriers by psychosis status. The model expects this for most deletion phenotypes, the calcium phenotype among them (Khan et al., 2020); such a result bears on what the deletion causes and not on penetrance.

A peripheral null obtained with an index that has not met the reliability, responsiveness and correspondence thresholds of Section S7.6. An unvalidated proxy returning no signal is uninformative about the quantity it was meant to proxy.

Remission without capacity recovery, provided demand is shown to have fallen. Section 11.3 permits two routes to remission, and a result consistent with the second is not evidence against the first.

An upper bound below δ reported as evidence that compensation does not exist. What such a bound rejects is an effect at least as large as δ; the distinction is fixed in Section S7.1 and is not a matter of interpretation after the fact.

## Supplementary Figure

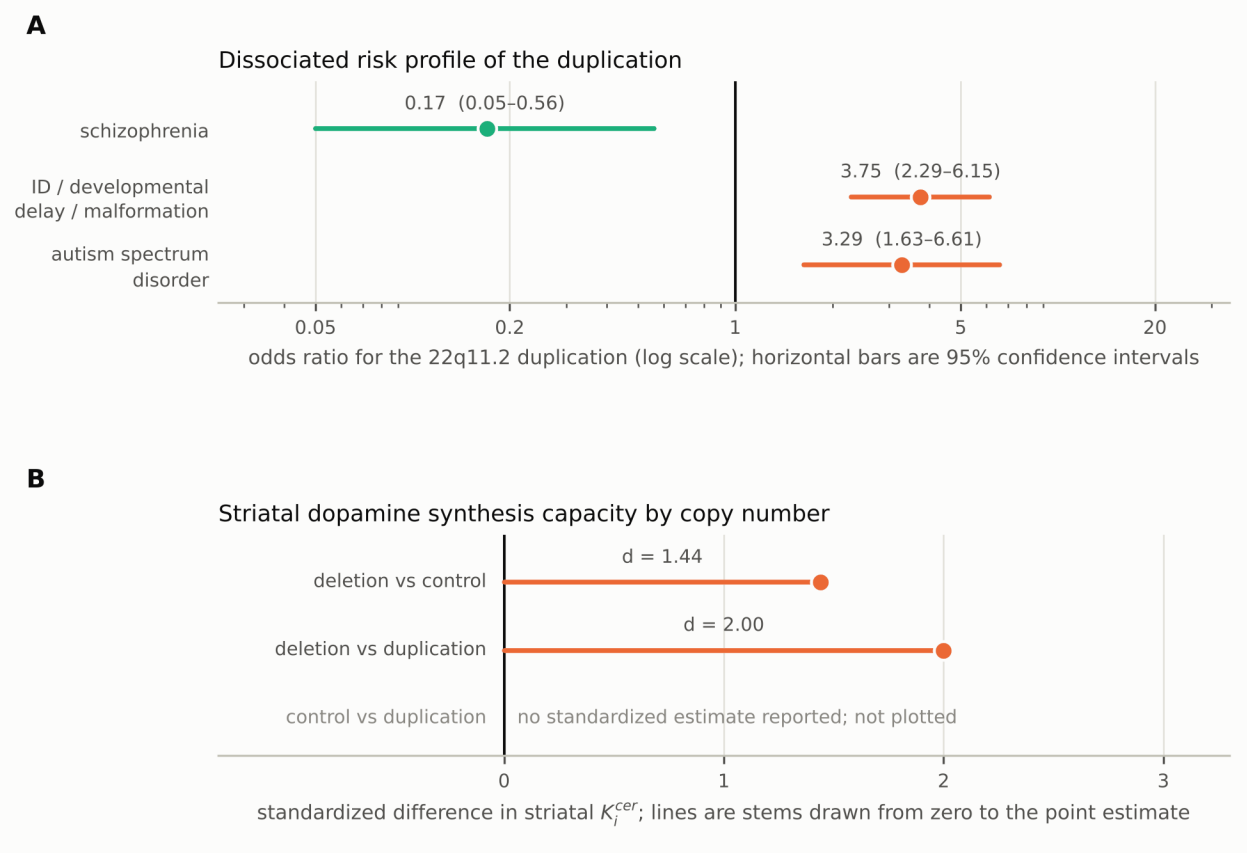



**Figure S1. The reciprocal copy-number series, showing only reported contrasts. (A)** Outcome risk for 22q11.2 duplication carriers relative to the general population, as odds ratios with 95% confidence intervals from Rees et al. (2014): schizophrenia 0.17 (0.05–0.56), intellectual disability, developmental delay and congenital malformation 3.75 (2.29–6.15), autism spectrum disorder 3.29 (1.63–6.61). Horizontal bars are confidence intervals. The deletion's roughly twentyfold schizophrenia risk is a relative-risk multiplier from other studies and is not plotted on this scale. **(B)** Striatal dopamine synthesis capacity across the copy-number series as reported by Rogdaki et al. (2023) in 21 deletion carriers, 12 duplication carriers and 26 controls, all antipsychotic-naive: an inverse linear effect of copy number on whole-striatal $K_i^{cer}$ ($B = -1.2 \times 10^{-3}$ min$^{-1}$ per copy, $SE = 2 \times 10^{-4}$, $p < 0.001$), with deletion carriers exceeding controls by Cohen's $d = 1.44$ and duplication carriers by $d = 2.00$ after adjustment for multiple comparisons. The horizontal lines here are stems drawn from zero to the point estimate, not uncertainty intervals. Only the two standardized contrasts the paper reports are plotted. The duplication-versus-control difference was examined voxelwise and appeared in bilateral caudate at $p < 0.05$ uncorrected but did not survive familywise-error (FWE) correction, so no standardized value exists for it and none is plotted; the row carries a text annotation instead, since any plotted position on an effect-size axis would communicate an estimate the source does not provide. The figure plots contrasts rather than group means for comparability across the two panels; the source does report group means with standard errors. Ordered group means are not evidence that every adjacent pair differs.

## Supplementary References

Alvino, F. G., Gini, S., Minetti, A., Pagani, M., Sastre-Yagüe, D., Barsotti, N., De Guzman, E., Schleifer, C., Stuefer, A., Kushan, L., Montani, C., Galbusera, A., Papaleo, F., Kates, W. R., Murphy, D., Lombardo, M. V., Pasqualetti, M., Bearden, C. E., & Gozzi, A. (2025). Synaptic-dependent developmental dysconnectivity in 22q11.2 deletion syndrome. *Science Advances, 11*(11), eadq2807. https://doi.org/10.1126/sciadv.adq2807

Bagautdinova, J., Zöller, D., Schaer, M., Padula, M. C., Mancini, V., Schneider, M., & Eliez, S. (2021). Altered cortical thickness development in 22q11.2 deletion syndrome and association with psychotic symptoms. *Molecular Psychiatry, 26*(12), 7671–7678. https://doi.org/10.1038/s41380-021-01209-8

Bassett, A. S., Lowther, C., Merico, D., Costain, G., Chow, E. W. C., van Amelsvoort, T., McDonald-McGinn, D., Gur, R. E., Swillen, A., Van den Bree, M., Murphy, K., Gothelf, D., Bearden, C. E., Eliez, S., Kates, W., Philip, N., Sashi, V., Campbell, L., Vorstman, J., … Marshall, C. R., & International 22q11.2DS Brain and Behavior Consortium. (2017). Rare genome-wide copy number variation and expression of schizophrenia in 22q11.2 deletion syndrome. *American Journal of Psychiatry, 174*(11), 1054–1063. https://doi.org/10.1176/appi.ajp.2017.16121417

Castellani, G., Ciampoli, M., Benedetti, A., Ferretti, V., Trigilio, G., Barcik, W., Busnelli, M., Contarini, G., Paolini, C., Devroye, C., Rodriguez Aburto, M., Cucinelli, A., Antonelli, F., Maltese, F., Braccia, C., Pacinelli, G., Managò, F., Rodríguez-Gimeno, A., Mazzarella, M. A., … Papaleo, F. (2025). Oxytocin seals the blood–brain barrier, improving 22q11.2 deletion syndrome trajectories. *Brain, 148*(9), 3184–3198. https://doi.org/10.1093/brain/awaf112

Cheng, M., Yin, Y., Engchuan, W., Heung, T., International 22q11.2 Brain Behavior Consortium, Morrow, B. E., Bassett, A. S., & Yuen, R. K. C. (2026). Genome-wide tandem repeat expansions modify schizophrenia risk in the presence of a 22q11.2 deletion. *Molecular Psychiatry, 31*, 4934–4946. https://doi.org/10.1038/s41380-026-03574-8

Chun, S., Du, F., Westmoreland, J. J., Han, S. B., Wang, Y.-D., Eddins, D., Bayazitov, I. T., Devaraju, P., Yu, J., Mellado Lagarde, M. M., Anderson, K., & Zakharenko, S. S. (2017). Thalamic miR-338-3p mediates auditory thalamocortical disruption and its late onset in models of 22q11.2 microdeletion. *Nature Medicine, 23*(1), 39–48. https://doi.org/10.1038/nm.4240

Chun, S., Westmoreland, J. J., Bayazitov, I. T., Eddins, D., Pani, A. K., Smeyne, R. J., Yu, J., Blundon, J. A., & Zakharenko, S. S. (2014). Specific disruption of thalamic inputs to the auditory cortex in schizophrenia models. *Science, 344*(6188), 1178–1182. https://doi.org/10.1126/science.1253895

Cleynen, I., Engchuan, W., Hestand, M. S., Heung, T., Holleman, A. M., Johnston, H. R., Monfeuga, T., McDonald-McGinn, D. M., Gur, R. E., Morrow, B. E., Swillen, A., Vorstman, J. A. S., Bearden, C. E., Chow, E. W. C., van den Bree, M., Emanuel, B. S., Vermeesch, J. R., Warren, S. T., Owen, M. J., … Bassett, A. S. (2021). Genetic contributors to risk of schizophrenia in the presence of a 22q11.2 deletion. *Molecular Psychiatry, 26*(8), 4496–4510. https://doi.org/10.1038/s41380-020-0654-3

Crabtree, G. W., Park, A. J., Gordon, J. A., & Gogos, J. A. (2016). Cytosolic accumulation of L-proline disrupts GABA-ergic transmission through GAD blockade. *Cell Reports, 17*(2), 570–582. https://doi.org/10.1016/j.celrep.2016.09.029

Crockett, A. M., Ryan, S. K., Hernandez Vásquez, A., Canning, C., Kanyuch, N., Kebir, H., Ceja, G., Gesualdi, J., Zackai, E., McDonald-McGinn, D., Viaene, A., Kapoor, R., Benallegue, N., Gur, R., Anderson, S. A., & Alvarez, J. I. (2021). Disruption of the blood–brain barrier in 22q11.2 deletion syndrome. *Brain, 144*(5), 1351–1360. https://doi.org/10.1093/brain/awab055

Das, S. C., Hjelm, B. E., Rollins, B. L., Sequeira, A., Morgan, L., Omidsalar, A. A., Schatzberg, A. F., Barchas, J. D., Lee, F. S., Myers, R. M., Watson, S. J., Akil, H., Bunney, W. E., & Vawter, M. P. (2022). Mitochondria DNA copy number, mitochondria DNA total somatic deletions, Complex I activity, synapse number, and synaptic mitochondria number are altered in schizophrenia and bipolar disorder. *Translational Psychiatry, 12*(1), 353. https://doi.org/10.1038/s41398-022-02127-1

Davies, R. W., Fiksinski, A. M., Breetvelt, E. J., Williams, N. M., Hooper, S. R., Monfeuga, T., Bassett, A. S., Owen, M. J., Gur, R. E., Morrow, B. E., McDonald-McGinn, D. M., Swillen, A., Chow, E. W. C., van den Bree, M., Emanuel, B. S., Vermeesch, J. R., van Amelsvoort, T., Arango, C., Armando, M., … Vorstman, J. A. S. (2020). Using common genetic variation to examine phenotypic expression and risk prediction in 22q11.2 deletion syndrome. *Nature Medicine, 26*(12), 1912–1918. https://doi.org/10.1038/s41591-020-1103-1

Devaraju, P., Yu, J., Eddins, D., Mellado-Lagarde, M. M., Earls, L. R., Westmoreland, J. J., Quarato, G., Green, D. R., & Zakharenko, S. S. (2017). Haploinsufficiency of the 22q11.2 microdeletion gene *Mrpl40* disrupts short-term synaptic plasticity and working memory through dysregulation of mitochondrial calcium. *Molecular Psychiatry, 22*(9), 1313–1326. https://doi.org/10.1038/mp.2016.75

Earls, L. R., Fricke, R. G., Yu, J., Berry, R. B., Baldwin, L. T., & Zakharenko, S. S. (2012). Age-dependent microRNA control of synaptic plasticity in 22q11 deletion syndrome and schizophrenia. *The Journal of Neuroscience, 32*(41), 14132–14144. https://doi.org/10.1523/JNEUROSCI.1312-12.2012

Fernandez, A., Meechan, D. W., Karpinski, B. A., Paronett, E. M., Bryan, C. A., Rutz, H. L., Radin, E. A., Lubin, N., Bonner, E. R., Popratiloff, A., Rothblat, L. A., Maynard, T. M., & LaMantia, A.-S. (2019). Mitochondrial dysfunction leads to cortical under-connectivity and cognitive impairment. *Neuron, 102*(6), 1127–1142. https://doi.org/10.1016/j.neuron.2019.04.013

Gokhale, A., Hartwig, C., Freeman, A. A. H., Bassell, J. L., Zlatic, S. A., Sapp Savas, C., Vadlamudi, T., Abudulai, F., Pham, T. T., Crocker, A., Werner, E., Wen, Z., Repetto, G. M., Gogos, J. A., Claypool, S. M., Forsyth, J. K., Bearden, C. E., Glausier, J., Lewis, D. A., … Faundez, V. (2019). Systems analysis of the 22q11.2 microdeletion syndrome converges on a mitochondrial interactome necessary for synapse function and behavior. *The Journal of Neuroscience, 39*(18), 3561–3581. https://doi.org/10.1523/JNEUROSCI.1983-18.2019

Greene, C., Kealy, J., Humphries, M. M., Gong, Y., Hou, J., Hudson, N., Cassidy, L. M., Martiniano, R., Shashi, V., Hooper, S. R., Grant, G. A., Kenna, P. F., Norris, K., Callaghan, C. K., Islam, M. N., O'Mara, S. M., Najda, Z., Campbell, S. G., Pachter, J. S., … Campbell, M. (2018). Dose-dependent expression of claudin-5 is a modifying factor in schizophrenia. *Molecular Psychiatry, 23*(11), 2156–2166. https://doi.org/10.1038/mp.2017.156

Guo, Y., Singh, L. N., Zhu, Y., Gur, R. E., Resnick, A., Anderson, S. A., & Alvarez, J. I. (2020). Association of a functional Claudin-5 variant with schizophrenia in female patients with the 22q11.2 deletion syndrome. *Schizophrenia Research, 215*, 451–452. https://doi.org/10.1016/j.schres.2019.09.014

Gur, R. E., McDonald-McGinn, D. M., Moore, T. M., Gallagher, R. S., McClellan, E., White, L., Ruparel, K., Hillman, N., Crowley, T. B., McGinn, D. E., Zackai, E., Emanuel, B. S., Calkins, M. E., Roalf, D. R., & Gur, R. C. (2023). Psychosis spectrum features, neurocognition and functioning in a longitudinal study of youth with 22q11.2 deletion syndrome. *Psychological Medicine, 53*(14), 6763–6772. https://doi.org/10.1017/S0033291723000259

Hamaker, E. L., Kuiper, R. M., & Grasman, R. P. P. P. (2015). A critique of the cross-lagged panel model. *Psychological Methods, 20*(1), 102–116. https://doi.org/10.1037/a0038889

Hiroi, N., Hiramoto, T., Harper, K. M., Suzuki, G., & Boku, S. (2012). Mouse models of 22q11.2-associated autism spectrum disorder. *Autism Open Access, S1*, 001. https://doi.org/10.4172/2165-7890.S1-001

Howes, O. D., & Onwordi, E. C. (2023). The synaptic hypothesis of schizophrenia version III: A master mechanism. *Molecular Psychiatry, 28*(5), 1843–1856. https://doi.org/10.1038/s41380-023-02043-w

Jacquet, H., Raux, G., Thibaut, F., Hecketsweiler, B., Houy, E., Demilly, C., Haouzir, S., Allio, G., Fouldrin, G., Drouin, V., Bou, J., Petit, M., Campion, D., & Frébourg, T. (2002). PRODH mutations and hyperprolinemia in a subset of schizophrenic patients. *Human Molecular Genetics, 11*(19), 2243–2249. https://doi.org/10.1093/hmg/11.19.2243

Jalbrzikowski, M., Lazaro, M. T., Gao, F., Huang, A., Chow, C., Geschwind, D. H., Coppola, G., & Bearden, C. E. (2015). Transcriptome profiling of peripheral blood in 22q11.2 deletion syndrome reveals functional pathways related to psychosis and autism spectrum disorder. *PLoS ONE, 10*(7), e0132542. https://doi.org/10.1371/journal.pone.0132542

Karayiorgou, M., & Gogos, J. A. (2004). The molecular genetics of the 22q11-associated schizophrenia. *Molecular Brain Research, 132*(2), 95–104. https://doi.org/10.1016/j.molbrainres.2004.09.029

Khan, T. A., Revah, O., Gordon, A., Yoon, S.-J., Krawisz, A. K., Goold, C., Sun, Y., Kim, C. H., Tian, Y., Li, M.-Y., Schaepe, J. M., Ikeda, K., Amin, N. D., Sakai, N., Yazawa, M., Kushan, L., Nishino, S., Porteus, M. H., Rapoport, J. L., … Paşca, S. P. (2020). Neuronal defects in a human cellular model of 22q11.2 deletion syndrome. *Nature Medicine, 26*(12), 1888–1898. https://doi.org/10.1038/s41591-020-1043-9

Kolar, D., Krajcovic, B., Kleteckova, L., Kuncicka, D., Vales, K., & Brozka, H. (2023). Review: Genes involved in mitochondrial physiology within 22q11.2 deleted region and their relevance to schizophrenia. *Schizophrenia Bulletin, 49*(6), 1637–1653. https://doi.org/10.1093/schbul/sbad066

Li, J., Ryan, S. K., Deboer, E., Cook, K., Fitzgerald, S., Lachman, H. M., Wallace, D. C., Goldberg, E. M., & Anderson, S. A. (2019). Mitochondrial deficits in human iPSC-derived neurons from patients with 22q11.2 deletion syndrome and schizophrenia. *Translational Psychiatry, 9*(1), 302. https://doi.org/10.1038/s41398-019-0643-y

Li, J., Tran, O. T., Crowley, T. B., Moore, T. M., Zackai, E. H., Emanuel, B. S., McDonald-McGinn, D. M., Gur, R. E., Wallace, D. C., & Anderson, S. A. (2021). Association of mitochondrial biogenesis with variable penetrance of schizophrenia. *JAMA Psychiatry, 78*(8), 911–921. https://doi.org/10.1001/jamapsychiatry.2021.0762

Lin, J.-R., Zhao, Y., Jabalameli, M. R., Nguyen, N., Mitra, J., International 22q11.2DS Brain and Behavior Consortium, Swillen, A., Vorstman, J. A. S., Chow, E. W. C., van den Bree, M., Emanuel, B. S., Vermeesch, J. R., Owen, M. J., Williams, N. M., Bassett, A. S., McDonald-McGinn, D. M., Gur, R. E., Bearden, C. E., Morrow, B. E., & Zhang, Z. D. (2023). Rare coding variants as risk modifiers of the 22q11.2 deletion implicate postnatal cortical development in syndromic schizophrenia. *Molecular Psychiatry, 28*(5), 2071–2080. https://doi.org/10.1038/s41380-023-02009-y

Liu, H., Heath, S. C., Sobin, C., Roos, J. L., Galke, B. L., Blundell, M. L., Lenane, M., Robertson, B., Wijsman, E. M., Rapoport, J. L., Gogos, J. A., & Karayiorgou, M. (2002). Genetic variation at the 22q11 PRODH2/DGCR6 locus presents an unusual pattern and increases susceptibility to schizophrenia. *Proceedings of the National Academy of Sciences, 99*(6), 3717–3722. https://doi.org/10.1073/pnas.042700699

Lu, T. M., Houghton, S., Magdeldin, T., Barcia Durán, J. G., Minotti, A. P., Snead, A., Sproul, A., Nguyen, D.-H. T., Xiang, J., Fine, H. A., Rosenwaks, Z., Studer, L., Rafii, S., Agalliu, D., Redmond, D., & Lis, R. (2021). Pluripotent stem cell-derived epithelium misidentified as brain microvascular endothelium requires ETS factors to acquire vascular fate. *Proceedings of the National Academy of Sciences, 118*(8), e2016950118. https://doi.org/10.1073/pnas.2016950118

Mancini, V., Rogdaki, M., Jauhar, S., Moretto, M., Veronese, M., Turkheimer, F., Howes, O. D., & McCutcheon, R. A. (2026). Striatal dopaminergic function and cortical functional connectivity in 22q11.2 deletion syndrome: An integrative multimodal 18F-DOPA PET and magnetic resonance imaging study. *Molecular Psychiatry*. Advance online publication. https://doi.org/10.1038/s41380-026-03839-2

Mancini, V., Saleh, M. G., Delavari, F., Bagautdinova, J., & Eliez, S. (2023). Excitatory/inhibitory imbalance underlies hippocampal atrophy in individuals with 22q11.2 deletion syndrome with psychotic symptoms. *Biological Psychiatry, 94*(7), 569–579. https://doi.org/10.1016/j.biopsych.2023.03.021

Mekori-Domachevsky, E., Taler, M., Shoenfeld, Y., Gurevich, M., Sonis, P., Weisman, O., Weizman, A., & Gothelf, D. (2017). Elevated proinflammatory markers in 22q11.2 deletion syndrome are associated with psychosis and cognitive deficits. *Journal of Clinical Psychiatry, 78*(9), e1219–e1225. https://doi.org/10.4088/JCP.16m11207

Moore, T. M. (2026). *Schizophrenia as ordered synaptic fragility* [Manuscript under review].

Nehme, R., Pietiläinen, O., Artomov, M., Tegtmeyer, M., Valakh, V., Lehtonen, L., Bell, C., Singh, T., Trehan, A., Sherwood, J., Manning, D., Peirent, E., Malik, R., Guss, E. J., Hawes, D., Beccard, A., Bara, A. M., Hazelbaker, D. Z., Zuccaro, E., … Eggan, K. (2022). The 22q11.2 region regulates presynaptic gene-products linked to schizophrenia. *Nature Communications, 13*(1), 3690. https://doi.org/10.1038/s41467-022-31436-8

O'Hora, K. P., Amir, C. M., Chiem, E., Schleifer, C. H., Grigoryan, V., Kushan-Wells, L., Chiang, J. J., Cole, S., Irwin, M. R., & Bearden, C. E. (2024). Differential inflammatory profiles in carriers of reciprocal 22q11.2 copy number variants. *Psychoneuroendocrinology, 169*, 107135. https://doi.org/10.1016/j.psyneuen.2024.107135

Passecker, J., Aloimonos, C. M., Dagunts, A., Wagner, F. F., Kupferschmidt, D. A., Gogos, J., & Gordon, J. A. (2025). Developmental selective GSK3α inhibition rescues working memory deficits in a mouse model of schizophrenia predisposition. *Complex Psychiatry, 11*(1), 131–141. https://doi.org/10.1159/000547800

Passecker, J., Chang, C.-Y., Dagunts, A., Aloimonos, C. M., Leitner, L., Petryk, A., Wagner, F. F., Myroshnychenko, M. V., Kupferschmidt, D. A., Gogos, J. A., & Gordon, J. A. (2026). Divergent transcriptomic pathways underlie sex-biased cognitive rescue by developmental GSK3B inhibition in a mouse model of 22q11.2 deletion syndrome. *Translational Psychiatry, 16*(1), 415. https://doi.org/10.1038/s41398-026-04108-0

Paterlini, M., Zakharenko, S. S., Lai, W.-S., Qin, J., Zhang, H., Mukai, J., Westphal, K. G. C., Olivier, B., Sulzer, D., Pavlidis, P., Siegelbaum, S. A., Karayiorgou, M., & Gogos, J. A. (2005). Transcriptional and behavioral interaction between 22q11.2 orthologs modulates schizophrenia-related phenotypes in mice. *Nature Neuroscience, 8*(11), 1586–1594. https://doi.org/10.1038/nn1562

Rao, S. B., Sun, Z., Brundu, F., Chen, Y., Sun, Y., Zhu, H., Shprintsen, R. J., Tomer, R., Rabadan, R., Leong, K. W., Markx, S., Kushner, S. A., Xu, B., & Gogos, J. A. (2025). Aberrant pace of cortical neuron development in brain organoids from patients with 22q11.2 deletion syndrome-associated schizophrenia. *Nature Communications, 16*(1), 6986. https://doi.org/10.1038/s41467-025-62187-x

Rees, E., Kirov, G., Sanders, A., Walters, J. T. R., Chambert, K. D., Shi, J., Szatkiewicz, J., O'Dushlaine, C., Richards, A. L., Green, E. K., Jones, I., Davies, G., Legge, S. E., Moran, J. L., Pato, C., Pato, M., Genovese, G., Levinson, D., Duan, J., … Owen, M. J. (2014). Evidence that duplications of 22q11.2 protect against schizophrenia. *Molecular Psychiatry, 19*(1), 37–40. https://doi.org/10.1038/mp.2013.156

Roberts, R. C., Barksdale, K. A., Roche, J. K., & Lahti, A. C. (2015). Decreased synaptic and mitochondrial density in the postmortem anterior cingulate cortex in schizophrenia. *Schizophrenia Research, 168*(1–2), 543–553. https://doi.org/10.1016/j.schres.2015.07.016

Rogdaki, M., Devroye, C., Ciampoli, M., Veronese, M., Ashok, A. H., McCutcheon, R. A., Jauhar, S., Bonoldi, I., Gudbrandsen, M., Daly, E., van Amelsvoort, T., Van Den Bree, M., Owen, M. J., Turkheimer, F., Papaleo, F., & Howes, O. D. (2023). Striatal dopaminergic alterations in individuals with copy number variants at the 22q11.2 genetic locus and their implications for psychosis risk: A [18F]-DOPA PET study. *Molecular Psychiatry, 28*(5), 1995–2006. https://doi.org/10.1038/s41380-021-01108-y

Schneider, M., Debbané, M., Bassett, A. S., Chow, E. W. C., Fung, W. L. A., van den Bree, M., Owen, M., Murphy, K. C., Niarchou, M., Kates, W. R., Antshel, K. M., Fremont, W., McDonald-McGinn, D. M., Gur, R. E., Zackai, E. H., Vorstman, J., Duijff, S. N., Klaassen, P. W. J., Swillen, A., … International Consortium on Brain and Behavior in 22q11.2 Deletion Syndrome. (2014). Psychiatric disorders from childhood to adulthood in 22q11.2 deletion syndrome: Results from the International Consortium on Brain and Behavior in 22q11.2 Deletion Syndrome. *American Journal of Psychiatry, 171*(6), 627–639. https://doi.org/10.1176/appi.ajp.2013.13070864

Sekar, A., Bialas, A. R., de Rivera, H., Davis, A., Hammond, T. R., Kamitaki, N., Tooley, K., Presumey, J., Baum, M., Van Doren, V., Genovese, G., Rose, S. A., Handsaker, R. E., Daly, M. J., Carroll, M. C., Stevens, B., & McCarroll, S. A. (2016). Schizophrenia risk from complex variation of complement component 4. *Nature, 530*(7589), 177–183. https://doi.org/10.1038/nature16549

Shin, D., Kim, C. N., Ross, J., Hennick, K. M., Wu, S.-R., Paranjape, N., Leonard, R., Wang, J. C., Keefe, M. G., Pavlovic, B. J., Donohue, K. C., Moreau, C., Wigdor, E. M., Larson, H. H., Allen, D. E., Cadwell, C. R., Bhaduri, A., Popova, G., Bearden, C. E., … Nowakowski, T. J. (2024). Thalamocortical organoids enable in vitro modeling of 22q11.2 microdeletion associated with neuropsychiatric disorders. *Cell Stem Cell, 31*(3), 421–432. https://doi.org/10.1016/j.stem.2024.01.010

Sigurdsson, T., Stark, K. L., Karayiorgou, M., Gogos, J. A., & Gordon, J. A. (2010). Impaired hippocampal–prefrontal synchrony in a genetic mouse model of schizophrenia. *Nature, 464*(7289), 763–767. https://doi.org/10.1038/nature08855

Stark, K. L., Xu, B., Bagchi, A., Lai, W.-S., Liu, H., Hsu, R., Wan, X., Pavlidis, P., Mills, A. A., Karayiorgou, M., & Gogos, J. A. (2008). Altered brain microRNA biogenesis contributes to phenotypic deficits in a 22q11-deletion mouse model. *Nature Genetics, 40*(6), 751–760. https://doi.org/10.1038/ng.138

Sun, D., Ching, C. R. K., Lin, A., Forsyth, J. K., Kushan, L., Vajdi, A., Jalbrzikowski, M., Hansen, L., Villalon-Reina, J. E., Qu, X., Jonas, R. K., van Amelsvoort, T., Bakker, G., Kates, W. R., Antshel, K. M., Fremont, W., Campbell, L. E., McCabe, K. L., Daly, E., … Bearden, C. E. (2020). Large-scale mapping of cortical alterations in 22q11.2 deletion syndrome: Convergence with idiopathic psychosis and effects of deletion size. *Molecular Psychiatry, 25*(8), 1822–1834. https://doi.org/10.1038/s41380-018-0078-5

Tamura, M., Mukai, J., Gordon, J. A., & Gogos, J. A. (2016). Developmental inhibition of Gsk3 rescues behavioral and neurophysiological deficits in a mouse model of schizophrenia predisposition. *Neuron, 89*(5), 1100–1109. https://doi.org/10.1016/j.neuron.2016.01.025

Tang, S. X., Moore, T. M., Calkins, M. E., Yi, J. J., McDonald-McGinn, D. M., Zackai, E. H., Emanuel, B. S., Gur, R. C., & Gur, R. E. (2017). Emergent, remitted and persistent psychosis-spectrum symptoms in 22q11.2 deletion syndrome. *Translational Psychiatry, 7*(7), e1180. https://doi.org/10.1038/tp.2017.157

Vergaelen, E., Schiweck, C., Van Steeland, K., Counotte, J., Veling, W., Swillen, A., Drexhage, H., & Claes, S. (2018). A pilot study on immuno-psychiatry in 22q11.2 deletion syndrome: A role for Th17 cells in psychosis? *Brain, Behavior, and Immunity, 70*, 88–95. https://doi.org/10.1016/j.bbi.2018.03.022

Vorstman, J. A. S., Breetvelt, E. J., Duijff, S. N., Eliez, S., Schneider, M., Jalbrzikowski, M., Armando, M., Vicari, S., Shashi, V., Hooper, S. R., Chow, E. W. C., Fung, W. L. A., Butcher, N. J., Young, D. A., McDonald-McGinn, D. M., Vogels, A., van Amelsvoort, T., Gothelf, D., Weinberger, R., … International Consortium on Brain and Behavior in 22q11.2 Deletion Syndrome. (2015). Cognitive decline preceding the onset of psychosis in patients with 22q11.2 deletion syndrome. *JAMA Psychiatry, 72*(4), 377–385. https://doi.org/10.1001/jamapsychiatry.2014.2671

Xu, B., Hsu, P.-K., Stark, K. L., Karayiorgou, M., & Gogos, J. A. (2013). Derepression of a neuronal inhibitor due to miRNA dysregulation in a schizophrenia-related microdeletion. *Cell, 152*(1–2), 262–275. https://doi.org/10.1016/j.cell.2012.11.052